

Open Research Online

The Open University's repository of research publications and other research outputs

Chromite Deposits And Their Ultramafic Host Rocks In The Oman Ophiolite

Thesis

How to cite:

Brown, Michael Anthony (1984). Chromite Deposits And Their Ultramafic Host Rocks In The Oman Ophiolite. PhD thesis The Open University.

For guidance on citations see [FAQs](#).

© 1983 The Author



<https://creativecommons.org/licenses/by-nc-nd/4.0/>

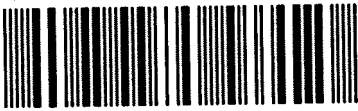
Version: Redacted Version of Record

Link(s) to article on publisher's website:

<http://dx.doi.org/doi:10.21954/ou.ro.00011868>

Copyright and Moral Rights for the articles on this site are retained by the individual authors and/or other copyright owners. For more information on Open Research Online's data [policy](#) on reuse of materials please consult the policies page.

oro.open.ac.uk



D 51281/84

UNRESTRICTED

CHROMITE DEPOSITS AND THEIR ULTRAMAFIC HOST ROCKS
IN THE OMAN OPHIOLITE

A thesis presented for the degree of
Doctor of Philosophy

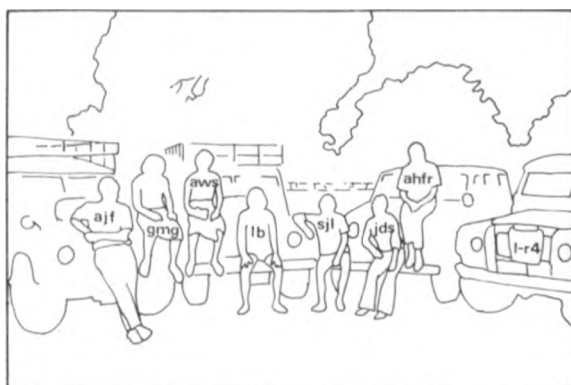
by

Michael Anthony Brown
B.Sc. Hons. University of Southampton

Authors no: HDE 6453
Date of submission: 1.1.83
Date of award: 9.5.84

Department of Earth Sciences
The Open University

December 1982



ajf	Andy Fleet
gmg	Gavin Graham
aws	Tony Shelton
lb	Tony Alabaster
sjl	Steve Lippard
jds	John Smewing
ahfr	Alistair Robertson

Frontispiece: On top of the Oman Ophiolite

"You may recognise some of these people"

see Endpiece

M.A. BROWN

Ph.D. Thesis

Chromite Deposits and their
Ultramafic Host Rocks in
the Oman Ophiolite

I am willing that this Ph.D Thesis
may be made available to readers
and may be photocopied, subject to the
discretion of the Librarian.

M. A. BROWN

21 May 1984

The Open University
Higher Degrees Office
23 MAY 1984

ACK.....
Pass to.....
Disposal.....

ABSTRACT

Chromite deposits in the Oman ophiolite are invariably associated with dunite bodies occurring dominantly within the upper part of the basal harzburgite unit of the ophiolite, the 'Mantle Sequence'. The host harzburgite and the dunite/chromitite suite show textural and geochemical evidence of origin by different genetic processes.

Harzburgite has tectonite textures from polyphase deformation and is homogeneous on a gross scale in its mineralogy and chemistry. Harzburgite mineral compositions suggest an origin as a refractory residue from one or more partial melting episodes, low fO_2 conditions, and show no systematic spatial variation. Large variations in accessory chromite are attributable to re-equilibration with variable bulk-rock alumina contents.

Dunite-chromitite bodies are less deformed than the harzburgite and contain primary igneous textures. Chromitite spinel compositions are least affected by silicate-chromite re-equilibration and show systematic variation with depth throughout the Mantle Sequence compatible with crystallization from a rising hydrous magma diapir. Pulses of chromite precipitation may have been initiated on periodic release of magma from the diapir into the overlying chamber. Coupled with crystal settling and/or boundary layer crystallization this is a possible mechanism for formation of massive chromite bodies and explains the congregation of large chromite deposits within a narrow depth zone at the top of the Mantle Sequence.

The presence of alkali-rich minerals and volatile phases in interstices and/or primary inclusions in massive chromite deposits are significant. Clearly alkalies and volatiles are intimately associated with the processes of transport and concentration of chromium, possibly involving immiscible liquids, but little is known of the phase relations of such complex systems at present.

Oman chromitites are not commercially very attractive for large scale investment but could be worked on a small scale and represent a further diversity in a world market dominated by two countries.

ACKNOWLEDGEMENTS

This work was supported by a studentship grant from the Ministry for Overseas Development (O.D.M.). My supervisors were Professor Ian Gass and Dr. Chris Neary who did their best to guide me through the research and were a great influence on the work achieved. I thank them for critically reading the manuscript and also Martin Menzies who reviewed part of the draft. The views expressed in this thesis do not necessarily coincide with those of the reviewers.

The staff of the Ministry of Agriculture, Fisheries, Petroleum and Minerals, notably Dr. Ismail Elboushi and Mohammed Kassim, were instrumental in gaining access for our group into Oman and accommodation in Sohar. From them I learned much about Arabic hospitality and administration methods. Geologists of Prospection Ltd. (Canada) and later Oman Mining & Co. showed me most chromite deposit locations either on maps or in the field and some, notably George Jeffs and Ken Brown, shared the delights of wadi wandering in the upper mantle.

The Sohar bunge was often the scene for a cast of thousands during my stay there. I would like to express my appreciation to the following friends with whom I spent most time; John Smewing, Adrian (Dr. Stig) Lewis, Gavin Graham, Mike Searle, Tony Shelton, Tony Alabaster and Steve Lippard. We may not have had too many wild discussions in the field about the origin of chromite deposits, but then who has? They kept me laughing and almost sane throughout a total of 12 months of field work. All those people we met in Muscat especially Geoff and Pauline Searle and other friends in P.D.O. were very hospitable making us feel very much at home. The people of the Hajar al Gharbi, particularly in Farfar and Rajmi, I thank for too much t'fadhal and their infectious optimism over wajid hadeed.

My three and a bit years at the Open University were very happy ones with more friends than I have room to mention. It has been a pleasure to know all the people with whom I have played sports of various descriptions; the parties were excellent. Special thanks go to Richie Holt for teaching me research and thesis writing techniques, Paul Browning for patient remedial help with the Cambridge dialects of Phoenix and Zed, Andy Tindle and Phil Potts for guidance with the electron microprobe, Ian Chaplin and all lab staff for dominantly willing sample preparation, John Taylor for aid with diagrams, maps and photos, and all of the secretarial staff of the O.U. Earth Sciences department over the years who have been willing to oblige in any way possible.

Amy Allen-Rowlandson not only typed and re-typed this thesis but also never complained in the slightest whenever I staggered in late for Sunday lunch after football and the pub, not even when I married her daughter. Laura was a great source of encouragement during the writing of this thesis, always insisting that my work should come first - right after plastering the bathroom, fixing the brakes on the mini,

My parents, Pat and Alan Brown should have the final mention. They paid my way through my B.Sc. degree at Southampton but never reminded me about it.

List of Contents

ABSTRACT

ACKNOWLEDGEMENTS

<u>CHAPTER ONE</u>	Introduction	
1.1	Oman : regional setting	1
1.2	Regional Geology.	1
1.2A	Tethyan ophiolite belt.	1
1.2B	Geology of the Northern Oman Mountains.	5
	Autochthonous units.	6
	Allochthonous units.	8
	Post-ophiolite autochthonous sediments	9
	Nappe emplacement.	12
1.3	Previous work	14
	Ophiolitic harzburgite sequences.	14
	Podiform chromite deposits.	16
1.4	Previous work on the Semail Ophiolite	22
1.5	The present study	25
 <u>CHAPTER TWO</u>	 Geology of the Oman Ophiolite.	 27
2.1	Introduction.	27
2.2	The Crustal sequence.	27
	Ophiolite sediments	27
	The extrusives.	30
	The sheeted dyke complex.	30
	The high level intrusive assemblage	31
	The cumulates	32

2.3	The Mantle sequence	33
	Harzburgite	33
	Dunite.	35
	Chromitite.	38
	The Mantle sequence upper boundary or 'Petrologic Iloho'	40
2.4	Mafic and ultramafic dykes.	43
<u>CHAPTER THREE</u>		
	Harzburgite	48
3.1	Introduction.	48
3.2	Mineral optical properties.	48
	Olivine	48
	Orthopyroxene	51
	Clinopyroxene	51
	Chromite.	51
3.3	Rock textures	56
3.4	Harzburgite mineral chemistry	62
	Olivine	64
	Orthopyroxene	64
	Clinopyroxene	69
	Chromite.	69
3.5	Covariance of harzburgite mineral chemistry	69
3.6	Spatial variations in harzburgite mineral chemistry	73
<u>CHAPTER FOUR</u>		
	Dunite and Chromitite	78
4.1	Introduction.	78

4.2	Rock textures	78
	Primary igneous textures.	78
	Deformation textures.	87
4.3	Mineralogy and chemistry.	89
	Introduction.	89
	Olivine	89
	Pyroxene.	91
	Chromite.	91
	Feldspar.	95
	Amphibole	100
	Sulphides	100
	Platinum group elements (PGE)	100
4.4	Covariance of dunite and chromitite mineral chemistry	102
4.5	Spatial variation in mantle sequence dunite and chromitite mineral chemistry.	102
	Single grains	102
	Variation within chromitite bodies.	105
	Spatial variations in chromite chemistry throughout the Onman mantle sequence.	107
<u>CHAPTER FIVE</u> Mafic and ultramafic dykes.		110
5.1	Introduction.	110
5.2	Rock textures	114
5.3	Mineral chemistry	117
<u>CHAPTER SIX</u> Secondary Minerals.		123
6.1	Introduction.	123

6.2	Serpentine.	123
6.3	Tremolite	125
6.4	Chlorite.	125
6.5	Iron oxides	128
6.6	Carbonates.	128
6.7	Ferritchromit	128
CHAPTER SEVEN	Genesis of the Oman chromitites and their host rocks	132
7.1	Physical conditions	132
	Geothermometry.	132
	Olivine-spinel geothermometer.	132
	Two-pyroxene geothermometer.	136
	Geobarometry.	138
	Oxygen fugacity	138
7.2	Genetic processes	141
	Introduction.	141
	Partial melting	142
	Early magma evolution	151
7.3	Mechanism for chromite concentration.	157
7.4	Textural evidence for mechanisms of chromite concentration	164
7.5	Genesis of the Oman chromitites and their host rocks : Summary.	170
CHAPTER EIGHT	Economic geology	174
8.1	Introduction.	174
8.2	Chromite prospection.	178
8.3	Evaluation of Oman chromitite	181

<u>APPENDIX ONE</u>	Rock Nomenclature.	185
A1.1	Petrological classification	185
A1.2	Textural classification	186
A1.3	Ophiolite definition.	189
 <u>APPENDIX TWO</u>	 Sample Locations	 190
A2.1	Harzburgite traverse sample locations	191
A2.2	Locations of chromite deposits and other microprobe analysed rocks MAPS 1 - 4.	192
A2.3	Locations of samples analysed for Platinum Group elements (PGE).	197
A2.4	Close up of PGE sample locations in Rayy-Rajmi area	198
 <u>APPENDIX THREE</u>	 Geochemical Data.	 199
A3.1	Microprobe analyses	199
A3.1.1	Sample preparation and analytical procedure	199
A3.1.2	Precision and accuracy.	200
A3.1.3	Silicate analyses	208
A3.1.4	Chromite data input program	217
A3.1.5	Chromite analyses	219
A3.2	Sulphides	242
A3.3	Platinum group elements	243
References.		244

List of Figures

CHAPTER ONE

fig. 1.1	Outcrop map of the Oman Mountains.	2
fig. 1.2	Tethyan ophiolites	3
fig. 1.3	Oman stratigraphy.	3
fig. 1.4	Geological sketch map of the Oman Mountains. . .	7
fig. 1.5	Model of rifting and passive margin formation. .	10
fig. 1.6	Reconstruction of the Hawasina basin	11
fig. 1.7	Model of formation of podiform chromite deposits (I).	18
fig. 1.8	Model of formation of podiform chromite deposits (II).	18
fig. 1.9	Chromite compositional fields in the spinel prism	21

CHAPTER TWO

fig. 2.1	Geological map of the Oman Ophiolite : Fizh and N. Salahi blocks.	28
fig. 2.2	Diagrammatic cross-section through the stratigraphy of the Oman ophiolite	29

CHAPTER THREE

fig. 3.1	Development of OPX retort shape by simple shear model.	52
fig. 3.2	Textural elements in Oman harzburgites	59
fig. 3.3	Mg/Mg+Fe x NiO ₂ : harzburgite olivines	66
fig. 3.4	Pyroxene quadrilateral : harzburgite pyroxenes .	67
fig. 3.5	Mg/Mg+Fe x Wt% Al ₂ O ₃ : harzburgite enstatite. . .	68

fig. 3.6	Coexisting Opx and Cpx in Oman harzburgites . . .	68
fig. 3.7	Spinel prism ; harzburgite accessory chromites. .	70
fig. 3.8	Cr/Cr+Al x TiO ₂ Wt% : harzburgite accessory chromites	71
fig. 3.9	Mg/Mg+Fe x MnO Wt% : harzburgite accessory chromites	71
fig. 3.10	Covariance of harzburgite mineral chemistry and modal composition	72
fig. 3.11	Sample locations on the Rayy-Rajmi harzburgite traverse.	74
fig. 3.12	Sample locations on the Bani Kharus harzburgite traverse.	74
fig. 3.13	Spatial variation of mantle sequence mineral chemistry : Rayy-Rajmi traverse	75
fig. 3.14	Spatial variation of mantle sequence mineral chemistry : Bani Kharus traverse.	77

CHAPTER FOUR

fig. 4.1A	Mg/Mg+Fe x NiO ₂ Wt% olivine : dunite and chromitite.	92
fig. 4.1B	Olivine compositions from paired harzburgite and dunite samples.	93
fig. 4.2	Pyroxene plots : dunite and chromitite.	94
fig. 4.3A	Chromite compositions: Cr/Cr+Al x Mg/Mg+Fe" dunite and chromitite	96
fig. 4.3B	Chromite compositions from paired harzburgite and dunite samples.	96
fig. 4.4	Chromite compositions: Mg/Mg+Fe" x Fe"/Cr+Al+Fe"	97
fig. 4.5	Chromite compositions: Cr/Cr+Al x TiO ₂ Wt%. . . .	98
fig. 4.6	Chromite compositions: Mg/Mg+Fe" x MnO Wt%. . . .	99
fig. 4.7	Amphibole compositions: chromitites	101
fig. 4.8	Covariance of mantle sequence dunite and chromitite mineral chemistry.	103

fig. 4.9	Analysis points in single chromite grain (OM 3962).	104
fig. 4.10	Chromite compositions plotted against horizon within chromite deposits	106
fig. 4.11	Chromite compositions plotted against horizon within mantle sequence	108

CHAPTER FIVE

fig. 5.1	Dyke orientations in mantle sequence	113
fig. 5.2	Diagram of mafic layered dyke.	115
fig. 5.3	Olivine compositions: dykes.	119
fig. 5.4	Pyroxene compositions: dykes	119
fig. 5.5	Spinel prism: dykes.	120
fig. 5.6	TiO ₂ and MnO contents of chromite: dykes	121

CHAPTER SIX

fig. 6.1	Chlorite compositions.	129
----------	--------------------------------	-----

CHAPTER SEVEN

fig. 7.1	Olivine-spinel geothermometer, (Roeder et al, 1979)	133
fig. 7.2	Olivine-spinel geothermometer, (Fabriès, 1979).	134
fig. 7.3	Correspondence between olivine/chromite ratio and mineral composition.	135
fig. 7.4	Oman chromitite compositions plotted in the spinel prism contoured for oxygen fugacity . .	140
fig. 7.5	Chromite compositions with intrinsic oxygen fugacity values plotted in spinel prism contoured for oxygen fugacity.	140
fig. 7.6	Projections in the C.M.A.S. tetrahedron. . . .	143

fig. 7.7	Projections in the basalt tetrahedron with polybaric phase boundaries.	149
fig. 7.8	Whole rock Wt% FeO(tot) x Wt% MgO	152
fig. 7.9	Olivine saturation surface.	153
fig. 7.10	Oman Ophiolite lithologic units: proportions used in calculation of the Oman Primary Magma composition OPM	153A
fig. 7.11	Liquidus phase relationships in $\text{MgO-Cr}_2\text{O}_3\text{-SiO}_2$	155
fig. 7.12	Enlarged portion of an olivine-silica-chromite plot.	155
fig. 7.13	Sketches of phase boundaries in the olivine-chromite-quartz system under different physical and chemical conditions.	156
fig. 7.14	$\text{Log}_{10} f\text{O}_2$ x temperature plots	158
fig. 7.15	Olivine-chromite binary system.	163

CHAPTER EIGHT

fig. 8.1	Main chromite deposits in the Fizh block and northern Salahi block	176
fig. 8.2	Gravity anomalies caused by chromitite bodies	180

APPENDIX ONE

fig. A1.1	Classification and nomenclature of gabbroic and ultramafic rocks.	185
-----------	---	-----

APPENDIX TWO

fig. A2.1	Harzburgite traverse sample locations in the Rayy-Rajmi and Bani Kharus areas.	191
fig. A2.2	Locations of chromite deposits and microprobe analysed rocks in the Fizh and Salahi blocks: Maps 1 - 4.	192-6
fig. A2.3	Locations of samples analysed for platinum group elements.	197
fig. A2.4	Locations in the Rayy-Rajmi area of samples analysed for platinum group elements.	198

APPENDIX THREE

fig. A3.1	Preparation of chromite blocks for analysis. . . .	202
fig. A3.2	Linescan of pentlandite.	242

List of Tables

CHAPTER THREE

Table 3.1	Harzburgite and lherzolites : modal analyses .	49
Table 3.2	Correlation of Oman harzburgite textural types and classifications of textural types of mantle tectonites from upper-mantle peridotite xenolith studies	61
Table 3.3	Harzburgite mineral chemistry.	643
Table 3.4	Olivine compositions of alpine peridotites/ ophiolite tectonites, ultramafic portions of layered intrusions and peridotite mantle nodules.	65 54

CHAPTER FOUR

Table 4.1	Modal analyses of Oman mantle sequence dunite and chromitite	79
Table 4.2	Dunite and chromitite mineral chemistry. . . .	90
Table 4.3	Variation of chromite chemistry : single grain	104A

CHAPTER FIVE

Table 5.1	Modal analyses of dykes in Oman mantle sequence	111
Table 5.2	Mafic and ultramafic dykes : mineral chemistry	118

CHAPTER SIX

Table 6.1	Secondary minerals : chemical composition. . .	126
Table 6.2	Comparison of 'ferritchromit' with primary chromite	126

CHAPTER SEVEN

Table 7.1	Wood & Banno OPX-CPX geothermometer.	137
Table 7.2	Powell OPX-CPX geothermometer.	137
Table 7.3	'Whole rock' analyses of harzburgite and lherzolite calculated from mineral compositions and modal analyses.	144
Table 7.4	Projection parameters for O'Hara (1968) polybaric phase diagram.	146
Table 7.5	Average chemical composition of Oman ophiolite lithologic units used in the calculation of the composition of an Oman Primary Magma (OPM)	148

Table 7.6	Projection parameters for basalt tetrahedron with polybaric phase boundaries (Stolper, 1980)	150
Table 7.7	Diagrammatic summary of chromite texture nomenclature	165
<u>CHAPTER EIGHT</u>		
Table 8.1	World Chromite Production.	175
Table 8.2	Possible reserves and grade of some Oman chromite deposits.	177
<u>APPENDIX ONE</u>		
Table A1.1	Textural classification : Mercier & Nicolas (1976)	186
Table A1.2	Textural classification : Pike & Schwarzmann (1977)	187
Table A1.3	Textural classification : Basu (1977).	188
<u>APPENDIX THREE</u>		
Table A3.1	Microprobe specifications.	201
Table A3.2	Microprobe vs. wet chemical analysis of basalt glass ABG.	203
Table A3.3	Analyses of secondary standards ADT (diopside) and ABX (chromite)	204
Table A3.4	Calculated errors on mineral compositional parameters obtained on the Open University microprobe	205
Table A3.5	Analysis of Cyprus chromite samples : Open University microprobe vs. Leeds University X.R.F..	207
Table A3.6	Key to index numbers in chromite analysis listing.	218
Table A3.7	Abundances of Platinum Group Elements in Oman chromitites	243

List of PlatesCHAPTER TWO

Plate 2.1	Harzburgite foliation.	34
Plate 2.2	Orthopyroxene segregation layers	34
Plate 2.3	Harzburgite/dunite layering.	34
Plate 2.4	Harzburgite/dunite layering and orthopyroxene segregation layers	36
Plate 2.5	Oikocryst of clinopyroxene in dunite	36
Plate 2.6	Harzburgite/dunite 'irregular-mix'	36
Plate 2.7	Dunite dyke in harzburgite	37
Plate 2.8	Dunite dyke with orthopyroxene enriched harzburgite at margins	37
Plate 2.9	Harzburgite/dunite layering cross-cut by dunite dykes	37
Plate 2.10	Sudi dunite body	39
Plate 2.11	Chromitite layers and small pods in a dunite layer	39
Plate 2.12	Pods and layers of massive chromitite in a dunite layer.	39
Plate 2.13	Maharah 1 chromite deposit	41
Plate 2.14	Cross-laminations of chromitite and dunite . .	41
Plate 2.15	Load structures at chromitite/dunite layer boundary	41
Plate 2.16	Al Ainah 1 chromite deposit.	42
Plate 2.17	Harrisitic olivines.	42
Plate 2.18	Dyke cutting petrological moho	42
Plate 2.19	Brecciated harzburgite and gabbro net veining	44
Plate 2.20	Basal 'cumulate' dunite layer.	44
Plate 2.21	Base of the Semail Nappe	44

Plate 2.22	The Banded Unit : mylonite horizons.	45
Plate 2.23	Pyroxenite dyke : brittle fracture	45
Plate 2.24	Pyroxenite dyke : ptygmatic folding.	45
Plate 2.25	Pyroxenite dykes : near isoclinal folding. .	47
Plate 2.26	Compound dyke of troctolite and leuco-gabbro	47
Plate 2.27	'Layered' gabbroic dyke.	47

CHAPTER THREE

Plate 3.1	Olivine porphyroclast : embayed margins. . .	50
Plate 3.2	Olivine porphyroclast : patchy extinction. .	50
Plate 3.3	Olivine porphyroclast : striped extinction .	50
Plate 3.4	Olivine neoblasts.	53
Plate 3.5	Tabulate porphyroclast of enstatite.	53
Plate 3.6	Elongate porphyroclast of enstatite.	53
Plate 3.7	Retort shaped porphyroclast of enstatite . .	54
Plate 3.8	Kink band in enstatite porphyroclast	54
Plate 3.9	Diopside exsolution lamellae curved across enstatite subgrain boundary.	54
Plate 3.10	Exsolution blebs of diopside cross-cutting kink-band in enstatite	55
Plate 3.11	Neoblasts of enstatite	55
Plate 3.12	'Graphic' chromite exsolution in enstatite .	55
Plate 3.13	Chromite at olivine/enstatite boundary . . .	57
Plate 3.14	Linear string of chromite grains	57
Plate 3.15	Tadpole shaped chromite porphyroclast. . . .	57
Plate 3.16	Holly-leaf shaped chromite porphyroclast . .	58
Plate 3.17	'Pull-apart' in accessory chromite grain . .	58
Plate 3.18	Brittle fracture in accessory chromite grains	58

CHAPTER FOUR

Plate 4.1	Mantle sequence dunite : intercumulus diopside	80
Plate 4.2	Cumulate sequence dunite : intercumulus diopside	80
Plate 4.3	Harrisitic olivine crystals.	80
Plate 4.4	Harrisitic olivine crystals with enveloping concentric chromitite layers	82
Plate 4.5	Harrisitic olivine crystal with core of olivine chromitite	82
Plate 4.6	Chromite net texture	82
Plate 4.7	Occluded silicate texture.	84
Plate 4.8	Occluded silicate in chromitite.	84
Plate 4.9	Occluded silicate in chromitite.	84
Plate 4.10	Layered phase graded chromite.	85
Plate 4.11	Fine grained silicate rich layer in chromitite	85
Plate 4.12	Fine grained olivine chromitite layer in massive chromitite	85
Plate 4.13	Chromite 'cluster texture'	86
Plate 4.14	Nodular chromite	86
Plate 4.15	Insipient nodular chromite	86
Plate 4.16	Massive chromitite	88
Plate 4.17	Nodular chromite in massive chromitite	88
Plate 4.18	Cigar-shaped occluded silicate	88

CHAPTER FIVE

Plate 5.1	Four generations of dykes in mantle sequence .	112
Plate 5.2 (A - E)	Photomicrographs of lithologies in 'layered' dyke	116
Plate 5.3	Kink-band in enstatite : deformed pyroxenite dyke	112
Plate 5.4	Strained xenocrysts of enstatite in undeformed dyke of micro-gabbro.	112

CHAPTER SIX

Plate 6.1	Serpentine mesh texture	124
Plate 6.2	Compound vein of chrysotile and lizardite/antigonite.	124
Plate 6.3	Fibrous aggregate of tremolite	124
Plate 6.4	Tremolite in chromite inclusion	127
Plate 6.5	Vein of chlorite and serpentine cut by vein of magnesite PPL	127
Plate 6.6	Vein of chlorite and serpentine cut by vein of magnesite XPL	127
Plate 6.7	Stringers of magnetite in serpentine mesh texture.	130
Plate 6.8	Replacement of plagioclase by micro- crystalline calcite stained with iron oxides	130
Plate 6.9	'Ferritchromit' rims on fractures and boundaries of chromite grains	130

LIST OF ABBREVIATIONS

Fo	=	forsterite
En	=	enstatite
Di	=	diopside
Ws	=	wollastonite
Fs	=	ferrosilite
Sp	=	spinel
Chr	=	chromite/chromitite
Opx	=	orthopyroxene
Ol	=	olivine
Cpx	=	clinopyroxene
Hzb	=	harzburgite
Dun	=	dunite
Lhz	=	lherzolite
OPM	=	Oman Primary Magma
PGE	=	platinum group elements
a-t c	=	alpine-type chromitites

PPL	=	plain polarised light
XPL	=	cross polarised light
fov	=	field of view
mag	=	magnification
LH	=	left hand
RH	=	right hand

photomicrographs

LIST OF ENCLOSURES

1. The Sumeini-Shinas Area, Oman Ophiolite Project Geological Map 1 (Brown, Searle & Smewing, 1979).
2. Wadi Jizi, Oman Ophiolite Project Geological Map 2 (Lippard, Robertson, Searle, Simonian, Smewing and Woodcock, 1980).
3. Chromites from Al'Ays Complex, Saudi Arabia and the Semail Complex, Oman, (Neary and Brown, 1979). Reprinted from Evolution and Mineralisation of the Arabian Shield (Al-Shanti, A.M.S., ed.) I.A.G.Bull.2, 193-205.
4. Textural and geochemical evidence for the origin of some chromite deposits in the Oman ophiolite, (Brown, 1980). Photocopy from Proceedings of the International Ophiolite Symposium, Cyprus, 1979, (Panayiotou, A., ed.), 714-721.
5. Palladium, platinum, rhodium, iridium and ruthenium in chromite-rich rocks from the Semail Ophiolite, Oman, (Page, Pallister, Brown, Smewing and Haffty, 1982). Reprinted from Canadian Mineralogist, v.20, 539-548.

CHAPTER ONE

Introduction

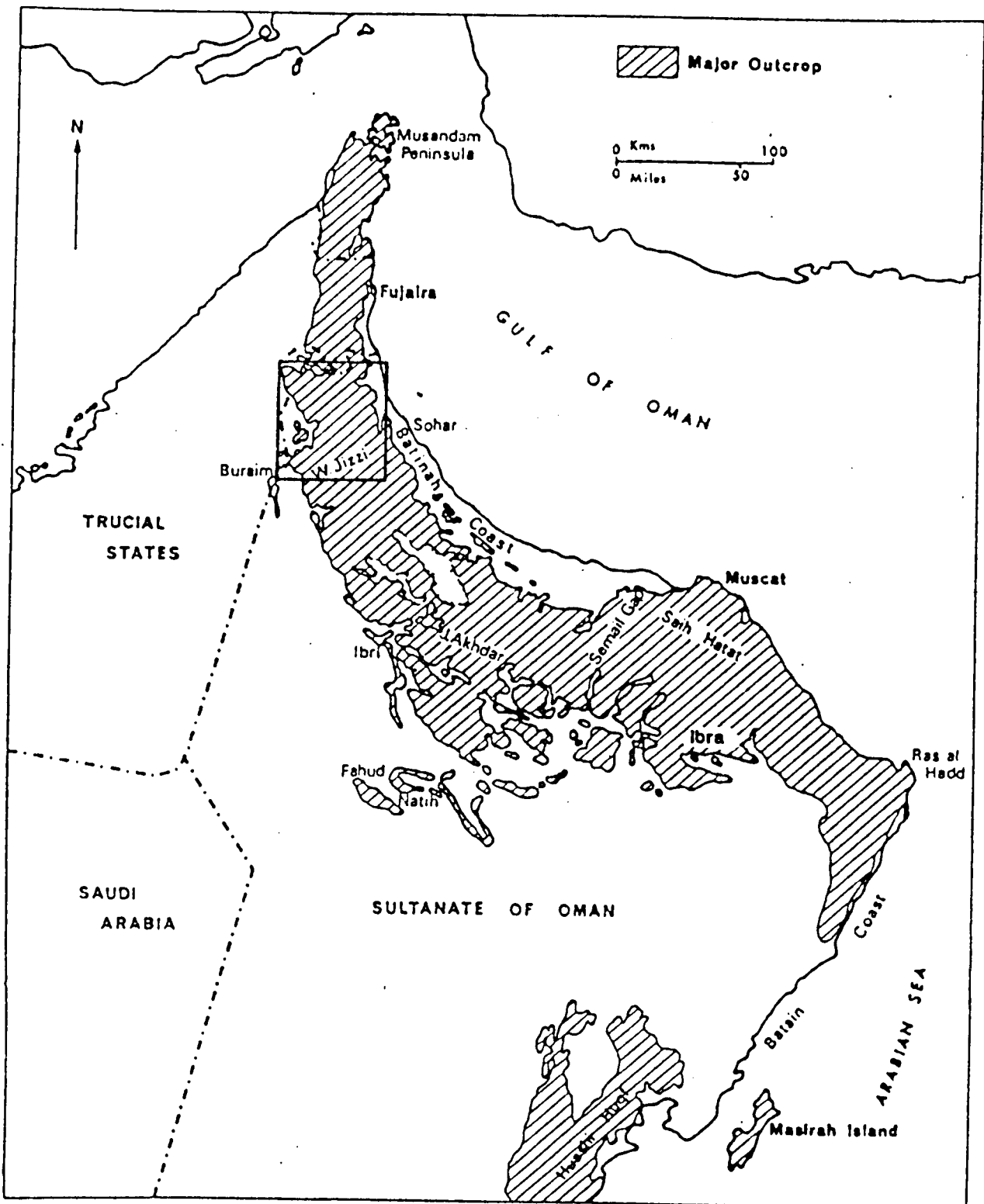
1.1 Oman : regional setting

The dominant geographical feature of Oman is the arcuate mountain chain bordering the eastern coast and passing southwards from the northern borders with the United Arab Emirates (U.A.E.) and the south-eastern-most point of the Arabian Peninsula, (fig.1.1). These mountains reach elevations of between 500 and 1000m in the area of study and are cut by deeply incised generally W-E – SE-NW trending wadis. Further to the south in the Jebal Akhdar range they rise to just over 3000m, the highest point being Jebal Ash Shams at 3019m above sea level. The extensive coastal plain bounded by the mountains and the Gulf of Oman is known as 'Al Batinah' or 'the coast' and consists of overlapping outwash fans produced during the geologically recent past by the intensive erosion of the mountain chain.

1.2 Regional Geology

Tethyan ophiolite belt

Palaeogeographic reconstructions (Smith, 1971; Dewey et al, 1973- and Stoneley, 1975) reveal that during the triassic an oceanic area(s) (Tethys) existed between 1) Africa, Arabia and India which were then part of Gondwanaland in the south and 2) Eurasia in the north. The evolution and eventual closure of Tethys are linked to the development of the present day Atlantic ocean (Dewey et al, 1973) and evidence for its existence can be seen in suture zones of the Alpine-Himalayan system extending from North Africa and Europe through the Middle East to the Himalayas, Burma, Malaysia and Indonesia. Along the suture zone there are Triassic volcanic sequences related to initial rifting, extensive shelf-slope-rise successions of passive margin sediments and ophiolite sequences that are remnants of oceanic lithosphere. Olistostromal and turbiditic trench sediments and volcanics, the products of subduction zone processes occur with the ophiolites (c.f. Wells, 1969; Glennie et al, 1974; Stoneley, 1975). The positions of the Tethyan sutures and the related ophiolites are shown in fig.1.2.



SIMPLIFIED OUTCROP MAP OF THE OMAN MOUNTAINS

fig. 1.1 The Oman Mountains
Main field area for this study shown in box

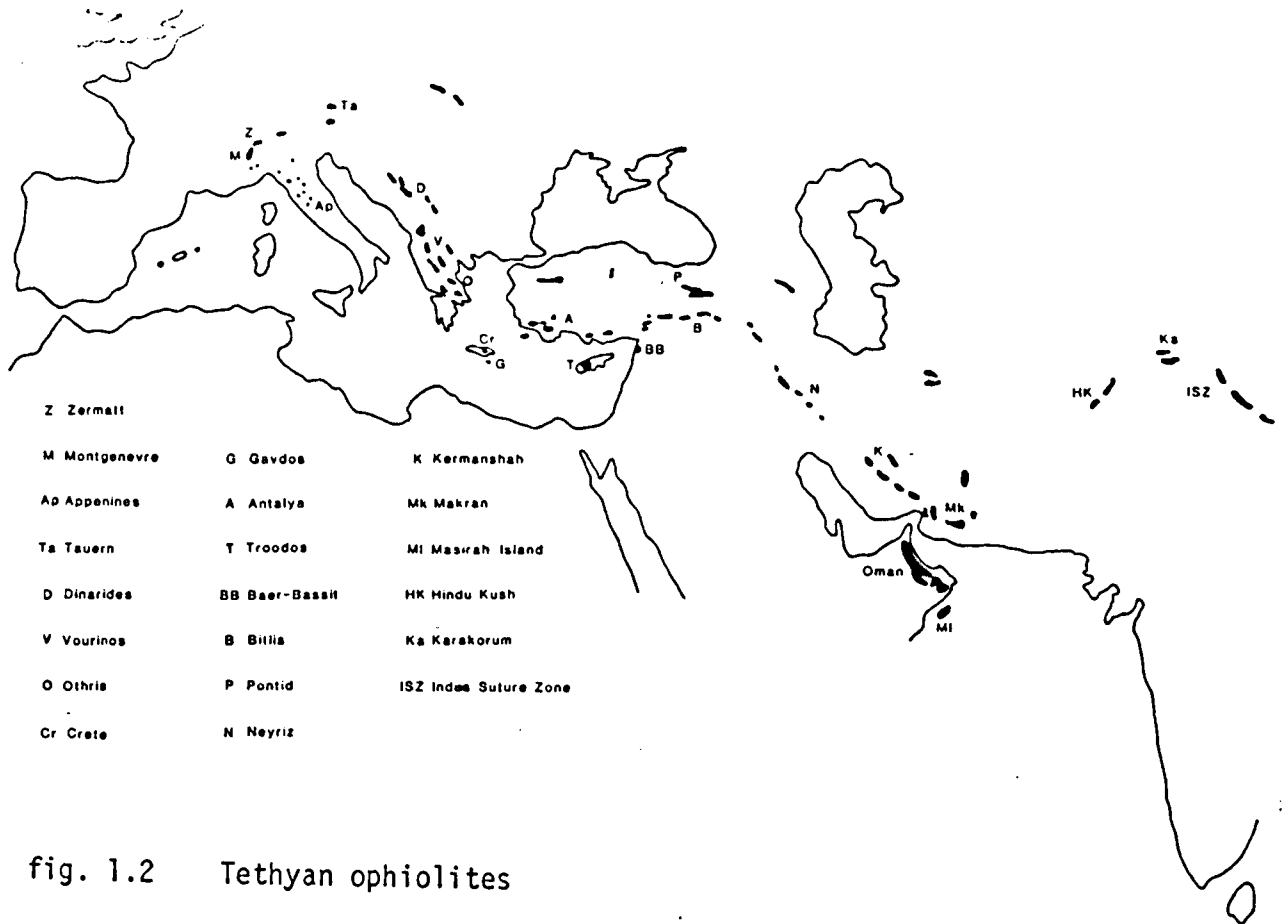


fig. 1.2 Tethyan ophiolites

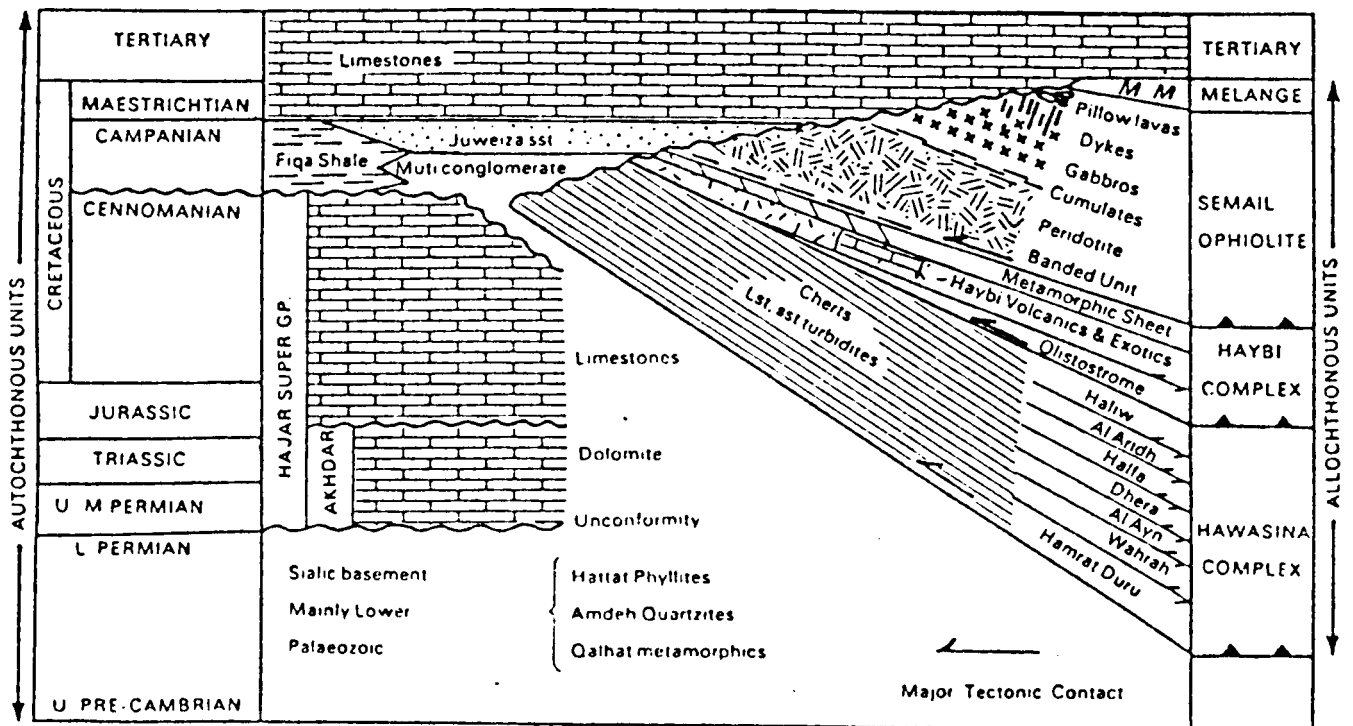


fig. 1.3 Oman stratigraphy (from Searle, '1980)

The evolution of the Alpine-Himalayan system did not involve a single plate boundary but a complex system of evolving ocean ridges, transform faults, trenches, island arcs, back arc basins and subsiding continental margins (Smith, 1971; Dewey et al, 1973). This has produced a variation in the age of formation and emplacement of ophiolite suites varying from Triassic to Upper Cretaceous.

Two types of ophiolite have been recognised in the western Tethyan belt (Rocci et al, 1975; Pearce, 1979) :

- 1) Early and middle Mesozoic ophiolites mostly occurring in the western Mediterranean, which have mid-ocean ridge to within-plate type basalts and a harzburgite mantle sequence.
- 2) Upper Cretaceous ophiolites with mid-ocean ridge to island-arc tholeiite type lavas with lower abundances of incompatible elements than those in the first group and a harzburgite mantle sequence.

Pearce (1979) has shown that few of the Tethyan ophiolite lava units show all the characteristics of normal mid-ocean ridge basalts and upper units from Troodos and Oman (group 2) resemble island-arc tholeiites (Miyashiro, 1973; Pearce, 1976; Alabaster et al, 1980). The intimate association of mid-ocean ridge type lower lavas and underlying sheeted dykes indicative of sea floor spreading with upper island-arc type lavas in the group 2 ophiolites suggests that they were formed by sea-floor spreading in marginal or back-arc basins above a shallow dipping subduction zone.

In the southern Tethyan suture Stoneley (1975) recognises two types of ophiolite complex using structural and sedimentological associations:

- 1) On the northern side of the suture are predominantly late Cretaceous small and fragmented ophiolites associated with deep-water sediments at the base of a Tertiary cycle of flysch sedimentation. Examples of this type are the interior of the Makran coastal belt (Gansser, 1955), associated with Indus flysch north of the Himalayas (Gansser, 1964) in the Arakan Yoma (Brunnschweiler, 1966), the Andaman Islands (Karunakaran, et al (1964), and in the islands of the outer Indonesian arc (van Bemmelen, 1949).

2) On the southern side of the suture are ophiolites which overlie or are found within a Mesozoic/Cenozoic passive margin sedimentary sequence and were all emplaced in the late Cretaceous (Campanian-Maestrichtian). Examples of this type have been described in Cyprus (Gass and Masson-Smith, 1963; Gass, 1968), Southern Turkey (Rigo de Righi and Cortesini, 1964; Brinkman, 1972), Iran (Wells, 1969; Ricou, 1971), Pakistan (Jones, 1961), the Himalayas (Gansser, 1959; 1964), and Oman (Reinhardt, 1969; Allemann and Peters, 1972; Glennie et al, 1973; 1974). These ophiolites are generally larger and more intact than the first type, Oman being the largest and best preserved of these with an estimated volume of 30,000km³. The mechanisms of emplacement of these two ophiolite types are markedly different (Stoneley, 1975). The first type, taking those in the Zagros Crush Zone, Iran, as an example, have been emplaced at a site of former subduction and where continental collision has taken place, in this case of Arabia into Asia. The second type are associated with passive margin sediments and have been earlier obducted there or are essentially autochthonous (e.g. Troodos, Cyprus, Gass and Masson-Smith, 1963). The proposed mechanisms of emplacement for the Oman ophiolite are briefly discussed in the next section which deals with the general geology, history of deposition and tectonism associated with the Oman ophiolite.

Geology of the Northern Oman Mountains

Geological study of the Oman started over 70 years ago with the pioneer work of Pilgrim (1908), and continued with work by Lees (1928), Hudson et al (1954), Morton (1959), Hudson and Chatton (1959), Hudson (1960), Tschopp (1967), Wilson (1969), Reinhardt (1969), Allemann and Peters (1972) and Glennie et al (1973). In 1974 Glennie and his co-workers presented a comprehensive volume forming the framework for most subsequent study. Since 1974, two research teams, one from the United States Geological Survey/University of California led by Dr.C.Hopson and the other from the Open University, U.K., led by Prof.I.G.Gass (of which the author is a member), have been engaged in field work in the Northern Oman Mountains. Numerous papers have been and will be published, most of which will be referred to in this work.

The stratigraphy in Oman can be divided into 7 major units (figs. 1.3 and 1.4). The lowermost two units are autochthonous basement with overlying sediments overlain tectonically by 4 allochthonous units; 1) the Sumeini group of carbonate and clastic shelf edge sediments, 2) the Hawasina complex of carbonate, clastic and pelagic basinal sediments, 3) the Haybi complex, a melange including a volcanic complex and 4) the Semail ophiolite. An uppermost unit consists of sediments unconformably laid down across all previous units. The allochthonous nature of the Semail ophiolite (Igneous Series) and the Hawasina Group was proposed by Lees (1928) but subsequent workers (Morton, 1959, Tschopp, 1967, Wilson, 1969), invoked an essentially autochthonous situation. Later work by Reinhardt (1969), Allemann and Peters (1972) and Glennie et al (1973; 1974) as well as the present studies support Lee's original allochthonous model and this is now almost universally accepted.

Autochthonous units

Crystalline basement is exposed at Jebal Ja'alan (fig. 1.4) where gneisses, amphibolites and schists are intruded by granites dated at 860my (Glennie et al, 1974) and later N-S trending dykes.

The oldest rocks in the northern Oman mountains are exposed in the cores of the anticlinal structures of Jebal Akhdar, Saih Hatat and Haushi-Huqf (fig. 1.4). They are a Cambrian to Carboniferous succession of quartzites, shales, carbonates and volcanics formed whilst the area was either emergent or covered by shallow continental seas. Deformation and local metamorphism of this pre-Permian succession took place during an early phase of the Hercynian orogeny. Continental rifting occurred in the area during the late Permian followed by a marine incursion resulting in a thick succession of Permian to Triassic dolomites of restricted facies (Akhdar group). By the mid-Triassic a block faulted continental margin existed with sedimentation controlled by differential subsidence (Graham, 1980(a)). The area was uplifted in the late Triassic probably prior to the onset of ocean floor spreading and continental separation signified by a late

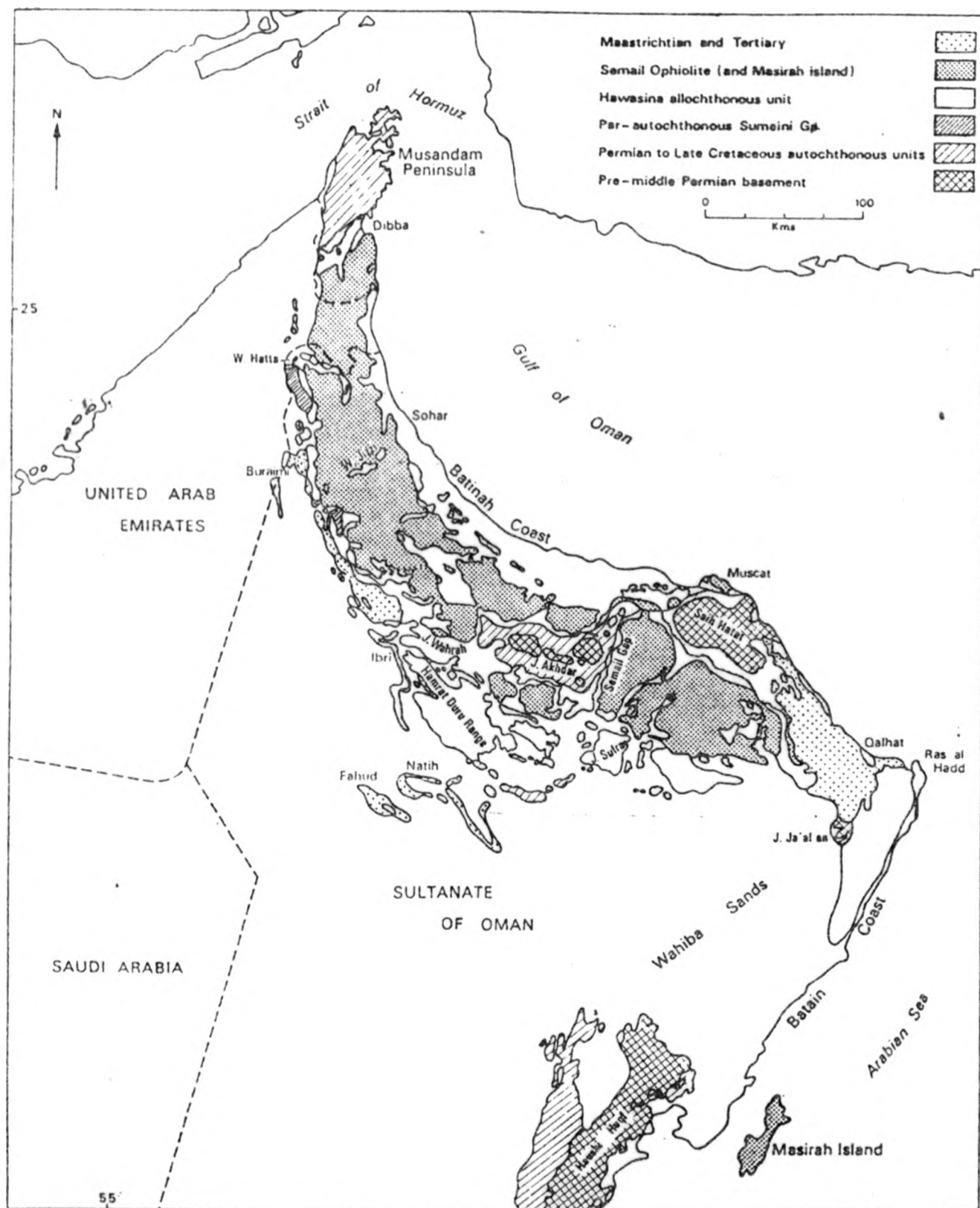


fig. 1.4 Geological sketch map of the Oman mountains
(from Graham, 1980)

Triassic unconformity over much of Oman. The early Jurassic saw gentle subsidence of the margin and the onset of shallow marine carbonate sedimentation which lasted until the mid-Cretaceous (Cenomanian), depositing the Sahtan, Kahmah and Wasia groups which, with the Akhdar group, make up the Hajar Super-Group. Regional uplift in the late Cretaceous was followed by the deposition of the Muti Formation (Coniacian to Campanian) consisting of shales and marls containing irregular lenses or thicker sequences of limestone conglomerate, calcareous turbidite and radiolarian chert. The conglomerates are more common towards the north-east where they are composed essentially of Permian clasts. The Muti Formation grades laterally south and west into shales and marls of the Figa formation. Overlying these two formations is the Juweiza Formation consisting of coarse grained clastic sediments and conglomerates which contain clasts of Hawasina sediments and ophiolite igneous rocks.

Allochthonous units

The lowermost allochthonous unit, occurring only in northern parts of the mountains, is the Sumeini Group, a Permian to Cenomanian sequence of reefal limestones, slump conglomerates, turbidites and calcareous mudstones. These are thought (Glennie et al, 1974) to be the shelf-edge facies equivalents of the shelf facies Hajar Super Group and as such are not considered to have moved very far during nappe emplacement. For this reason the Sumeini Group is termed the 'parautochthonous series' (Glennie et al, op cit).

Tectonically overlying the Sumeini Group is the Hawasina Complex which consists of several thin imbricated nappes of pelagic sediments, limestone and sandstone turbidites and cherts. The Hawasina Complex has been divided on the basis of lithology or lithologic sequence into 7 tectonically bound lithostratigraphic units, each deposited between the mid-Triassic and mid-Cretaceous (except for unit 7, the limestone exotics) (Glennie et al, 1973). There is an obvious trend of deepening environment of deposition passing up the structural section (Glennie et al, op cit; Graham 1980(b)). The continental rifting and

passive margin formation proposed for Oman during the deposition of the Hajar Super Group, Summeini Group and Hawasina Group sediments from the early Permian to early Cretaceous by Graham (1980(b)) is shown diagrammatically in fig.1.5. A reconstruction of the Hawasina basin by Glennie et al, (1974), is shown in fig.1.6.

Tectonically overlying the Hawasina complex is a complicated internally imbricated sheet of olistostromal sediments, alkaline lavas and pyroclastics often enclosing large blocks of Permian and Triassic exotic limestones, tholeiitic, mainly pillowed lavas and a metamorphic sheet of serpentinite and lower greenschist to upper amphibolite meta-sediments and meta-volcanics. This tectonic unit is the Oman mélangé of Glennie et al (1974) and the Haybi Complex of Searle (1980). Searle (op cit) divides the Haybi complex into an Upper Cretaceous sedimentary mélangé, Upper Permian to Mid?-Cretaceous volcanic rocks (the Haybi Volcanics), isolated Upper Permian and Upper Triassic limestone exotics, sub-ophiolitic metamorphic rocks and serpentinites.

The Semail Nappe or Oman Ophiolite overlies the Haybi Complex from which it is separated by the Semail Thrust. The ophiolite nappe is up to 15km thick and consists of a thick harzburgite unit in turn overlain by layered mainly gabbroic rocks a sheeted dyke complex and pillow lavas. A complete, coherent and largely undeformed ophiolite sequence, as defined by the 1972 Penrose conference (appendix I) is present. The various lithologies that make up the ophiolite sequence are described and discussed in detail in chapters 2, 3, 4, 5 and 7.

Post-ophiolite autochthonous sediments

Shallow marine bioclastic limestones of Maestrichtian age (the Simsima Formation) unconformably overlie all of the autochthonous units and on the eastern side of the Oman mountains conformably overlie the Campanian to Maestrichtian Juweiza Formation and possibly the Fiqa formation (Glennie et al, 1974). The Simsima formation either grades upwards into Palaeocene limestone or is overlain unconformably by late Eocene or early Miocene sediments (Glennie, 1977).

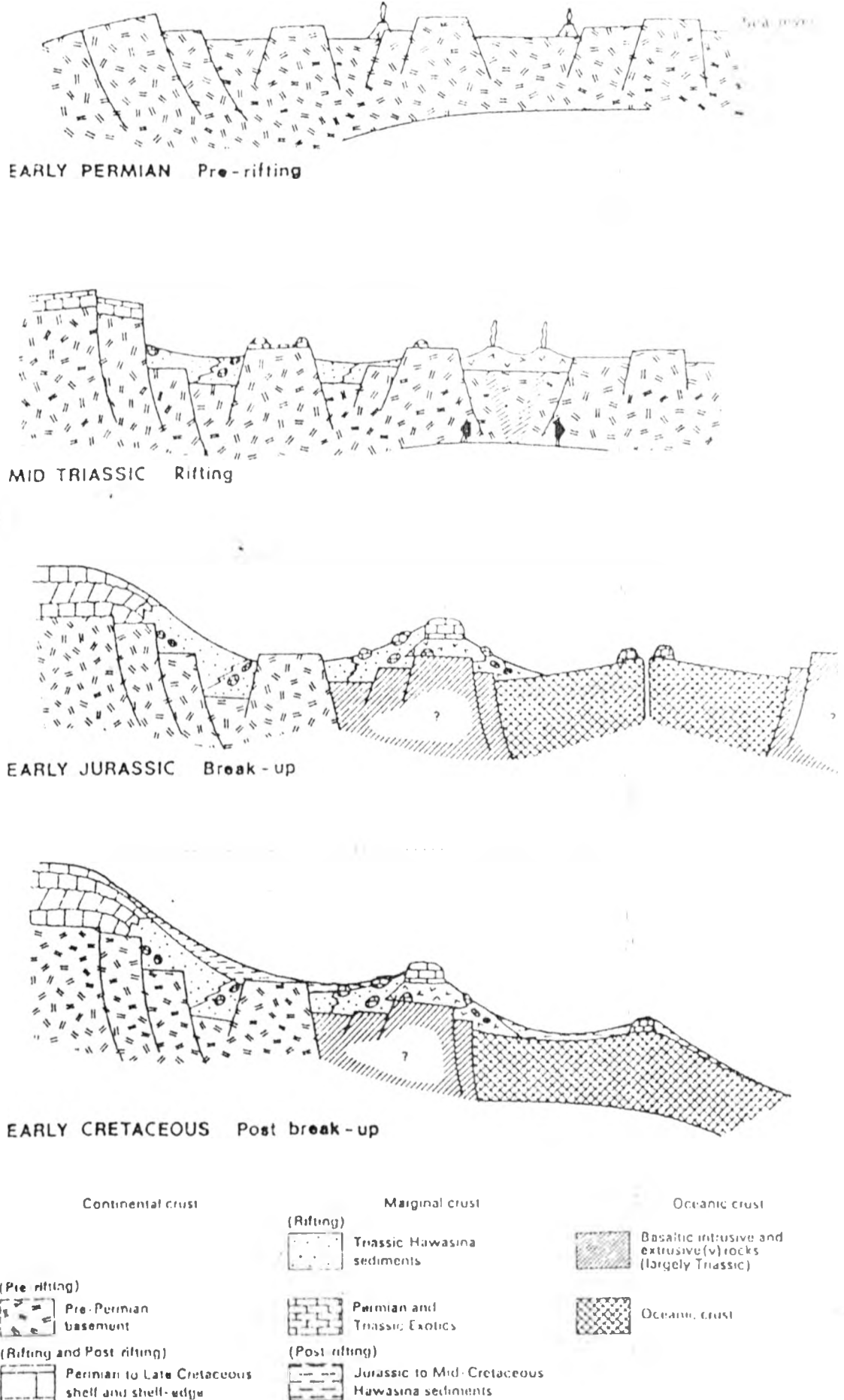


fig. 1.5 Model of rifting and passive margin formation (from Graham, 1980(b))

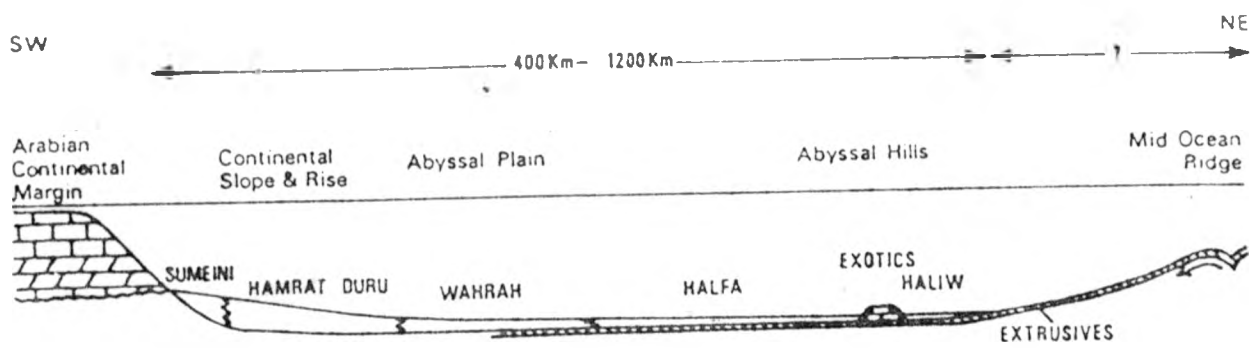


fig. 1.6 Reconstruction of the Hawasina basin
(from Glennie et al, 1974)

Nappe Emplacement

Accumulation of a thick Cretaceous shelf succession throughout Oman was followed by uplift, erosion and deposition of the Muti shales and conglomerates. This represented increased instability of the shelf which directly preceded emplacement of the nappes. The ophiolite is dated as Cenomanian/Turonian (Glennie et al, 1974; Tippit and Pessagno, 1979). It was emplaced after the deposition of the Muti Formation (Coniacian to Campanian) but prior to the onset of shallow marine sedimentation in the Maestrichtian. The processes causing the initial movement of the ophiolite slab have been the subject of some speculation. Various models that have been suggested are:

- 1) gravity gliding from the north-east (Glennie et al, 1974)
- 2) gravity spreading (Elliott, 1976)
- 3) collision between a passive margin and the fore-arc limb of an island arc complex (Gealey, 1977)
- 4) accretion above a north-easterly dipping subduction zone followed by partial continental collision (Welland and Mitchell, 1977), and
- 5) initial displacement of the ophiolite by continental under-thrusting of ocean floor and later emplacement by gravity gliding/spreading (Searle, 1980; Graham, 1980(b)).

The existence of a north-easterly dipping subduction zone is consistent with evidence from Iran (Takin, 1972) but Welland and Mitchell's (1977) model of accretion as thrust wedges above a subduction zone does not account for the ophiolite remaining as one competent slab during emplacement. They also suggest that the origin of the ophiolite suite is to the south-west of the subduction zone, at a mid-ocean spreading ridge. The upper lavas of the ophiolite have island arc/back arc affinities (Alabaster et al, 1980) and are separated from the lower lavas by little or no sediments suggesting that the upper lavas were erupted soon after the lower lavas and so the ophiolite was probably formed above a gently dipping subduction zone. Gealey's (1977) model, therefore, appears appropriate but does not satisfactorily explain all the features present. The fore-arc limb of an island arc system

would represent some of the oldest oceanic crust present and would be expected to have a Permo-Triassic age. It is much younger and was emplaced very soon after its formation. Island arcs are known to be amongst the most rapidly uplifted of tectonic features and although the arc volcanics present in the Oman ophiolite are less than 1km thick the arrival of a passive margin at a subduction zone beneath a rising insipient arc with subsequent underthrusting and isostatic rebound by the continental margin (Graham, 1980(b), Searle, 1980) may be the most likely mechanism for uplift. This would provide the driving force for the gravity emplacement models earlier suggested by Glennie et al (1974) and Elliot (1976), and invoked by Graham (op cit) and Searle (op cit) for final emplacement of the Oman ophiolite onto the continental margin of Arabia. In this passive margin/arc collision model the absence of the old component of the fore-arc limb still remains a problem. It is possible that it may have been lost by 'peeling off' into the subjacent subduction zone, but this is purely conjectural. Underthrusting of an island arc by a passive continental margin has occurred in New Guinea (Hamilton, 1973; Branson 1978) although in this case subduction proceeded for longer and the arc was therefore more developed. Continental underthrusting at considerable depth is supported by the presence in the Haybi Complex in Oman of upper amphibolite facies meta-sediments and volcanics.

Following ophiolite emplacement regional uplift occurred during which the ophiolite was subject to a brief period of emergence producing laterites preserved in the southern part of the mountains near Ibra (fig.1.1). Then the whole of Oman was covered in shallow seas from the Maestrichtian onwards until Oligocene and Miocene uplift (Glennie et al, 1974) resulted in a regression and the exposure of progressively lower strata in the anticlinal structures of Jebel Akhdar, Saih Hatat and Haushi-Huqf (fig.1.4). The ophiolite consists of a series of large blocks tens of kilometres across with comparatively little internal deformation. This division into blocks occurred either during emplacement or as a result of Tertiary folding and erosion (Graham, 1980(b)). Graham (op cit) defines the main controlling factors on the distribution of these ophiolite blocks as:

- 1) Tertiary fold axes
- 2) The location of tectonic culminations and depressions beneath the Semail Thrust, and
- 3) Major basement faults.

The rapid uplift and erosion during the Tertiary has produced thick wadi gravels and fanglomerates which now form the flat coastal plain (Al Batinah) which borders the coast of the Gulf of Oman (fig.1.1).

1.3 Previous work

This section is a summary of geological data on the genesis of 1) ophiolitic harzburgite sequences and 2) podiform chromite deposits current at the initiation of this research. This will then lead to the rationale of the present study (1.5).

Ophiolitic harzburgite sequences

Tectonite peridotites are present as the lowermost unit in all ophiolite sequences (Penrose, 1972, see appendix I) and form a floor to the crustal magma chamber in which the overlying layered gabbros and peridotites were formed. Ophiolite tectonites are texturally and chemically similar to ultramafic rocks of Alpine-Peridotite Complexes (Thayer, 1960) and are assumed to be of similar origin. Both consist mainly of harzburgite or less commonly lherzolite with minor inhomogenities present as foliated or non-foliated patches of dunite and veins of dunite pyroxenite and gabbro which are intimately associated with and closely linked genetically to the harzburgite (Menzies and Allen, 1974).

The harzburgite is widely thought to be a depleted mantle residue from which melt fractions have been almost completely extracted after partial melting of primary mantle (Wilson, 1959; Carswell, 1968; Viljoen and Viljoen, 1969; Boudier and Nicolas, 1972; Menzies and Allen, 1974). From experimental studies, an assemblage of olivine and orthopyroxene is the expected residue after moderate degrees of

partial melting of aluminous peridotite upper mantle (O'Hara, 1968) and removal of basaltic melt (Hamilton and Mountjoy, 1965; Himmelberg and Loney, 1973). Bulk compositions of harzburgite are lower in Al, Ca, K and Na and higher in Mg, Mn, Ni and Cr than would be compatible with projected primary upper mantle compositions (Green and Ringwood, 1967; Menzies, 1973).

An interpretation of ophiolite and alpine-type harzburgite sequences as deformed cumulates has been suggested (Thayer, 1967) but major objections have been raised to this hypothesis:

- 1) The high proportion of harzburgite to overlying cumulates precludes the possibility that they formed by cumulate processes from a basaltic magma (Menzies and Allen, 1974) and cumulus origin from an ultramafic magma requires large volumes of that magma (harzburgite sequences usually constitute over half of ophiolite volume), which is extremely rare amongst lavas and so its existence at depth is questionable (Dickey, 1975).
- 2) No cryptic mineralogical or bulk chemical variations in Mg/Mg+Fe or Cr have been established in the harzburgites as might be expected in cumulate systems. The harzburgites appear to be very homogeneous (Menzies and Allen, 1974) and there is little or no evidence of inter-cumulus liquids (Dickey, 1975).
- 3) Co-precipitation of olivine and orthopyroxene to form these harzburgites would be prevented, at low pressures, by the olivine-orthopyroxene reaction relationship which persists to 5kbar in anhydrous systems and to higher pressures with high water contents (Kushiro et al, 1968).

Plagioclase lherzolite occurring as 'patches' in harzburgite sequences (Nicolas and Jackson, 1972; Menzies and Allen, 1974) and spinel lherzolites occurring as a basal layer (Malpas and Strong, 1975; Malpas, 1978) have been interpreted as primary or only partially modified mantle material. Evidence of incomplete extraction of a basaltic melt can be seen as pods or schlieren of gabbroic assemblages and intergranular partial melt textures (Menzies, 1973).

Incomplete separation and in-situ crystallization of generated basaltic extract have also been recorded in garnet lherzolites as garnet and clinopyroxene peridotites (Carswell, 1968- Kornprobst, 1969). Bulk compositions of these lherzolites are similar to those expected for primary mantle from experimental studies (Ringwood, 1966; Green and Ringwood, 1967; Ringwood, 1970; O'Hara, 1970).

Dunite patches and veins were previously grouped with harzburgites as residual tectonites (e.g. Moores and Vine, 1971) but have later been interpreted as the result of crystallization of olivine and chromite from liquids trapped in the harzburgite during its convective ascent (Allen, 1975; Malpas, 1978). No evidence has been presented so far for residual 90-100% olivine dunites which would be expected to have a much higher Cr, Ni and lower Ti, Fe and Mn contents than refractory harzburgites (Burns, 1973).

A calculated primary magma from approximately 20% partial melt at about 20kbar of spinel lherzolite is a picritic tholeiite which would start to crystallize at depths of less than 60km (Malpas, 1978- Cawthorn and Strong, 1975). The nature of crystallization would depend on the rate of uprise of a magma diapir, different rates resulting in different proportions of chromite, olivine, orthopyroxene and clinopyroxene obtained by crystallization under high pressures whilst plagioclase enters the assemblage under lower pressures explaining the various modal proportions of these minerals comprising veins in the tectonites (Malpas, 1978).

Podiform chromite deposits

Podiform chromite deposits (Thayer, 1960) include all pod-like, tabular and lenticular bodies of chromitite that occur in tectonite peridotites and basal dunite cumulates of ophiolites and alpine type peridotites (the first and last categories appearing for the most part to be synonymous). This association of podiform deposits with ophiolites restricts their occurrence to island arcs and mobile mountain belts mainly of Palaeozoic or younger age (Thayer, 1970), although Upper Proterozoic ophiolite podiform chromite deposits in

N.W. Saudi Arabia have been described (Neary, 1974) and the Selukwe deposits in Zimbabwe (>3200 b.y.) have both stratiform and podiform characteristics (Cotterill, 1969). By comparison Thayer (1970) notes that all economic stratiform type chromitites which are relatively undeformed and occur in stable shield areas, are of Precambrian age. The more extensive studies of stratiform type chromitites give important insights into some conditions under which the crystallization of chromite can take place. This may be relevant, as nowhere in podiform deposits are chromitites found outside of the types of host rocks in which they occur in stratiform complexes (Thayer, 1970) where they form by crystal settling (c.f. Worst, 1960) from mafic magma containing low (1-2%) concentrations of chromium (Irvine, 1967). Distinctive relict settled textures, more or less deformed by magmatic flowage, are preserved in most podiform chromite in alpine peridotites (Thayer, 1970). This has been taken as *prima facie* evidence that their primary host rocks were differentiated by crystal settling from a fluid mafic magma in a similar manner to stratiform complexes but various evidence has already been presented as to why at least the harzburgites, forming the main body of ophiolite tectonites and alpine peridotites are not at present generally considered to be magmatic cumulates. Attempts have been made to reconcile the undoubted cumulate origin of the chromitites with the residual nature of the harzburgite. The most simple mechanism is the formation of the chromitites at the base of the overlying cumulate sequence. Dickey (1975) suggests that the elongate shapes of the deposits may represent the forms of the original magma chambers as they formed in long narrow magma pockets along plate margins, in a turbulent zone of mixed liquids and solids, where nodular textures may originate by 'snowballing' and recrystallization of chromite crystals. Chromite concentration is by winnowing within this zone with massive chromitites and olivine chromitites with fine cumulus textures forming in magma pockets. The massive chromitites sink as dense autoliths into the underlying peridotite to a maximum of about 600m depth below the cumulate base (fig.1.7). Greenbaum (1972) describes a more placid environment at a constructive margin for the deposition of the Troodos (Cyprus) chromitites (fig.1.8). Here the chromite concentrations originate in hollows on the harzburgite

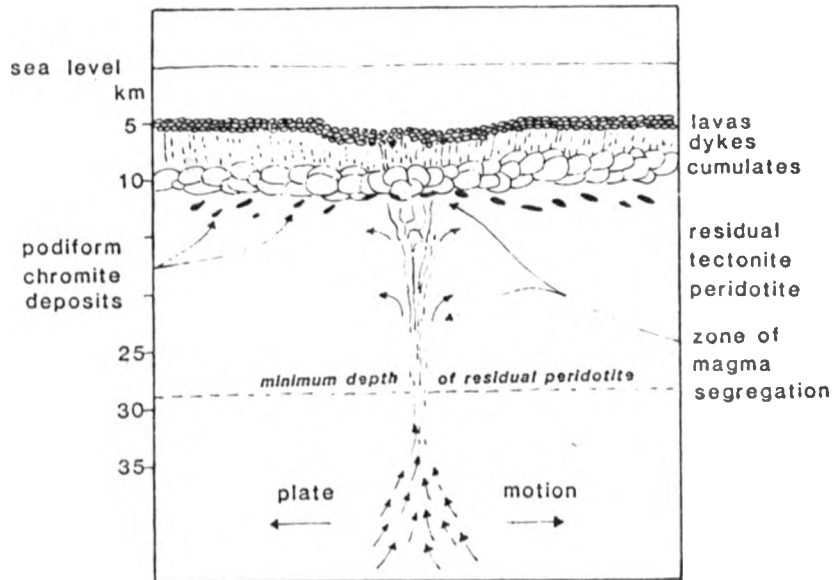


fig. 1.7 Model of formation of podiform chromite deposits (from Dickey, 1975)

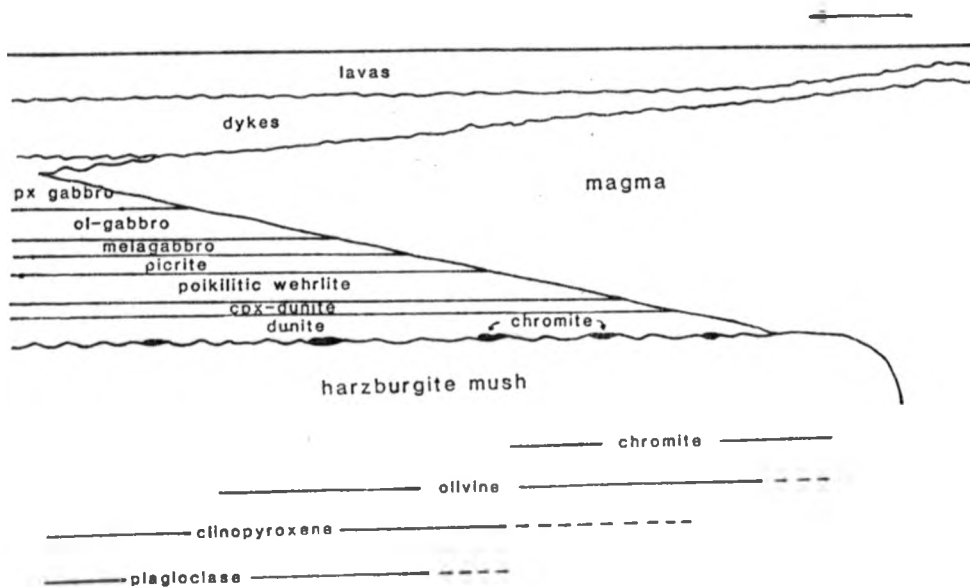


fig. 1.8 Model of formation of podiform chromite deposits (from Greenbaum, 1972)

floor by crystal settling with undercooling of the magma and supersaturation with chromium leading to dendritic growths and separation of chromium-rich immiscible liquid responsible for nodular and orbicular textures. He invokes later infolding of the basal dunite layer and contained chromitites into the tectonite peridotite. Neary (1975) proposes an origin by settling of chromite crystals at the sites of partial melting in magma pockets within the dunite/Harzburgite tectonite unit of the Upper Proterozoic Al'Ays complex in N.W. Saudi Arabia. The chromites are, then, residual with the observed chromite chemical variation across the complex being due to the dependence of Cr compositions on temperature, (Dickey and Yoder, 1972; O'Hara, 1973), with the most chromian chromites occurring at the base of the sequence. This segregation mechanism does seem to require rather large degrees of partial melting to form in situ magma pockets, however, and as Thayer (1970) notes, there is no evidence that chromitite masses can be formed by melting or recrystallizing a small part (e.g. 15-20%) of any solid rock containing accessory chromites or chromium-bearing silicates. However, this mechanism does attempt to explain the chemical variation with depth that is not easily explained by hypotheses invoking chromite masses sinking from the overlying cumulates. Podiform chromite deposits are invariably surrounded by a sheath or halo of dunite (e.g. Thayer, 1960, 1964, 1970; Dickey, 1975) and dunite bodies containing disseminated chromite and chromite schlieren have been attributed to cumulate processes acting within the tectonite peridotite (Allen, 1975; Dick, 1977; Malpas, 1978). This may provide a valuable clue to the origin in chromitites which show apparent cumulate textures within tectonised and residual host rocks.

Podiform chromitites are texturally distinct from stratiform chromitites in that the former is commonly comprised of coarse (> 3cm) anhedral interlocking grains and can display nodular and orbicular textures whilst the latter commonly bears smaller euhedral grains and lacks these textures, (Thayer, 1970). The nodular textures have encouraged some writers to propose an origin by liquid immiscibility on the basis of the field of immiscibility at 1 atm. above 1700°C in the system $MgO = Cr_2O_3 = SiO_2$ (Shams, 1964; Chakraborty and Mallik, 1971) but Dickey (1975) stated that this was unlikely both due to the

geologically unreasonable high temperatures and that the two liquids yielded in the system are unlike natural magmas.

The matrices of podiform chromitites are most commonly composed of olivine usually more or less altered to serpentine although plagioclase and clinopyroxene have been reported by Thayer (1964, 1969) and amphibole by Pamic (1970). Despite the clinopyroxene seen in the matrix of one deposit Thayer (1964) has noted that no chromitites occur in host rocks with essential clinopyroxene, i.e. lherzolites and wehrlites. The association of chromitites with plagioclase or their proximity to gabbroic cumulates due to their tendency to lie close beneath the tectonite/cumulate boundary means that their crystallization is restricted to pressures below 8-10kb (Kushiro and Yoder, 1966; O'Hara, 1967; Dickey, 1975) or depths of less than 25-30km under oceanic regions. Chromite deposits are never found in association with rocks of high pressure mineral assemblages such as eclogite or garnet peridotite (Jackson and Thayer, 1972), perhaps because at elevated (~ 10 kb) pressures chromium is extracted from the magma by direct precipitation of chrome diopside and other chromium-bearing silicates.

Chemical characteristics of podiform chromites include a large variation in chromium:aluminium ratio, low titanium and ferric iron contents and a fairly uniform magnesium:ferrous iron ratio contrasting with stratiform type chromites which have more widely varying magnesium:ferrous iron ratios and may have higher ferric iron contents (fig.1.9). The main factors controlling chromite composition are:

- 1) Residual or cumulate origin and magma evolution; the residual spinels produced during partial melting in magmagenesis would be the most chromian and cumulus chromites subsequently precipitated from the resulting magma will be increasingly aluminous as Cr is depleted and Al enriched in the liquid (Dickey, 1975). Ti will be strongly partitioned into the melt and Fe⁺⁺⁺ content will depend on the oxygen fugacity of the magma.
- 2) Temperature; spinels in equilibrium with silicate melt and clinopyroxene become more chromian with increasing temperature, (Dickey and Yoder, 1972; O'Hara, 1973).

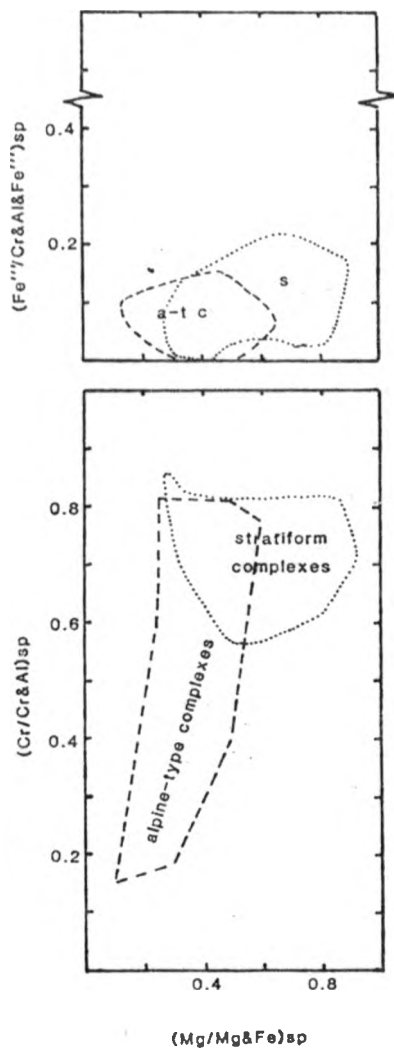


fig. 1.9 Chromite compositional fields of alpine type complexes (podiform or ophiolite chromite deposits) and stratiform type chromite deposits (adapted from Irvine, 1967 and Irvine & Findlay, 1972)

3) Bulk rock composition: the influence of bulk rock Cr:Al ratio on the composition of included spinel is strong in simple systems (Dickey and Yoder, 1972) and many, though not all, aluminous chromites occur in plagioclase-bearing host rocks. The Mg:Fe'' ratios of chromites are buffered by surrounding mafic silicates, (Irvine, 1967).

1.4 Previous work on the Semail Ophiolite

The first geological account of Oman was by Pilgrim (1908) who used the terms "Basic Igneous Series" and later the "Semail Intrusive Series" for the ophiolites. Lees (1928) renamed them the "Semail Igneous Series" as he identified extrusives within the sequence. He also recognised the allochthonous nature of the sequence, coined the term "Semail Nappe", subdivided the rock types within the series and put these in order of outcrop importance as serpentine, gabbro and diorite, all of which are penetrated by minor intrusions.

No particular advance occurred in the study of the ophiolite and in particular the basal peridotite unit until the 1960's. Reinhardt (1969) recognised the ophiolite suite as a "polygenetic association of igneous and metamorphic rocks" wherein the basal peridotite member consisted mainly of enstatite peridotite, formed 60% of the total volume and represented the oldest generation of the suite which was "possibly formed at an oceanic ridge". The environment of equilibration of these peridotites was calculated as high temperature (ca. 1400°C) and high pressure (10-20kb or 30-60km depth), (Peters, 1968).

Wilson (1969) also noted that the main body of the Semail Igneous Series was a peridotite and that layering "by crystal segregation" was common, the selective weathering of which gave the whole igneous body a bedded appearance. He proposed that the field relations supported the interpretation that the Semail Igneous Series was extruded in a liquid or viscous state. Internal layers were formed in a similar manner to those in stratiform intrusions such as the Bushveld Complex whilst heat and liquidity were retained by a fast accumulating body at abyssal depths.

Alleman and Peters (1973) supported Reinhardt's (1969) interpretation of the ophiolite as possible oceanic lithosphere and added that it did not develop from a single magma reservoir but probably from a basaltic magma generated more or less continuously from the mantle and that such a magma could be produced by partial melting of a peridotite with pyrolytic, spinel lherzolitic or garnet lherzolitic composition leaving a residue of harzburgite and dunite. They observed that the basal peridotite of the ophiolite consisted mostly of harzburgite with discontinuous dunite bands which sometimes contain stringers of tabular and pod-like chromitite bodies more or less parallel to the upper contact with the gabbro. Cross cutting dykes of pyroxenite and gabbro were described without chilled margins and lherzolites as rare showing no overall pattern of occurrence. In deeper parts of the peridotite 'layering', sometimes on a microscopic scale was thought by Alleman and Peters (1973) to be of tectonic origin due to overthrusting at the base of the Semail Nappe. They calculated equilibration temperatures for the peridotites, using Boyd and Schairer's (1964) and O'Hara's (1967) methods, of between 1000°C and 1250°C, lower values than those proposed by Reinhardt (1969).

Glennie et al (1973) recognised changes in P, T, pH₂O and pO₂ for each unit of the ophiolite and the marked similarity to models developed for spreading oceanic ridges and part of the underlying upper mantle. The major processes proposed for ophiolite formation were:

- 1) Partial melting of upper mantle rocks at relatively shallow depths (30-50km) as a result of depressurization and/or a rising geothermal gradient.
- 2) Separation of mafic melt from refractory residue, the latter being a 4-phase peridotite (ol-opx-cpx, Al-sp), the barren or burned-out peridotite of O'Hara (1967).
- 3) Upward flow of melt combined with fractional crystallization leading to differentiation of mostly mafic igneous rocks (chromitite, layered peridotites, and gabbros and diabase), with
- 4) extrusion and solidification of the magma at the surface to produce basalts.

Glennie et al (1974) support most of the observations made by Peters (1968), Reinhardt (1969) and Allemann and Peters (1973). They add that sudden compositional variations are observed at the top of the basal peridotite formation above a poorly defined level 200m or so below the contact with the overlying cumulate sequence where dunitic rocks are prevalent occasionally containing accumulations of chromite which bear textures suggesting crystallization from a melt. Large accumulations of chromite had only been observed in the north of the mountains and were aligned more or less parallel to the upper contact within this dunitic zone. They listed chromite occurrences using Peters (1968) subdivisions:

- 1) Stringers of tabular and pod-like bodies more or less parallel to the gabbro contact usually massive in the basal part and showing a gradational transition to almost chromite-free peridotite above.
- 2) Lens-shaped bodies of massive ore with long axes parallel to the stringers mentioned above with the contact with host rocks often faulted but with relics of the gradual transition to peridotites occasionally preserved.
- 3) Single crystals (0.1-1mm dia.) or small clusters of chromite disseminated through the peridotite.
- 4) Dykes of chromite cutting through peridotites and having sharp contacts which are usually associated with some other types of deposit.

Carney and Welland (1974) divided the chromitite bodies in Oman into podiform, stratiform, and banded types although it seems that the first two terms were used *sensu lato* to describe parallel sided or pod-like appearance in the field rather than to divide them into genetic types. They described apparent graded bedding in the deposits suggesting an origin by crystal accumulation but added that overprinting had taken place possibly by a flow-layering (Thayer, 1963) and/or a metamorphic fabric. The origin of chromitite concentrations in peridotite, they suggest, could have been during an early phase of crystal accumulation, possibly associated with mantle processes at a mid-ocean ridge system. The disruption into lenses and pods may well have been consequent upon later tectonic emplacement of the ophiolite.

1.5 The present study

Following the comprehensive documentation, over the last decade, of the similarity between ophiolites and oceanic lithosphere it is assumed that the Oman ophiolite was formed by sea-floor spreading. This work investigates upper mantle processes in this framework rather than to further demonstrate the similarity. As the Oman ophiolite possesses the largest expanse of onland oceanic upper mantle known at present it offers one of the best opportunities for studies of this kind. At the onset of this work the following main points presented themselves for further investigation:

- 1) If the harzburgite sequence was homogeneous or displayed abundant mineralogical or chemical layering, and if so how was this related to primary magmatic or later tectonic events?
- 2) Were there any remnants of primary mantle lithologies (i.e. lherzolites) within the sequence or any partial melt textures or trapped melts within the harzburgites?
- 3) What position do dunite bodies assume within the sequence and what form do they take?
- 4) What is the nature of the dykes that cross-cut the harzburgite sequence and are they genetically related to their host rocks?
- 5) What forms do massive podiform chromite deposits take, where do they occur within the sequence, what are their host rocks and how do they relate to the overall genesis of the sequence?
- 6) What do the textures in the chromitites represent? Are they primary magmatic structures and if so can they help to explain the concentration of chromite into massive bodies? What textures are modified or solely due to later tectonic processes?
- 7) Does the chemistry of the chromite suggest a residual or cumulate origin, are there any systematic spatial chemical variation and if so how is it explained?

All these detailed points are directed at a further understanding of the processes of formation of the tectonised sequence of peridotitic rocks that underlie the main cumulate series of an ophiolite complex

and, in particular to the genesis of the chromite concentrations therein. Associated questions of direct economic importance are:

- 8) Are the chromite deposits of economic size and grade, what are the possible reserves and are there any other economic minerals associated with them?
- 9) Can further exploration areas be suggested from the distribution of known deposits and do any useful exploration methods arise from this study?

CHAPTER TWO

Geology of the Oman Ophiolite

2.1 Introduction

The Semail Nappe consists almost entirely of igneous rocks and is up to 14km thick. The igneous rocks present conform in both their composition and structure to the Penrose (1972) definition of an ophiolite (see Appendix 1.2). The main rock units in descending order are: a thin carapace of pelagic sediments overlying pillow lavas, a sheeted dyke section, plagiogranites and high-level gabbros, cumulate gabbros and peridotites with tectonised harzburgite containing dunite and chromitite at the base (see figs. 2.1 and 2.2). Due to the similarities in petrological and seismic properties with the rocks of present day ocean floors this sequence of rocks is generally thought to represent ancient oceanic lithosphere formed at a fossil constructive plate margin (see Appendix 1.2). The lowermost of the above-named units is, in the framework of the oceanic lithosphere model, assumed to be a fragment of the uppermost mantle and is commonly termed the 'mantle sequence' (Allen, 1975; Malpas, 1978; Smewing, 1980a), a term that will forthwith be used here.

The Mantle Sequence is the main concern of this thesis and will be described in terms of the petrography and geochemistry of its constituent rock types but first, to set the scene, this chapter contains a brief description of the field relations of the Oman ophiolite.

2.2 The Crustal Sequence

Ophiolite sediments:

These consist of pelagic, sometimes metalliferous, sediments which overlie and are intercalated with lava flows. The main lithologies are red haematitic shales, ferromanganoan mudstones (umbers) and grey laminated limestones which may be up to 20m in thickness (Fleet and Robertson, 1980). Radiolaria from these sediments give Cenomanian-Turonian ages (Tippet et al, 1981).

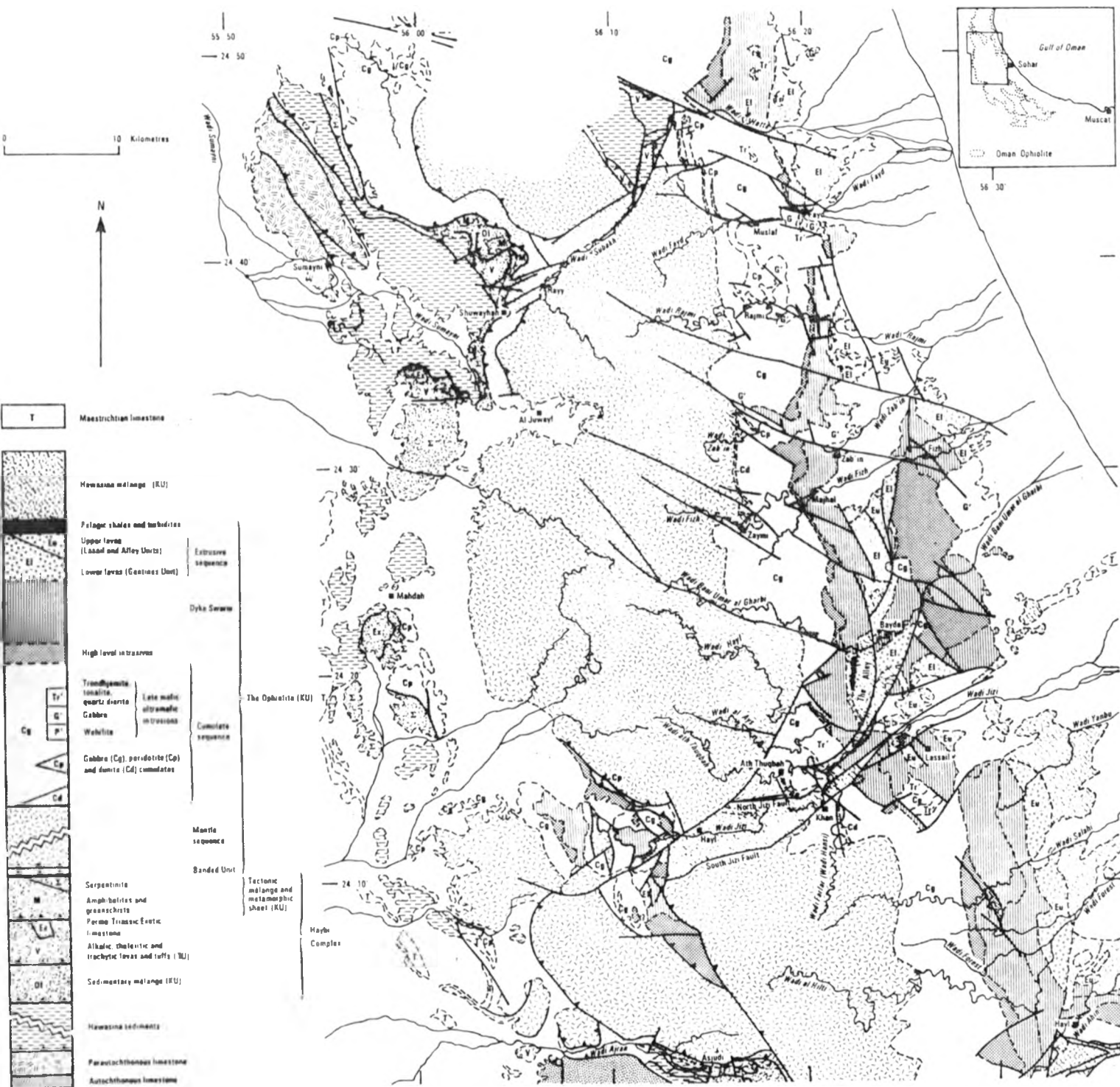


fig. 2.1 Geological map of the Oman ophiolite in the area of study for this thesis:- the Fijh block and the northern Salahi block

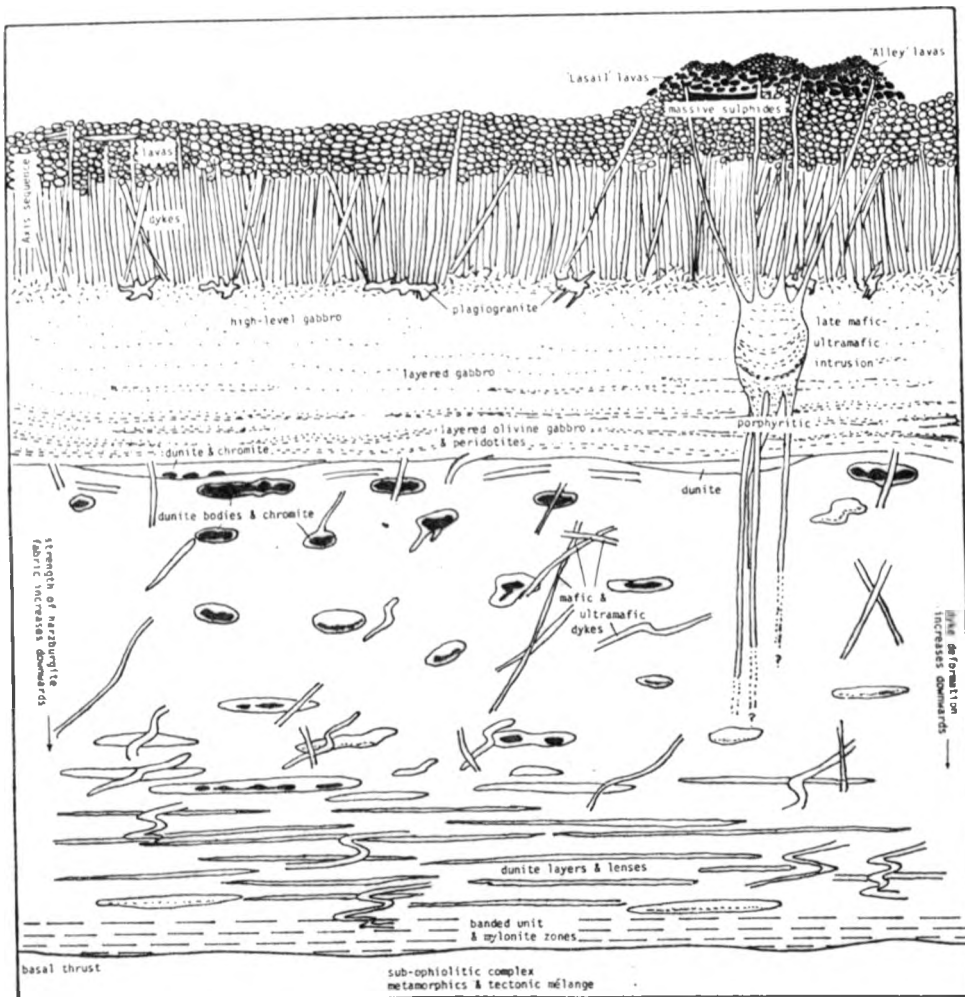


fig. 2.2 Diagrammatic cross-section through the stratigraphy of the Oman ophiolite

The extrusives :

The extrusive rocks are mostly pillowed but do include sheet flows, flow breccias and hyaloclastites and are intruded by dykes and sills. The extrusives are divided into 3 distinct division on the basis of primary and secondary mineralogies.

The lowermost unit, named the Geotimes Unit (Alabaster et al, 1980), is consistently present in the ophiolite sequence throughout Oman. It consists of interlayered pillows and structureless flows of aphyric basalt hydrothermally altered to greenschist facies. The pillows are large (1 - 2m), grey-brown, and poorly vesicular, whilst the sheet flows commonly show columnar jointing. Due to the gradational contact and similarity in composition and metamorphism of the Geotimes Unit with the underlying dyke swarm they are thought to be co-magmatic; both being part of the oceanic crust produced at a constructive plate margin.

In certain areas the Geotimes Unit is unconformably overlain by a series of lavas varying in composition from picrite basalts through basalts and andesites to rhyolites and obsidian. The stratigraphy of these lavas varies along the length of the ophiolite and discrete eruptive centres, about 20-30km apart, have been recognised by Alabaster et al (1980). Within these areas the upper lavas can be divided into two types: a lower unit, metamorphosed to greenschist facies which is termed the Lasail Unit after the type locality and an upper type, metamorphosed to zeolite facies, called the Alley Unit. Both units contain rock series from basalt to rhyolite but picrite basalt is restricted to the Alley Unit. Massive sulphide deposits can occur within these eruptive centres stratigraphically between the Geotimes Unit and Lasail Unit. An example of this can be seen at the type area for the latter unit where the largest known massive sulphide deposit in Oman is situated. Discordant mafic and ultramafic plutons and dykes occurring in the upper crustal levels of the ophiolite represent the magma chambers and feeder dykes associated with the upper lavas (fig.2.2).

The sheeted dyke complex :

The lowermost part of the Geotimes Unit contains basic dykes

which increase in abundance downwards until within 100-200m no lava is present. Most of the dykes are aphyric, greenish-grey in colour and composed of a greenschist facies metamorphic assemblage which has replaced but not destroyed original sub-ophitic basic igneous texture. No directional fabric is present. At the base of the sequence dykes have been metamorphosed under amphibolite facies conditions. The dykes may possess two, one or no chilled margins and are mostly aligned north-south throughout the northern part of the ophiolite but strike at 120° between Wadi Hatta and Wadi Zabin (see fig.2.1) in a possible transform fault zone (Smewing, 1980 (a)). The lower boundary of the sheeted dykes with the plutonic rocks beneath is also gradational. Due to the complex intrusive relationships of the high level plutonic series any member may appear subjacent to the dykes.

The high level intrusive assemblage:

This rock assemblage varies from a few metres to 200m thickness of a variety of lithologies: olivine and pyroxene gabbros with primary and secondary hornblende, ferrogabbros rich in magnetite, diorites, quartz diorites, tonalites and plagiogranites. The most abundant lithologies are the coarse grained plagiogranites and gabbros varying from microgabbro to pegmatitic varieties. The intermediate and acidic members of the assemblage tend to occur higher in the sequence. All rocks have been hydrothermally metamorphosed to upper greenschist/lower amphibolite facies. The mode of occurrence of the high level intrusives varies from diffuse patches a few metres across in host cumulate or dyke rocks to discrete intrusions which may reach 100m in thickness and a km. or so across. Xenoliths from the host dyke swarm are common and have undergone varying amounts of magmatic resorption. The lower boundary of the high level intrusives is also gradational. Here the underlying layered cumulate rocks merge upwards over a few metres into isotropic gabbros of the high level assemblage. The high level series rocks are commonly cross-cut by basaltic dykes which are rare in the underlying cumulates, suggesting that the high level intrusives formed at the roof of a magma chamber, possibly by underplating, whilst a melt precipitated cumulates below this roof and fed dykes and extrusives above it.

The cumulates:

The cumulates are comprised of a thick unit of gabbros and peridotites exhibiting phase layering, planar crystal orientation and intercumulus growth. The maximum thickness in the northern part of the ophiolite is about 3½km, but thicknesses of up to 6½km have been reported by Hopson and Pallister(1981) in the south. The cumulate phase layers generally have planar boundaries and mostly lack structures attributed to magma currents from steep magma chamber walls that are seen in many cumulate stratiform complexes. The most important texture is adcumulate suggesting a slow cumulate build-up, again contrasting with continental stratiform complexes where orthocumulates are more common being due to rapid build-up trapping intercumulus liquids. Cumulate layers are generally impersistent along strike such that sections through the cumulates vary considerably. Rhythmic repetition of sequences comprised of ultramafic cumulates (dunites, wehrlites and clinopyroxenites) followed by mafic cumulates (olivine gabbros and pyroxene gabbros) occurs within the cumulates with olivine persisting in basal layers to high levels. This implies that patterns of fractional crystallization of magma have been repeated for each unit.

Hydrothermal alteration is evident in the uppermost ½km of the cumulate sequence where gabbro is replaced by aggregates of hornblende, intermediate plagioclase, epidote and sulphides and, deeper in the cumulates, joints and fractures contain amphibolite assemblages (Smewing, 1980 (b)). The lower cumulates appear to be mainly free of hydrothermal alteration but δO^{18} data has shown that pervasive sub-solidus exchange with circulating sea-water has taken place to within 2km of the base of the cumulates (Gregory and Taylor, 1981).

The base of the cumulate sequence is a sharp contact where structures in the underlying mantle sequence are truncated. In other ophiolite complexes this contact has been termed the 'petrological moho', (e.g. Cann, 1969; Gass and Smewing, 1973; and Malpas, 1978), where it is envisaged that crustal magmatic rocks are underlain by rocks of the mantle sequence that are believed to be the solid residue from partial melting.

2.3 The Mantle Sequence

The rocks of the mantle sequence are composed of six primary solid solution minerals: olivine, orthopyroxene, clinopyroxene, chromite and more rarely plagioclase feldspar and amphibole. These primary phases have been altered to secondary assemblages of lizardite, chrysotile, antigorite, various iron oxides, amphiboles, chlorite and carbonates. Alteration is present in all samples and in some cases is total. The rocks are classified in terms of their primary mineralogies (Appendix 1).

The mantle sequence consists of 85-95% Harzburgite with associated minor cpx harzburgites and lherzolites and (15-5%) dunite which is gradational through chromitiferous dunite and olivine chromitite with chromitite which forms < 1%. These rocks are invariably coarse grained with maximum grain dimensions varying from 2mm to 50mm.

Harzburgite

The harzburgite is composed of olivine and orthopyroxene in approximately 80:20 proportions. Chromite is a constant accessory mineral varying from 0.5 to just over 1% of the mode and clinopyroxene may be present as up to 9% of the mode (see table 3.1), which makes the rock nominally a lherzolite.

In the field the harzburgite appears mainly brown due to weathering of olivine with conspicuous greenish grey orthopyroxene and black chromite. The weathering only persists a centimetre or two in from the surface and fresh harzburgite is dark green. Throughout the mantle sequence the harzburgite has a foliation defined by the planar orientation of orthopyroxenes and chromites (see plate 2.1). Mineral orientation may also define a lineation on the foliation surfaces. The foliation appears to increase in intensity downwards until at the base of the mantle sequence chromites are flattened in the plane of foliation.

Although the harzburgites are homogeneous on a gross scale a ratio segregation into more dunitic and more pyroxenitic layers is common. The layers are invariably parallel to the foliation and usually less than 3cm thick (plate 2.2). A different scale of harzburgite/dunite layering is prevalent in the lower part of the mantle sequence where layers are up

Plate 2.1 Foliation in harzburgite defined by planar orientation of orthopyroxenes and chromites.

Plate 2.2 Orthopyroxene rich segregation layers in harzburgite.

Plate 2.3 Harzburgite/dunite layering.

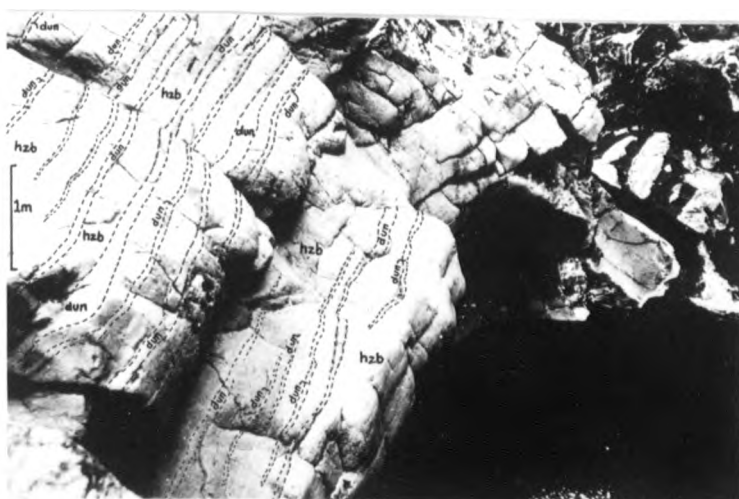
pl 2.1



pl 2.2



pl 2.3



to 30cm or so thick (plate 2.3). Where these two styles of layers occur together (plate 2.4) they are readily distinguishable.

As well as being interlayered with dunite, the harzburgite is also cross-cut by dunite bodies of various shapes and sizes, described in the following section.

Dunite

The dunite in the Oman mantle sequence consists almost entirely of olivine, now more or less altered to serpentine minerals with accessory chromite usually forming 1-2% of the mode. Chromite concentrations only occur within dunite. All gradations exist between dunite, chromitiferous dunite, olivine chromitite and chromitite. Clinopyroxene is occasionally present as oikocrysts enclosing olivine grains (plate 2.5). The weathering of dunite produces a smooth brown surface lacking the green tinge induced by orthopyroxene in harzburgites, and harzburgite and dunite are easily distinguishable when seen together. Chromite grains are conspicuous on weathered dunite surfaces. Various cross-cutting dunite bodies include lenses, dykes and more irregular shaped masses at least some of which interrupt the pervasive harzburgite foliation. Their regularity and concordance with the metamorphic fabric of the host harzburgite increases downwards through the sequence.

In the uppermost part of the mantle sequence dunite bodies may be very irregular anastomosing through and apparently enclosing blocks of the harzburgite (plate 2.6), and have been described by Neary and Brown (1979) as an 'irregular mix'. Straight sided dykes of dunite up to 30cm thick and discordant to the foliation also occur in the upper parts of the sequence (plate 2.7). Harzburgite bordering these dykes is often enriched in orthopyroxene (plate 2.8). In the middle parts of the sequence where the foliation is more intense and harzburgite/dunite layers are more common, irregular and anastomosing dykes of dunite often occur cross cutting the layers and the foliation (plate 2.9). Throughout the mantle sequence lenses of dunite occur varying in size from a metre or so to 500m long. They all bear concentrations of chromite invariably parallel to the long axis of the lens and varying from single grain layers to massive seams of chromitite. The grains of chromite in the dunite lenses are generally larger than accessory

Plate 2.4 Harzburgite/dunite layering and orthopyroxene rich segregation layers.

Plate 2.5 Oikocryst of clinopyroxene in dunite layer. Layering is parallel but clinopyroxene crystal is discordant to the foliation in the enclosing harzburgite.

Plate 2.6 Irregular mix of harzburgite and dunite. Dunite bodies anastomose through and often enclose blocks of harzburgite.

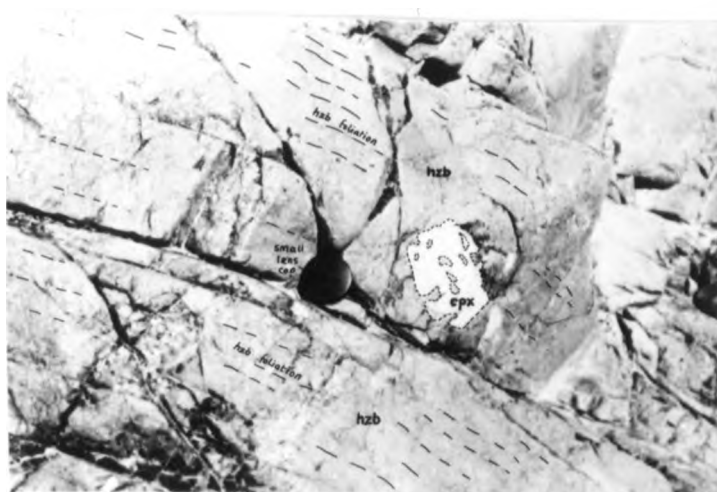
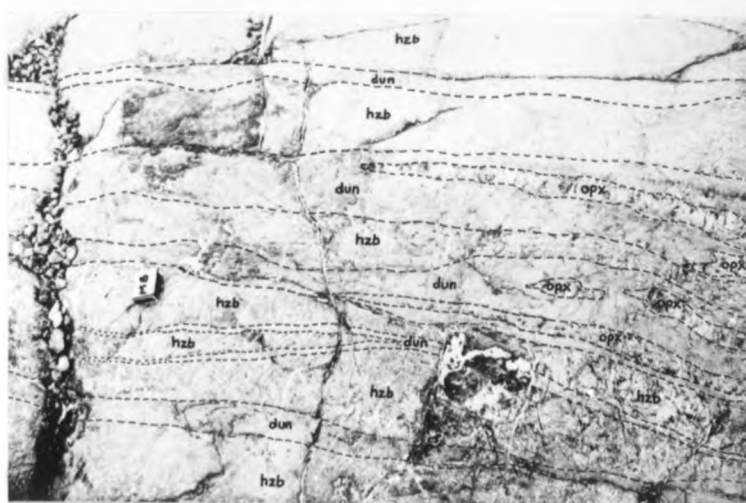


Plate 2.7 Straight, sharp sided dyke of dunite discordant to the foliation in the host harzburgite.

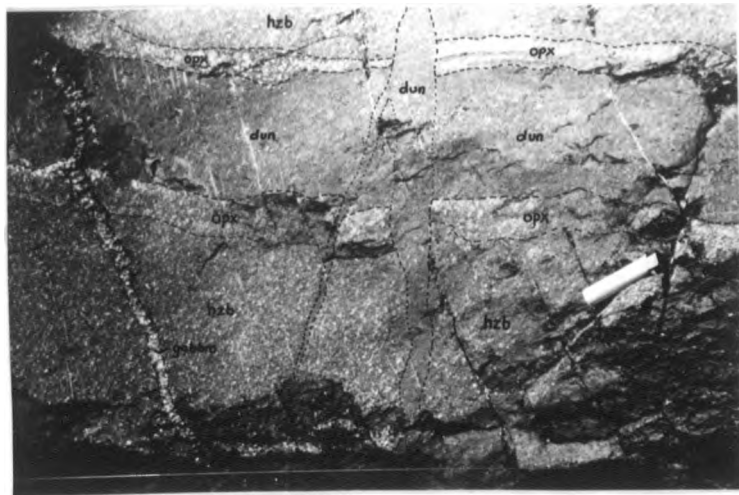
Plate 2.8 Orthopyroxene enriched harzburgite adjacent to the margin of a dunite dyke. Both dunite dyke and orthopyroxene segregations are cut by a later dunite dyke.

Plate 2.9 Harzburgite/dunite layering (dunite I) cross-cut by irregular anastamosing dunite dykes (dunite II).

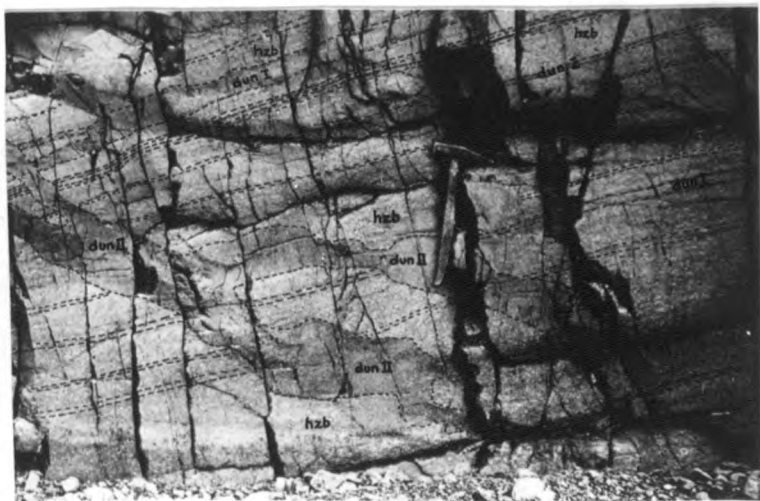
pl 2.7



pl 2.8



pl 2.9



chromites in surrounding harzburgite. One of the largest dunite lenses found so far is the Sudi dunite body (plate 2.10) situated close to the base of the ophiolite near al Juwayf (Appendix 2) and containing several chromite concentrations consisting of olivine chromitite and chromitite layers up to 5cm thick that display occluded silicate and chromite net textures (Thayer 1969, and table 7.7 this thesis). Chromitite sometimes occurs within dunite inter-layered with harzburgite (plate 2.11) where it often forms strings of isolated pods a few centimetres long rather than a continuous layer as in the dunite lenses.

Chromitite

Chromitites consist of over 90% chromite with interstitial silicates; usually olivine or its alteration products but clino- & orthopyroxene, amphibole and plagioclase feldspar also occur. Chromitites appear black to brown on weathered surfaces. The brown colouration is due to 'desert varnish', a very thin coat of secondary iron oxides, and obscures colour differences between rock types in all places except water-worn surfaces.

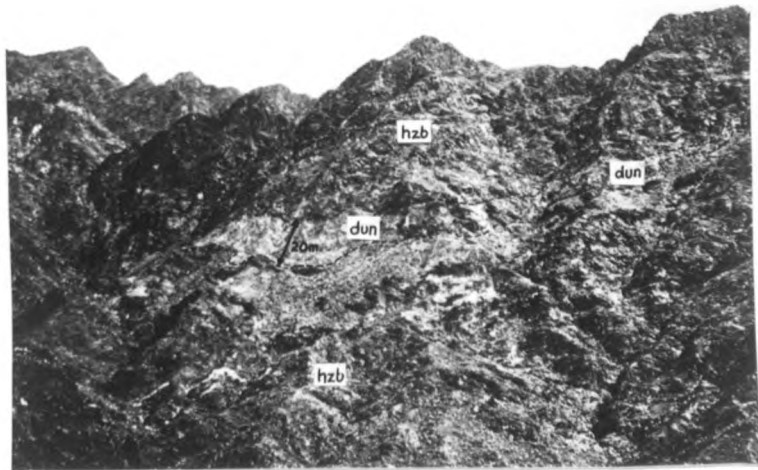
As described above, chromite grains are sometimes concentrated in dunite bodies and all gradations between pure dunite and nearly pure chromitite occur. Chromitite bodies show a large variation in size and form. In the lower part of the mantle sequence they are of limited size (c.f. the centimetre scale layers in the Sudi dunite, and the pods in dunite layers: plate 2.11). Larger pods than those in plate 2.11 do occur in dunite layers (e.g. in Wadi Rayy, plate 2.12) and the size of chromitite bodies increases up through the sequence until individual pods may reach up to 15m in thickness and 40-50m long. Also chromitite-rich zones consisting of groups of pods can be 500m across. The largest known such zone or deposit of chromite in Oman is the Maharah 1 deposit in the Wadi Rajmi district (plate 2.13). The deposit is composed of pods resembling the shape of the small chromitite pods of Wadi Rayy (plate 2.12). The large pods of the Maharah 1 deposit and many similar, smaller, deposits consist of olivine chromitite or 'massive' chromitite with little or no silicate matrix. These are inevitably surrounded by an envelope or halo of dunite varying from a few centimetres to a few metres thick but not necessarily related to the size of the chromitite body.

Plate 2.10 Sudi dunite body orientated along the plane of the strong harzburgite foliation near the base of the Semail Nappe near Al Juwayf.

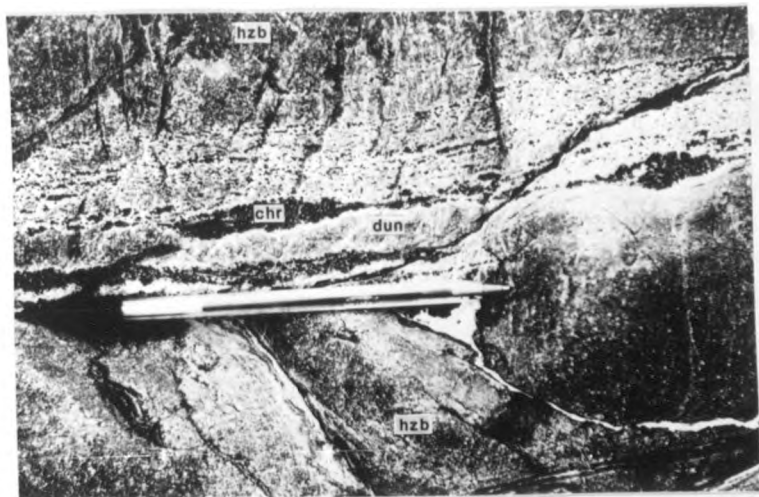
Plate 2.11 Chromitite layers and small 'pods' in a dunite layer. All layering is parallel to the foliation in the enclosing harzburgite.

Plate 2.12 Pods and layers of massive chromitite in a dunite layer. Layers are parallel to the foliation in the enclosing harzburgite.

pl 2.10



pl 2.11



pl 2.12



Shearing is common between the chromitite pods and their dunite hosts and the pods often have marginal serpentine filled shear zones a few centimetres across. The dunite envelopes surrounding the chromitite pods often contain small centimetre scale layers and lenses of chromitite which suggest that prior to the formation of the marginal shears the chromitite pods interdigitated with their dunite hosts. Some of the layers can still be traced back into the pods where marginal shearing is less intense.

In the Farfar 2 chromite deposit (Appendix 2) just beneath the cumulate sequence, cross laminations of fine chromitite and dunite layers can be seen between a large chromitite layer above and a dunite layer below (plate 2.14), and at the base of the upper chromitite are structures resembling load casts where dome-like protrusions of dunite extend up into the chromitite with flame-like downward extensions of chromitite around their margins (plate 2.15). Much lower in the sequence in Wadi Al Ainah (plate 2.16) all gradations from dunite to chromitite are displayed in one exposure as well as occluded silicate texture and ovoid aggregates of chromite grains which may be an incipient nodular texture and in Wadi Rajmi (locality - Appendix 2) graded bedding of chromite crystals and 'harrisitic' growth of olivine can be observed (plate 2.17).

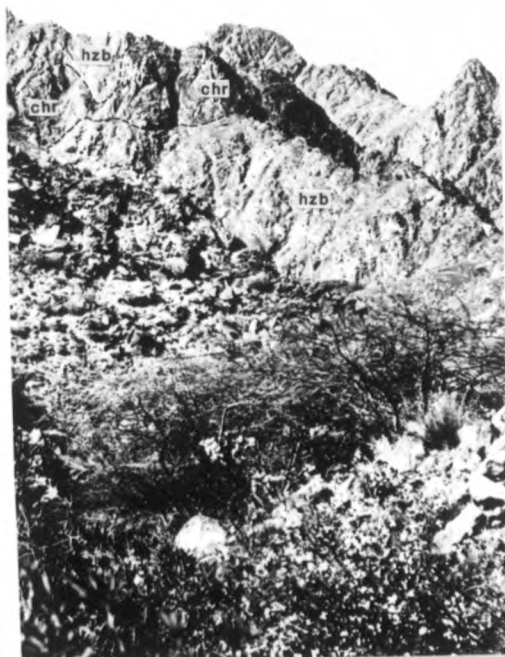
The Mantle Sequence Upper Boundary or 'Petrologic Moho'

The contact between the tectonized ultramafic rocks and the overlying layered mafic or ultramafic rocks of the cumulate sequence is here termed the petrological moho. No chilled margins have been observed along this contact and xenoliths of mantle sequence rocks are common in the lowermost part of the cumulates where they interrupt the cumulate layering. The type of cumulate directly overlying the mantle sequence varies laterally. In many places plagioclase-bearing rocks lie directly above the mantle sequence. A typical example is at Rajmi in Wadi Maharrah (Appendix 2) where cumulate gabbros overlie tectonite harzburgite. Here shearing at the contact has introduced a strong lineation into the cumulate layering. Also in this area gabbro sills 2 - 3 metres thick, bearing layers apparently similar to those in the cumulates, lie parallel to the moho about 10m below it and small gabbro dykes 5cm or so thick cut through the mantle sequence and moho and then become less distinct as they merge into gabbro cumulates (plate 2.18). Commonly, brecciation of the harzburgite has taken place at the moho

Plate 2.13 Large pods of massive chromitite in the largest known deposit, Maharah 1, near Rajmi. Photo is taken from about 0.5 km away

Plate 2.14 Cross-laminations of fine chromitite and dunite layers between a chromitite layer above and a dunite layer below. Farfar 2 chromite deposit

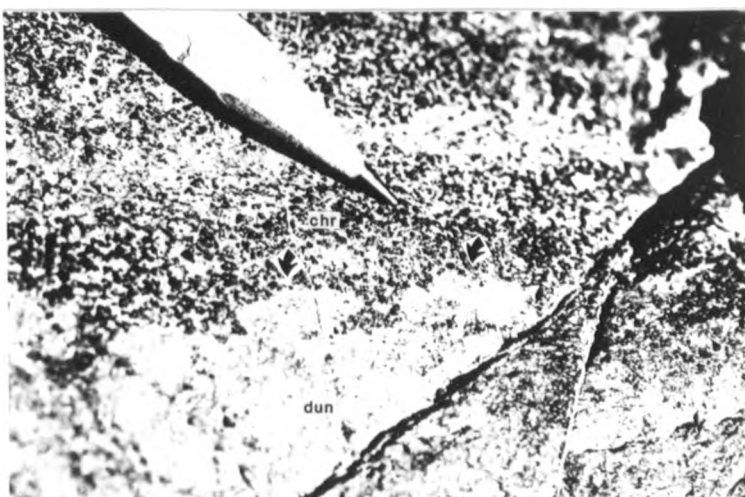
Plate 2.15 Possible load structures in the Farfar 2 chromite deposit. Dome-like protrusions of dunite extend up into an overlying chromitite layer



pl 2.13



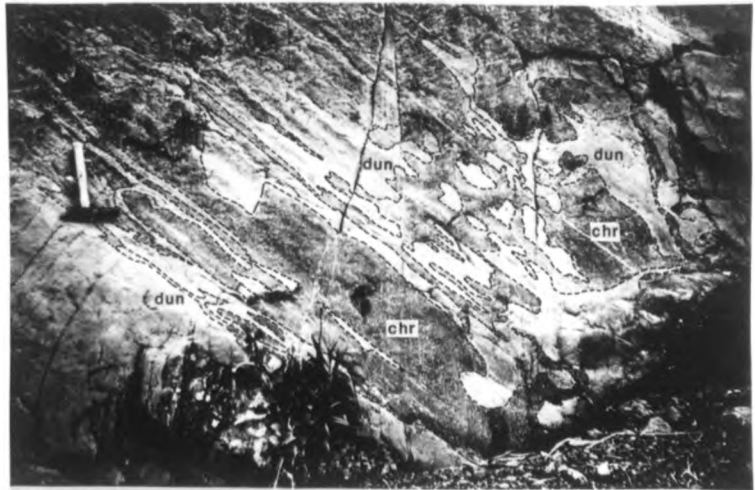
pl 2.14



pl 2.15

- Plate 2.16 Chromite deposit in Wadi Al Ainah composed of discontinuous layering of chromitite and dunite with large volumes of dunite occluded in chromitite. Deposit also exhibits gradational margins between dunite and chromitite, fine occluded silicate structure and cluster texture, described in Chapter 4.
- Plate 2.17 Harrisitic olivines: large tooth-like crystals of olivine protrude from a dunite layer into an irregular chromitite layer.
- Plate 2.18 The Mantle Sequence-Cumulate Sequence boundary or petrological mocho. A small dyke of gabbro cuts the Mantle Sequence harzburgite and merges into the gabbro layer above the 'mocho'.

pl 2.16



pl 2.17



pl 2.18



and invasion by gabbro has produced a net veined system (plate 2.19).

In other areas (e.g. Farfar and Ath Thuqbah: see Appendix 2) up to 100m of ultramafic rocks, dominantly dunite with interlayered cpx-dunite and wehrlite, form the basal cumulate layer (plate 2.20). In many cases these basal dunite layers are lensoid and appear to occupy depressions in the surface of the underlying harzburgite.

Mantle Sequence Lower Boundary: Base of the Semail Nappe

The mantle sequence is underlain, across a thrust contact, by the Haybi Complex (Searle, 1980) the uppermost unit of which is a locally developed tectonic *mélange* of pervasively foliated blocks or slices of amphibolites and greenschists in a matrix of serpentine. In places where the tectonic *mélange* is fully developed, upper amphibolite facies rocks occur directly beneath the ophiolite and metamorphic rocks of progressively lower grade are found at successively lower levels. Where the *mélange* is not developed the ophiolite directly overlies the 'Exotic' limestones and Haybi volcanic rocks. A full sequence from ophiolite down across the thrust contact, through the tectonic *mélange* and into the Haybi volcanics and limestone exotic blocks is illustrated in plate 2.21.

The lowermost 50-100m of the mantle sequence consists of harzburgites and dunites often separated by cataclastic or mylonitic shear zones that are parallel to the base of the nappe. Dunites and harzburgites are interlayered on centimetre and larger scales. As with the mylonite zones this layering is parallel to the thrust contact and gives the zone a conspicuous striped appearance. Searle (1980) terms this the Banded Unit (plate 2.22).

2.4 Mafic and Ultramafic Dykes

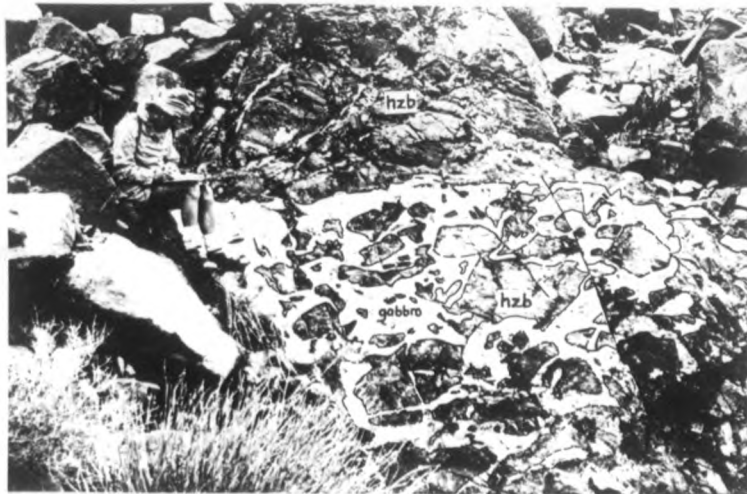
The mantle sequence is cross-cut by numerous dykes with sharp unchilled margins. The dykes have varied primary mineral assemblages consisting of combinations of one, two or three phases from olivine, orthopyroxene, clinopyroxene, plagioclase feldspar and hornblende with chromite or chromian spinel sometimes present as an accessory mineral. Plagioclase is absent from dykes at the base of the sequence but becomes more abundant upwards through the sequence. In the upper and

Plate 2.19 Brecciated harzburgite at the Mantle Sequence-Cumulate Sequence boundary with net veining of gabbro.

Plate 2.20 Basal layer of 'cumulate' dunite above the Mantle Sequence-Cumulate Sequence boundary or 'petrological moho'.

Plate 2.21 Base of the Semail Nappe passing down from mylonitised harzburgite (Banded Unit) in the east, through a tectonic mélangé with a serpentine matrix, into the Haybi Complex containing large blocks of 'exotic' limestone and volcanic rocks in the west. All units are bounded by thrust faults.

pl 2.19



pl 2.20



W

E

pl 2.21

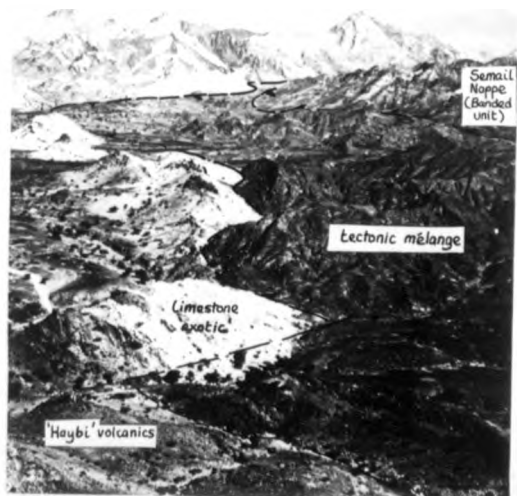


Plate 2.22 The Banded Unit: interlayered dunite and harzburgite containing mylonite zones at the base of the Semail Nappe.

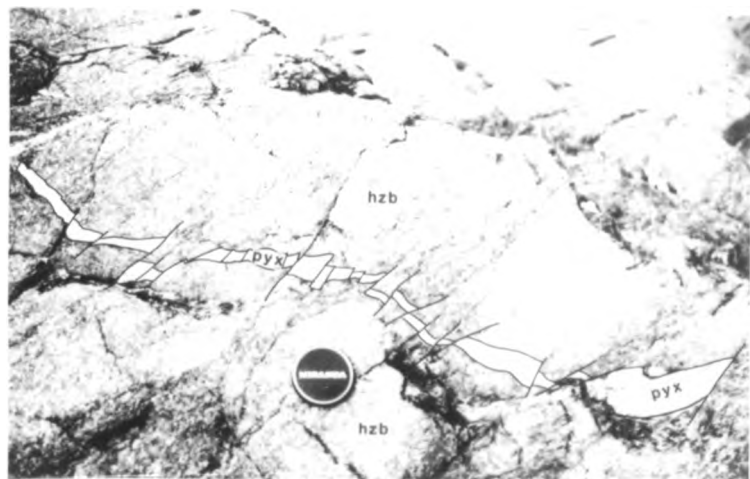
Plate 2.23 Small dyke of pyroxenite in harzburgite fragmented by brittle fracture.

Plate 2.24 Pyroxenite dyke in harzburgite showing ptygmatic folding with extreme thickening of fold noses and attenuation of fold limbs.

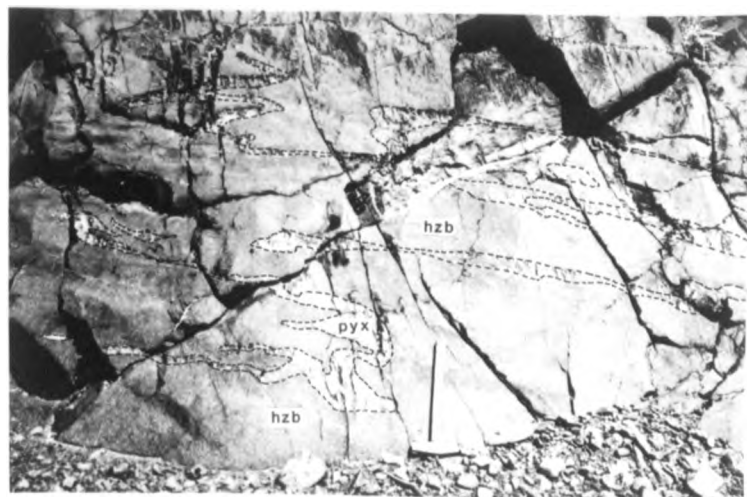
pl 2.22



pl 2.23



pl 2.24



middle parts of the sequence the dykes are straight sided, truncate all mantle sequence rocks and are only affected by later brittle deformation (plate 2.23). Deformation of the dykes increases in towards the base of the sequence and in the lowermost 2-3km dykes are folded, often ptgmatitically (plate 2.24) or almost isoclinally and may be boudinaged (plate 2.25).

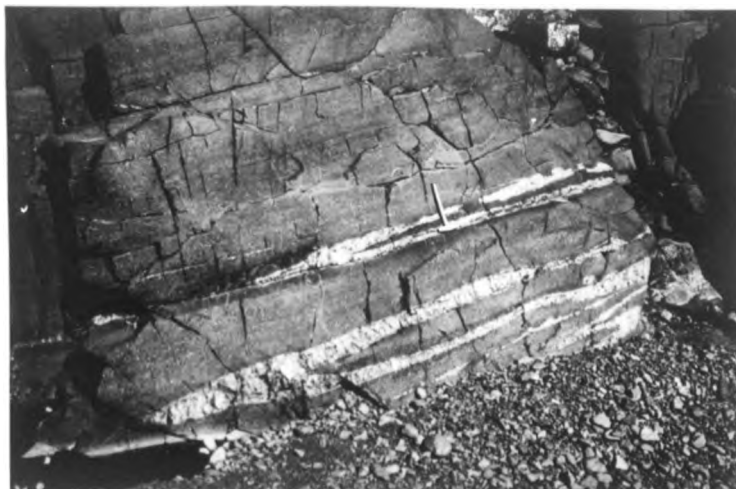
Ultramafic dykes are found mainly in the lower and middle parts of the sequence although they do occur throughout. They are usually between 5 and 30cm wide, the main rock types being coarse grained (< 6cm) orthopyroxenite, websterite and olivine websterite, and fine grained prophyritic picrite.

Mafic dykes are restricted to the middle and upper parts of the mantle sequence and are also common intrusions in the cumulate sequence. They are usually between 5 and 50cm thick, their grain size varies from micro-gabbroic to pegmatitic and composition from olivine gabbros and troctolites, through one and two pyroxene to hornblende gabbros. In some cases multiple intrusion has occurred with later usually more feldspathic dykes intruded either down the centre or at one margin of the previous dyke (plate 2.26).

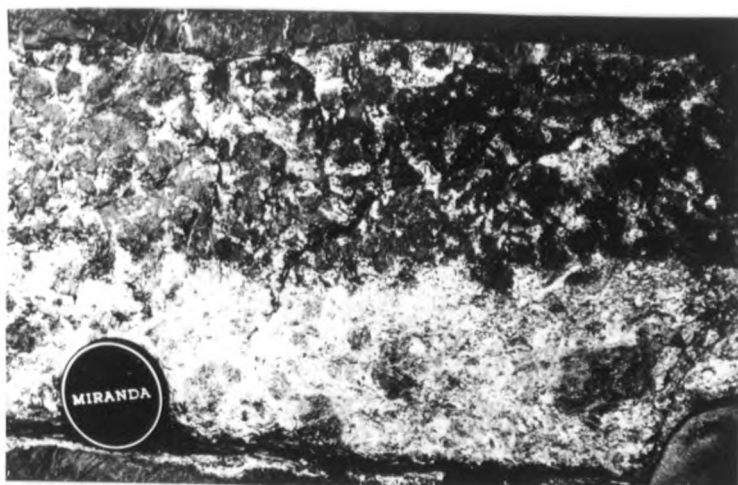
Some mafic dykes possess a planar phase layering parallel to their margins (plate 2.27) very similar in appearance to phase layering in the cumulate sequence. Coarse grained (< 4mm) irregular leucocratic patches composed mainly of feldspar cross-cut the layering within the dykes but do not cross the margins of the dyke. Comb textures are common in the mafic dykes, especially in the coarse pegmatitic varieties, where crystals of hornblende up to 3cm long have grown inwards from the dyke margins.

- Plate 2.25 Tight almost isoclinal folding of pyroxenite dykes showing fold axes parallel with harzburgite foliation and extreme attenuation/boudinage of fold limbs.
- Plate 2.26 Compound dyke composed of coarse grained troctolite (upper part) and leucocratic gabbro containing large diopside phenocrysts (lower part).
- Plate 2.27 Layered dyke cutting harzburgite. Dyke layers are mostly parallel to margins varying from troctolite, through gabbro, to anorthosite. An irregular coarser grained lens of leucogabbro cross-cuts dyke layers but not dyke margins.

pl 2.25



pl 2.26



pl 2.27



CHAPTER THREE

Harzburgite

3.1 Introduction

Harzburgites form 80 to 95% of the Oman mantle sequence and consist mainly of olivine and orthopyroxene in the ratio of about 80:20 although considerable variations may occur due to the ratio phase layering illustrated in plate 2.2. Chromite occurs as a constant accessory at 0.5 to 1% and clinopyroxene may be present forming up to 9% of the mode. Two samples out of 80 studied contain over 5% clinopyroxene and are strictly lherzolites. Modal analyses of 15 harzburgite and 2 lherzolite samples are presented in table 3.1. All mineral phases in the Oman harzburgite have suffered alteration to some degree. The primary phases are described in sections 3.2 to 3.4 inclusive. The optical and chemical properties of their alteration products are described in chapter 6.

3.2 Mineral optical properties

Olivine

All olivine in the Oman harzburgite is highly magnesian and optically positive (i.e. $> \text{Fo}_{87}$). Recrystallization is common with two grain types present: i) Porphyroclasts*, or relict original grains (plate 3.1) are large (up to 10mm), irregularly shaped, with curved or serrated boundaries where they interlock with surrounding grains. They are often elongate with length/width ratios of up to 7/1 and long axes mutually parallel. Extinction of porphyroclasts is undulose indicating that lattice strain has taken place. Subgrains and deformation lamellae parallel to (100) are sometimes present giving grains a patchy or striped appearance in cross polarised light, (plates 3.2 and 3.3). ii) Neoblasts*, or recrystallized grains (plate 3.4) of olivine are smaller than the porphyroclasts, usually in the range 0.1 to 1.0mm, and have straight to curvi-linear margins with equant polygonal shapes and triple points between grains with 120° margin intersections. The grains have normal extinction and lack sub-grains or internal deformation structures.

* For explanation of the use of these terms see appendix 1.1

HARZBURGITES									
Sample No.		2320	2342	4063	4065	4048	4064A	4080A	4165
Modal %	Olivine	74.4	92.6	80.3	78.1	68.4	65.9	87.1	80.6
	Enstatite	24.4	6.9	19.2	18.4	30.1	32.9	12.4	18.9
	Diopside	0.2	-	-	0.8	1.2	-	-	-
	Chromite	1.0	0.5	0.5	2.7	0.3	1.2	0.5	0.4

HARZBURGITES									AVERAGE HZB.MODE
Sample No.		4167	6609	6616	6622	4075A	4136	4091A	
Modal %	Olivine	89.5	86.7	83.3	76.3	68.0	84.8	84.3	80.0
	Enstatite	8.9	12.8	16.1	22.1	31.5	14.1	14.7	18.9
	Diopside	0.1	-	-	1.3	-	-	-	0.2
	Chromite	1.5	0.5	0.6	0.3	0.5	1.1	1.0	0.9

LHERZOLITES			
Sample No.		4032A	2315
Modal %	Olivine	63.7	76.0
	Enstatite	29.0	14.9
	Diopside	5.4	8.8
	Chromite	1.8	0.3

Table 3.1 Harzburgite and lherzolites modal analyses
(1000 counts)

Plate 3.1 Porphyroclast of olivine with irregular
embayed margins.

XPL
fov = 3mm

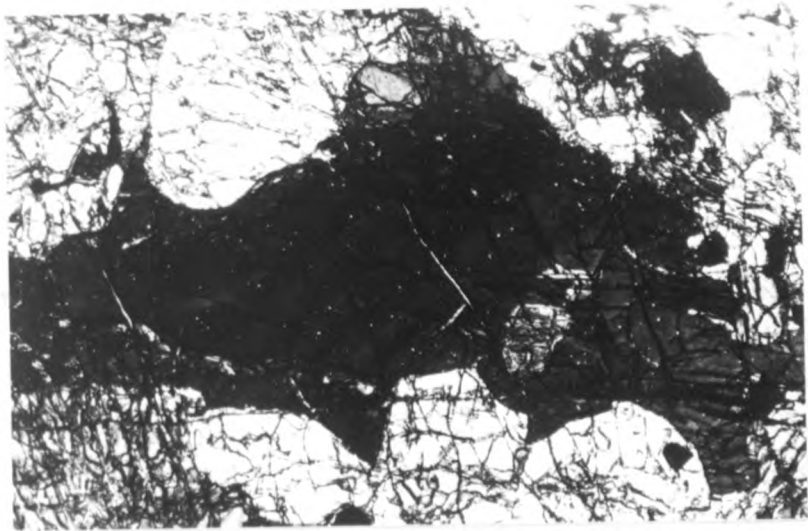
Plate 3.2 Porphyroclast of olivine showing
patchy extinction. Grain is crossed
by veins of lizardite.

XPL
fov = 3mm

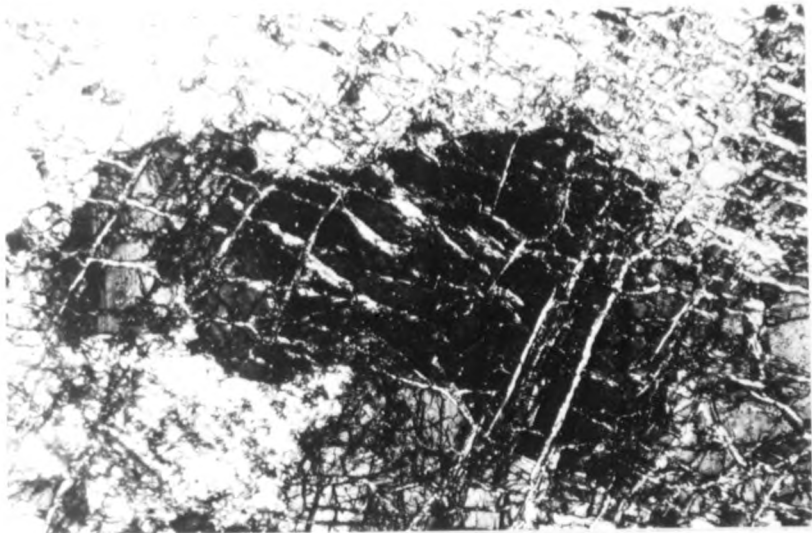
Plate 3.3 Porphyroclast of olivine with striped
extinction due to deformation lamellae
parallel to (100). Grain is crossed
by veins of lizardite.

XPL
fov = 3mm

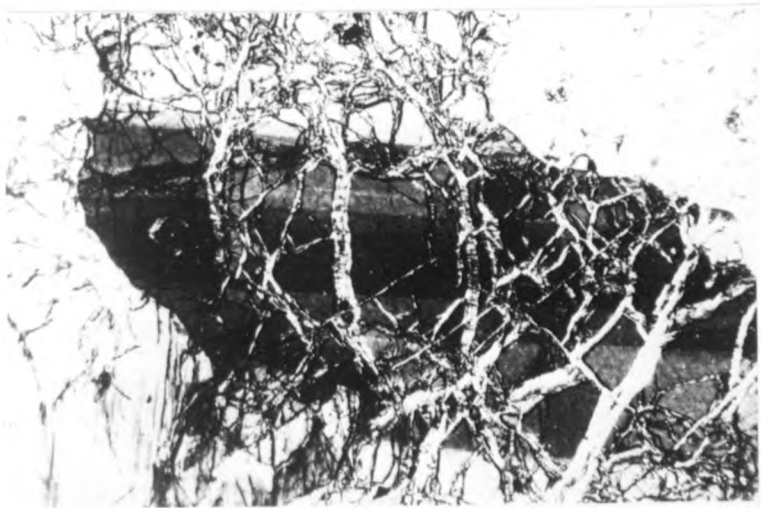
pl 3.1



pl 3.2



pl 3.3



Orthopyroxene

All orthopyroxene in the Oman harzburgite is enstatite. It is colourless, non-pleochroic and has straight extinction, high relief and an optically positive interference figure with a large axial angle. Like olivine, some enstatite grains have been recrystallised and two grain types can be distinguished. i) Porphyroclasts of enstatite are large (up to 12mm) and may be tabulate (plate 3.5), elongate (plate 3.6), irregular or 'retort shaped' (Basu 1977, see plate 3.7 and fig. 3.1). Porphyroclast grain boundaries are both curved and serrated, the latter having interlocking projections with olivine porphyroclasts. Cleavage in orthopyroxene porphyroclasts is often distinctly curved and extinction is undulose (see plate 3.5). Sub-grains are often present, sometimes divided by kink-bands across which the cleavage of the sub-grains change in orientation (see plate 3.8). Clinopyroxene exsolution lamellae, as thin parallel sided sheets or flattened blebs parallel to 100, are ubiquitous in enstatite porphyroclasts. The parallel sided lamellae are always deformed and can be curved or kinked (plate 3.9). Most of the blobs also are deformed but some appear to transgress deformation features such as kink-bands and therefore are post-deformational (plate 3.10). ii) Neoblasts of enstatite (plate 3.11) occur in clusters as straight sided polygonal grains with 120° margin intersections. They are smaller than the porphyroclasts and are usually 1-2mm across with straight cleavage, normal extinction, and no exsolution lamellae.

Clinopyroxene

Clinopyroxene in the Oman harzburgite occurs as rare, ragged sub to anhedral grains (up to 2mm) often with orthopyroxene exsolution lamellae. Strain features are similar to those in orthopyroxene with curved cleavages, exsolution lamellae and undulose extinction. Recrystallisation of clinopyroxene porphyroclasts is evident in some specimens where they are replaced by aggregates of small (up to 5mm) straight sided, strain free grains.

Chromite

Chromite occurs as small (< 1mm) grains in the Oman harzburgite,

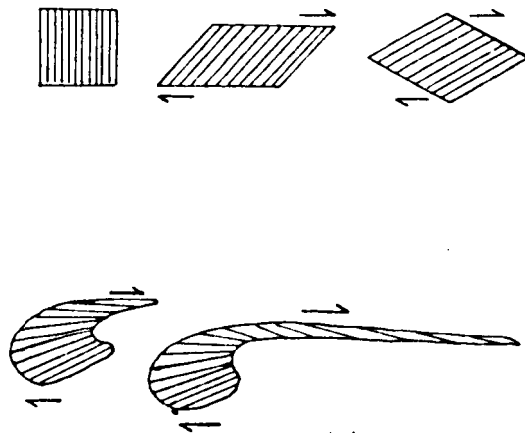


fig. 3.1 Development of retort shape
in orthopyroxene by a simple
shear model
(from Basu, 1977)

Plate 3.4 Straight sided, unstrained neoblasts of olivine. 120° grain triple boundaries are common. Grains have been altered marginally to lizardite.

XPL

fov = 3mm

Plate 3.5 Tabulate porphyroclast of enstatite with curved exsolution lamellae of diopside.

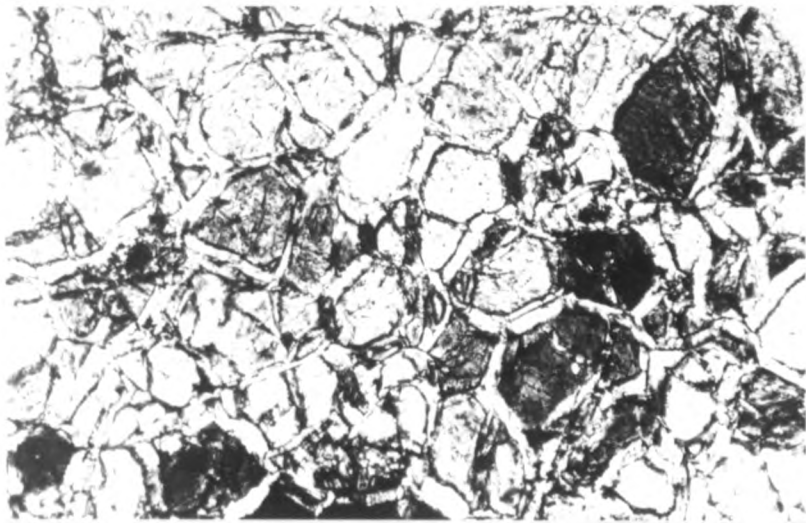
XPL

fov = 3mm

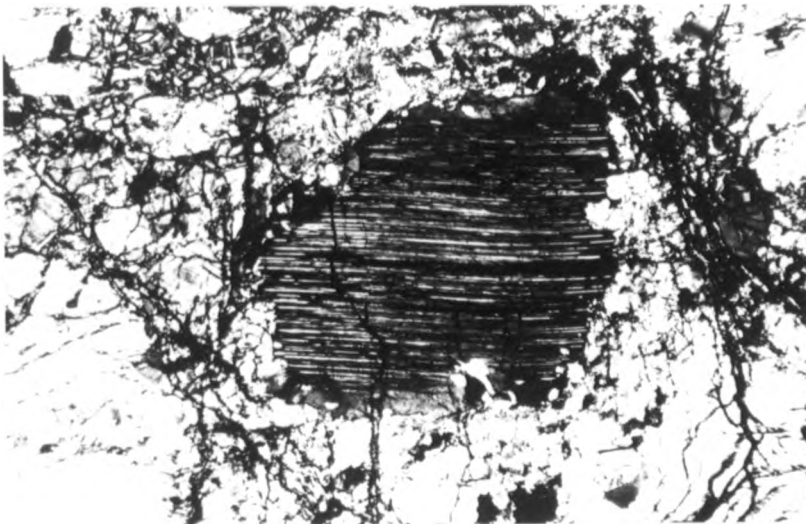
Plate 3.6 Elongate porphyroclast of enstatite with curved and kinked exsolution lamellae of diopside

XPL

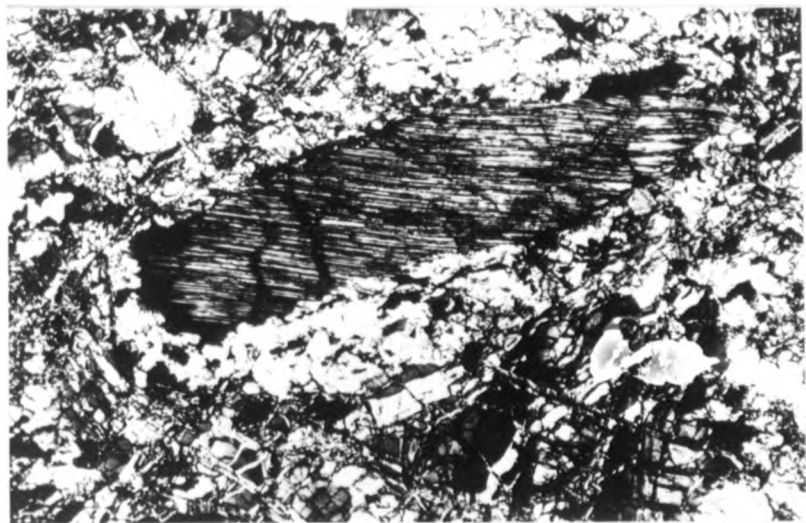
fov = 3mm



pl 3.4



pl 3.5



pl 3.6

Plate 3.7 Retort shaped porphyroclast of
 enstatite with kink band affecting
 diopside exsolution lamellae and cleavage.
 Exsolution blebs of diopside are located at
 kink-band boundaries

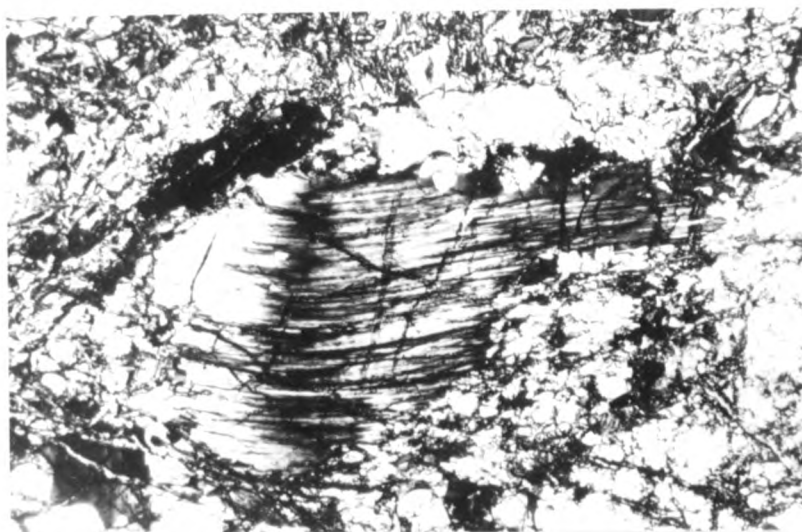
XPL
fov = 3mm

Plate 3.8 Kink band in enstatite porphyroclast
 showing deflection of cleavage.

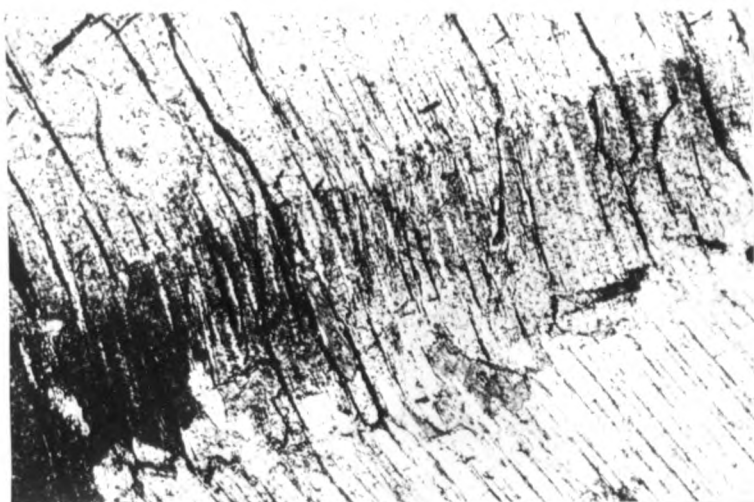
XPL
fov = 1mm

Plate 3.9 Exsolution lamellae of diopside curved
 across a subgrain boundary in an
 enstatite porphyroclast.

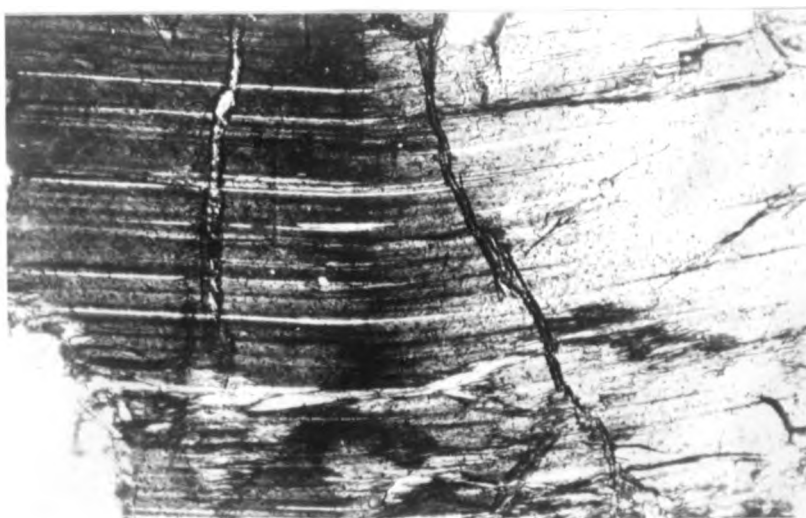
XPL
fov = 1mm



pl 3.7



pl 3.8



pl 3.9

Plate 3.10 Exsolution blebs of diopside cross-cutting a kink band at subgrain margin in enstatite porphyroclast.

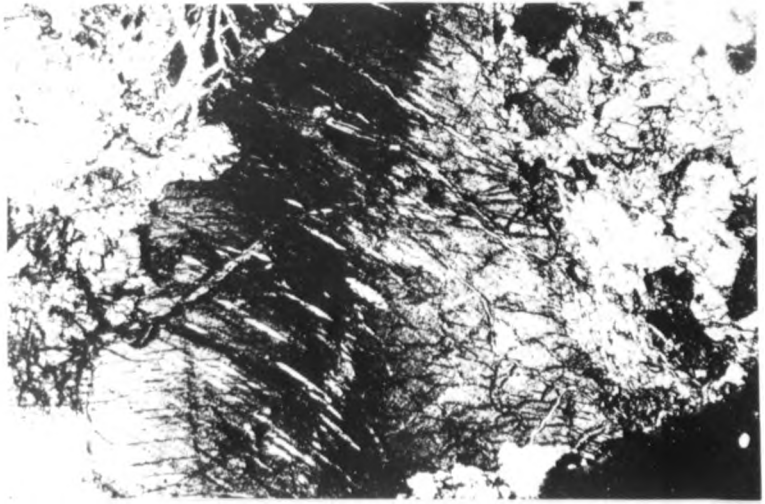
XPL
fov = 3mm

Plate 3.11 Neoblasts of unstrained enstatite with straight sides and frequent 120° triple grain boundaries.

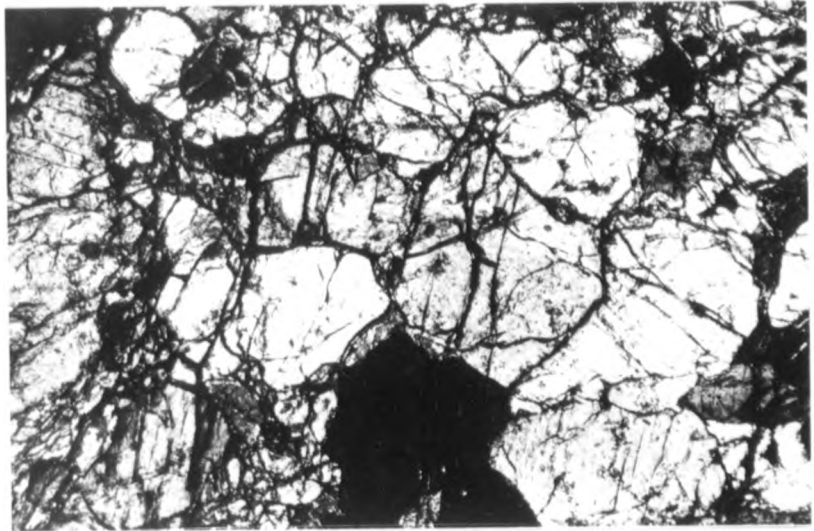
XPL
fov = 3mm

Plate 3.12 'Graphic' exsolved chromite in grain of enstatite.

PPL
fov = 3mm



pl 3.10



pl 3.11



pl 3.12

and varies in colour (in plane polarised light) from deep red in clinopyroxene-free harzburgites to straw yellow in cpx-harzburgites and lherzolite. The chromite grains occur in three main habits: i) exsolved lamellae in enstatite (plate 3.12), ii) sub to anhedral, sometimes vermicular, grains at enstatite/olivine grain contacts often with olivine and enstatite inclusions (plate 3.13), iii) sub to anhedral grains in linear strings sub-parallel to long axes of enstatite and olivine grains, i.e. the tectonic fabric of the harzburgite (plate 3.14). These chromite grains may be 'tadpole-shaped' (Talkington and Malpas, 1980) possessing tail-like extensions (plate 3.15) or 'holly-leaf' type (Mercier and Nicolas, 1975, see plate 3.16).

Chromite grains in the Oman harzburgite show evidence of brittle fracture, most prominently as sets of "pull-apart" cracks (Thayer, 1960) (plate 3.17) and secondly as slivers of chromite which appear to have been separated from the margins of grains (plate 3.18).

3.3 Rock textures

The main textural elements in the Oman harzburgite are summarised in fig. 3.2. These are schematic drawings not taken from any particular rock samples and elements A, B and C can be recognised in most sections.

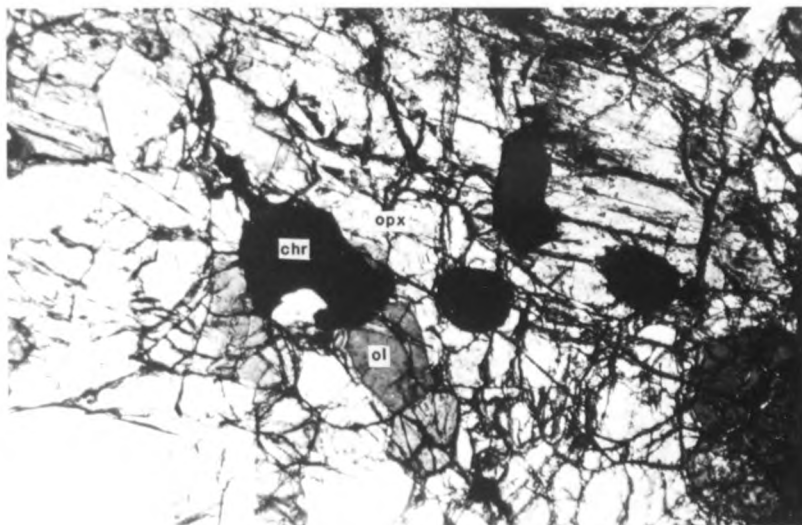
Type 'A' in fig. 3.2 is characterised by lobate and cusped grain boundaries which are thought to be due to resorption or dissolution-reprecipitation creep (Spry, 1969). The latter process could be facilitated by melt present during deformation acting as a medium for dissolution at the pressure points formed by impinging grain boundaries and for re-precipitation in areas where grains do not impinge (Dick, 1977). Type 'A' therefore could be interpreted as a partial melting texture.

Type 'B' in fig. 3.2 is dominated by elongate, mutually sub-parallel, porphyroclasts of olivine with sub-grains, orthopyroxene with curved cleavages, exsolution lamellae and blebs in cleavage and kink-bands and chromite aligned in the foliation at olivine intergranular

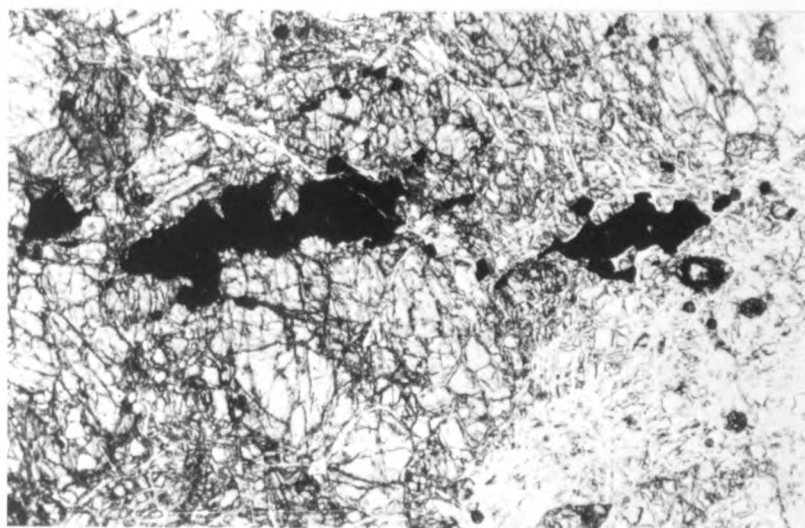
Plate 3.13 Subhedral rounded chromite grains
 at enstatite/olivine grain boundary
 XPL
 fov = 2mm

Plate 3.14 Linear string of anhedral chromite
 grains in strongly foliated (highly
 altered) harzburgite.
 PPL
 fov = 6mm

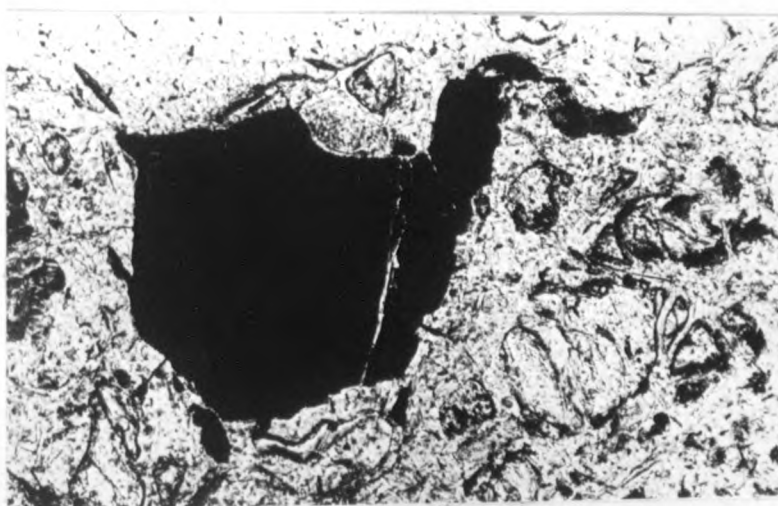
Plate 3.15 Tadpole shaped chromite porphyroclast.
 PPL
 fov = 2mm



pl 3.13



pl 3.14



pl 3.15

Plate 3.16 Holly leaf shaped chromite porphyroclast.

PPL

fov = 2mm

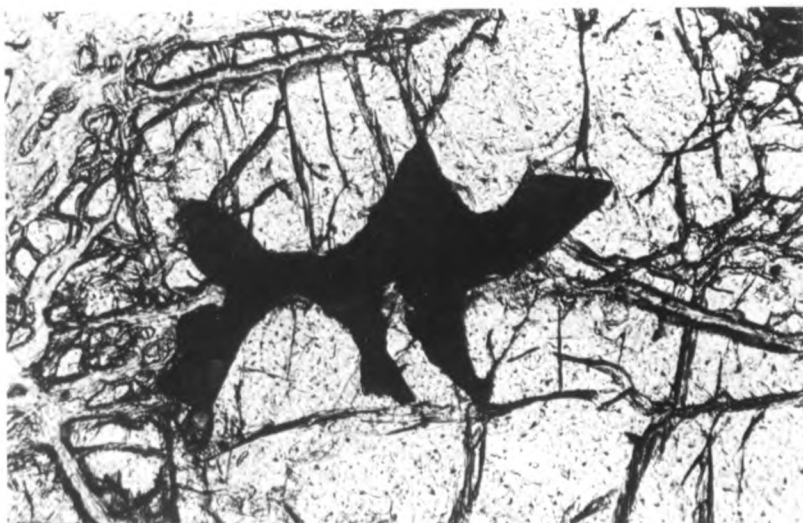
Plate 3.17 Chromite grain crossed by 'pull-apart' cracks.

PPL

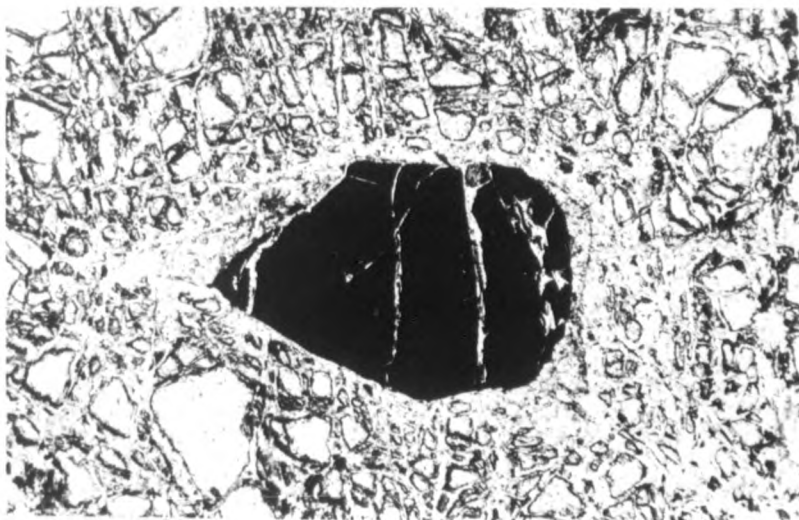
fov = 2mm

Plate 3.18 Chromite grains with 'pull-apart' crack (LH grain) and marginal sliver (arrowed) separated from (RH) chromite grain in serpentine filled fracture.

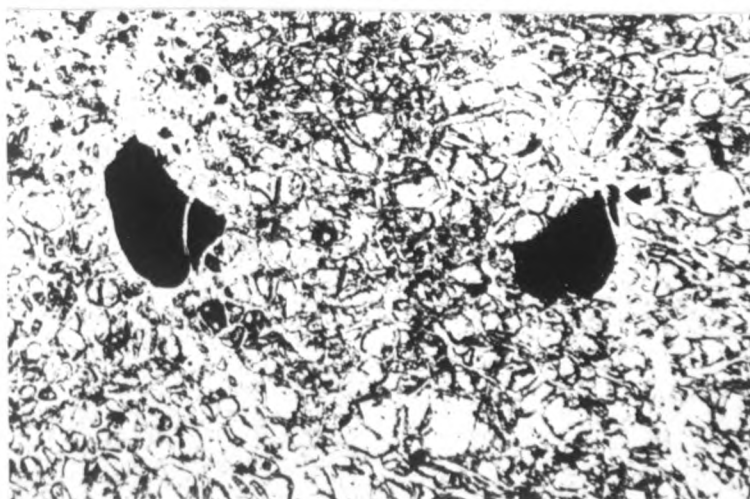
pl 3.16

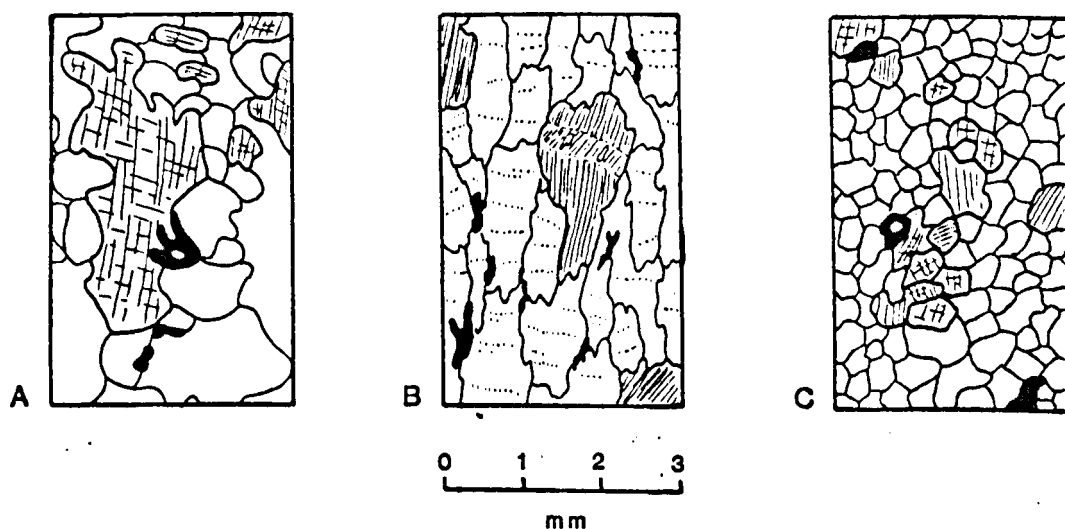


pl 3.17



pl 3.18





Schematic drawings of the dominant textures present in the Oman harzburgites.

A Lobate and cusped grains with interlocks. Vermicular spinel common at opx/ol boundaries.

B Elongate strained porphyroclasts of olivine with deformation lamellae and sub-grains, orthopyroxene with curved cleavage and exsolution lamellae and exsolution blebs in kink bands, and chromite grains aligned with foliation at olivine intergranular sites.

C Polygonal strain free grains (neoblasts) of olivine and to a lesser extent orthopyroxene, with 120 degree grain margin intersections.

Elements of A, B and C can be recognised in most thin-sections.

fig. 3.2 Textural elements in Oman harzburgites

sites. It is in the orthopyroxene porphyroclasts that exsolution blebs can be seen to be kink controlled. Post-kink exsolution may occur demonstrating that deformation took place at elevated temperatures.

Type 'C' in fig.3.2 consists of neoblasts of olivine and orthopyroxene, usually strain free with 120° grain margin intersections. This texture is due to a high temperature static recrystallisation of porphyroclasts and is mostly post-deformational (Type 'B' deformation) although some neoblasts do show slight elongation alignment and signs of stress.

A fourth textural type, of limited occurrence, consists of much smaller, granulated and extensively altered grains in mylonitic shear zones found only in the 'banded unit' near the base (lowermost 50 - 100m) of the Semail Nappe. This is due to lower temperature deformation associated with the emplacement of the ophiolite, (Searle, 1980).

There are various systems of nomenclature for mantle tectonite rock textures based on studies of ultramafic upper mantle xenoliths, (Mercier and Nicolas, 1975; Pike and Schwarzmans 1977; Basu, 1977). The most appropriate terms from these classifications for the textural elements observed in the Oman harzburgite are shown in table 3.3. It is stressed that the textures observed in any one sample of the Oman harzburgite are composed of a mixture of these textural elements indicating a complex history of deformation and recrystallization and it would be inappropriate to fit them into any one of these categories which are, in any case, intergradational.

Petrofabric studies of the Oman harzburgite have been carried out by Christensen and Smewing (1980) and Boudier and Coleman (1981). These studies show that two successive deformations are imprinted in the harzburgite sequence, confirming the conclusions from field evidence (2.3). Firstly a high temperature, low-stress deformation has affected the whole mantle sequence. High temperatures are inferred from several criteria: i) The activated slip-gliding systems in olivine (010) [100] and {okl} [100] are indicative of temperatures above 950°C in the pressure range 5-10 kbar, (Carter and Ave Lallemant, 1970; Nicolas et al, 1980); ii) the recrystallization of enstatite and olivine are intense shown by sharp sub-boundaries

Oman harzburgite textural element	Mantle tectonite classifications from xenolith studies		
	Mercier and Nicolas (1975)	Pike and Schwarzmann(1977)	Basu (1977)
Type A	Protagranular	Allotriomorphic	Coarse granular
Type B	Porphyroclastic	Porphyroclastic	Porphyroclastic
Type C	Equigranular	Equigranular mosaic	Equigranular mosaic (+ Tabular mosaic)

Table 3.2 Correlation of Oman harzburgite textural types and classifications of textural types of mantle tectonites from upper-mantle peridotite xenolith studies

and polygonal crystal shapes (Nicolas and Poirer, 1976); iii) at least part of the deformation took place under peridotite sub-solidus or even hypersolidus conditions. Stress conditions estimated from microstructural parameters such as neoblast size and sub-boundary spacings (Nicolas, 1978) using experimental calibrations (Post, 1973 and Mercier, 1976) vary from 250 to 375 bars for the high temperature deformation (Boudier and Coleman, 1980). The second deformation has obliterated the first in the lower part of the sequence where the activation of the low temperature ($< 950^{\circ}\text{C}$) slip system $(110) [001]$ in harzburgite olivine and parallel structures in the amphibolites and quartzites directly beneath the ophiolite suggest that this deformation occurred under amphibolite facies metamorphic conditions (Boudier and Coleman, 1980). Microstructures are indicative of high stress (> 1500 bars) for this second deformation (Nicolas et al, 1980). Strain related to this deformation is particularly high in the lower 500m where it is concentrated in mylonite bands but occurs as much as 2km higher where close-spaced microstructures in the olivine are indicative of rapid attenuation of strain.

Boudier and Coleman (1980) have deduced the kinematics of plastic flow from the structures and fabrics measured in the Oman harzburgite. The flow plane is approximated by the foliation and the flow line by the spinel lineation (Nicolas et al, 1973) and the sense of shear from relative orientations of foliation or flow plane and of lineation or flow line. The sense of shear shows that during the high temperature deformation the upper part of the sequence was displaced north-eastwards relative to the lower part and that this shear flow was responsible for isoclinal folding of pyroxenite dykes (plate 2.24) and phase ratio layering (plate 2.2). The sense of shear in the high stress deformation overprinted on the lowest part of the harzburgite sequence indicates that the upper part of the sequence is displaced westwards relative to the lower part.

3.4 Harzburgite mineral chemistry

The variations in composition of mineral grains from 42 harzburgite samples are presented in table 3.3. (Details of sample preparation and analytical procedure are contained in appendix 3.1). The

Number of harzburgite samples analysed = 42				
Mineral	Number of analyses	Zoning of grains	Total compositional range	Max.compn.range in 2 x 4 cm thin section
Olivine	100	None detected	(Mg/Mg + Fe)OL or Fo 0.892 - 0.917 NiO ₂ Wt% 0.25 - 0.51	0.0086 0.17 34% 65%
Orthopyroxene -Enstatite	94	None detected	(Mg/Mg + Fe + Ca)OPX or En 0.843 - 0.906 (Fe/Mg + Fe + Ca)OPX or Fs 0.078 - 0.097 (Ca/Mg + Fe + Ca)OPX or Wo 0.006 - 0.077 Al ₂ O ₃ Wt% 0.78 - 5.01	0.014 0.010 0.047 1.89 22% 53% 66% 45%
Clinopyroxene -Diopside	5	None detected	(Mg/Mg + Fe + Ca)CPX En 0.470 - 0.542 (Fe/Mg + Fe + Ca)CPX Fs 0.030 - 0.048 (Ca/Mg + Fe + Ca)CPX Wo 0.410 - 0.504	Insufficient data available
Spinel Chromite and Chrome-spinel	97	Fe rich rims see Ch.6.	(Cr/Cr + Al)SP 0.117 - 0.702 (Mg/Mg + Fe ²⁺)SP 0.441 - 0.710 (Fe ³⁺ /Cr + Al + Fe ³⁺)SP 0 - 0.061 TiO ₂ Wt% 0.03 - 0.17 MnO Wt% 0.09 - 0.25	0.059 0.136 0.012 0.05 0.08 10% 50% 20% 36% 50%

Table 3.3 Harzburgite mineral chemistry

silicate minerals (olivine, orthopyroxene and clinopyroxene) are highly magnesian and restricted in composition. The oxide minerals (chromite and chrome spinel) on the other hand show much larger compositional variations. Most chemical parameters in these minerals reach considerable percentages of the overall variation in one thin section (table 3.3), i.e. over a distance of about 2cm.

Olivine

The composition of olivine from the Oman harzburgite is compared with the composition of olivines from i) alpine type or ophiolite tectonite peridotites, ii) ultramafic upper mantle nodules, and iii) ultramafic portions of layered intrusive complexes in table 3.4. The olivine in the Oman harzburgite is highly magnesian and has a restricted compositional range.

The Mg/Mg+Fe ratios of olivine from the Oman harzburgite are plotted against their NiO Wt% contents in fig.3.3. There appears to be no correlation within the limited compositional ranges. Most (86%) of harzburgite olivine grains sampled in the Oman harzburgite contain between .40 and .44 Wt% NiO.

Orthopyroxene

Orthopyroxene compositions from the Oman harzburgite are plotted in the pyroxene quadrilateral in fig.3.4 and compared with those from other ophiolites and layered complexes. Most enstatite compositions from the Oman and other ophiolite harzburgite sequences lie between the start of the layered complex orthopyroxene trend (Boyd and Schairer, 1964), and Mg-rich compositions on the En-Fs join and define the 'Alpine-Enstatite trend' (Dick, 1977). A few enstatite grains from the Oman harzburgite contain over 5% CaSiO₃, amounts usually only encountered in orthopyroxenes with FeSiO₃ contents of over 28% in 1 atm. systems (Boyd and Schairer, 1964). The Al₂O₃ contents of enstatite grains from the Oman harzburgite are plotted against their Mg/Mg+Fe ratios and compared with enstatite compositions from other ophiolite harzburgite sequences in fig.3.5. There is an overall trend of decreasing Al₂O₃ with increasing Mg/Mg+Fe values as defined by enstatite compositions from several ophiolite harzburgite sequences. No one single locality defines the trend due to the limited compositional ranges in each.

	Body	Location	Composition Fo%	Source
Alpine peridotites/ ophiolite tectonites	Lizard	Cornwall	89.1 - 91.0	Green (1964), Kirby (1979)
	Burro Mountain	California	91.1 - 91.4	Loney et al (1971)
	Troodos	Cyprus	90.7 - 91.2	Greenbaum (1972)
	Bay of Islands	Newfoundland	87.8 - 92.2	Irvine and Findlay (1972)
	Papua	Papua, New Guinea	91.6 - 93.6	England and Davis (1973)
	Beni Bouchera	Morocco	89.1 - 90.5	Kornprobst (1969), Dickey (1969)
	Josephine	Oregon	89.5 - 91.2	Dick (1977)
	Semail	Oman	89.2 - 91.7	This thesis
	Harzburgite type tectonites		88 - 94	Jackson and Thayer (1972)
Ultramafic portions of layered intrusions	Lherzolite type tectonites		87 - 94	Jackson and Thayer (1972)
	Great dyke	Zimbabwe	81.0 - 92.2	Bichan (1969)
	E. Bushveld	South Africa	84.8 - 87.2	Cameron (1978)
	Stillwater	Montana	80 - 94	Jackson (1961)
	Turnagain	Br. Columbia	80.1 - 96.1	Clark (1978)
	Ultramafic portions of layered intrusions		75 - 94	Jackson and Thayer (1972)
	Ludlow	California	90.7	Ross, Foster and Myers (1954)
	Pendot Cove	Arizona	90.2	
	Dreiser	Germany	90.5	
	Kapfenstein	Austria	90.8	
	Meng Chian	China	90.9	
	Ichinomegata	Japan	89.1	
	Salt Lake Crater	Oahu	91.0	
	Camargo	Hawaii	90.8	
Ultramafic nodules from basaltic rocks		Mexico	91.1	

Table 3.4 Olivine compositions of alpine peridotites/ophiolite tectonites, ultramafic portions of layered intrusions and peridotite mantle nodules.

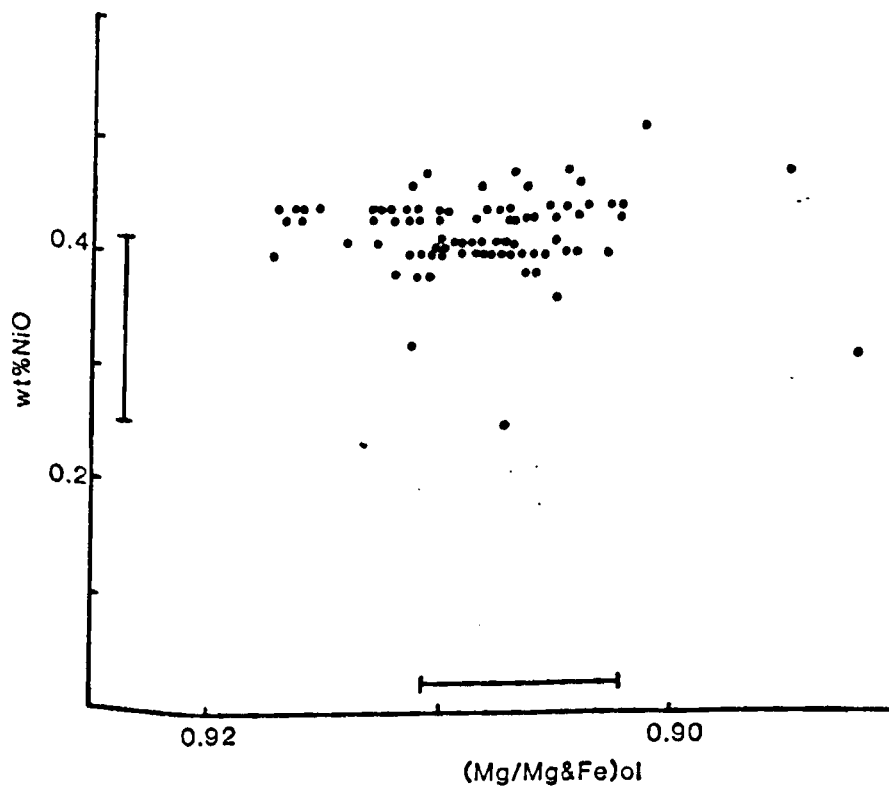


fig. 3.3 Mg/Mg+Fe x NiO₂ Wt% of olivine grains from Oman harzburgite. Bars adjacent to axes show maximum variation found in one thin section. The Mg/Mg+Fe ratios of the olivines show no correlation with their NiO₂ content. The variation of both in one thin section is a considerable proportion of the overall variation. The majority of olivine grains in the Oman harzburgite (86%) contain between 0.40 and 0.44 Wt% NiO₂ inclusive.

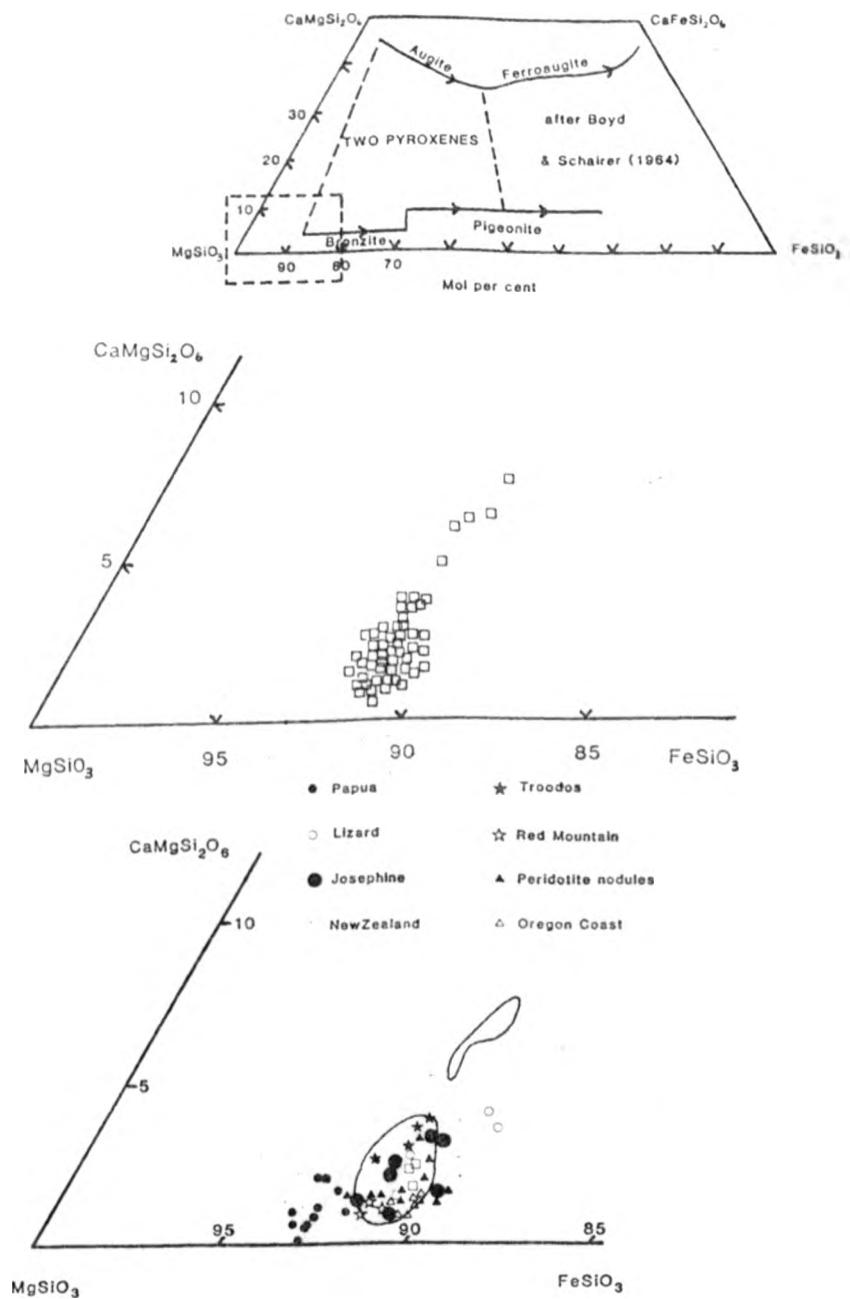


fig. 3.4 Enlarged sections of the pyroxene quadrilateral showing enstatite compositions from the Oman harzburgite (squares in central diagram) and from harzburgite sequences of 7 ophiolites and 9 mantle nodules from kimberlites. The entire pyroxene quadrilateral is shown above with compositional evolution trends from layered complexes for comparison. The Oman harzburgite enstatite compositions fall mainly between the start of the 'layered' orthopyroxene trend and Mg rich compositions near the En-Fs join. Enstatite from other ophiolites and mantle nodules also plot in this area forming the 'alpine enstatite trend' (Dick, 1977). 5 analysed enstatite grains contain over 5% CaSiO₃, compositions only usually encountered in orthopyroxenes with FeSiO₃ contents of over 28% (see layered trend).

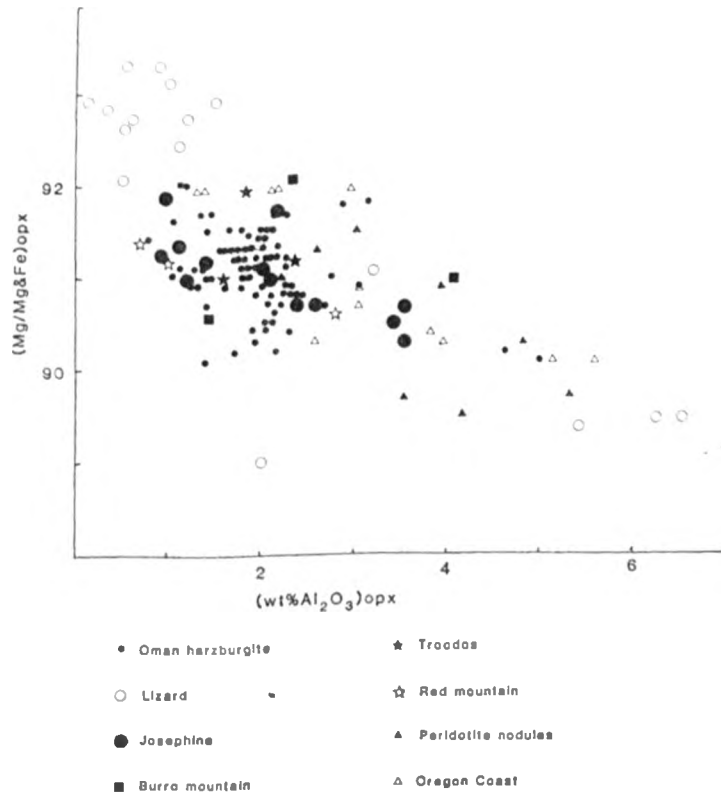


fig. 3.5 Enstatite Mg/Mg+Fe x Wt% Al₂O₃ in the Oman harzburgite, 6 other ophiolites and mantle nodules. There is a clear trend of decreasing Al₂O₃ with increase in Mg/Mg+Fe ratios.

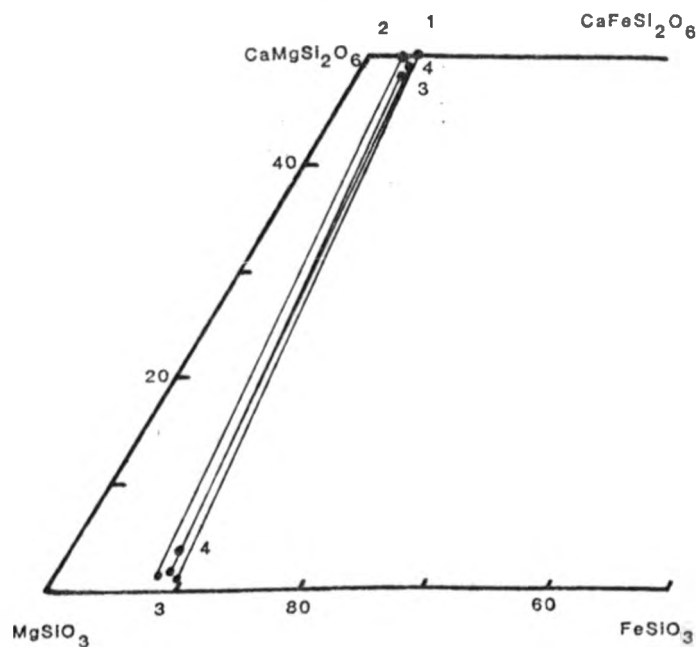


fig. 3.6 Plot of coexisting enstatite and diopside in Oman cpx-harzburgites. The most Ca poor enstatite does not always occur with the most Ca rich diopside. The pyroxene solvus geothermometer is inapplicable in this case (Chapter 7.1).

Clinopyroxene

The compositions of diopside grains from the Oman harzburgite are plotted in the pyroxene quadrilateral in fig.3.6 and joined by tie lines to associated enstatite compositions. The most diopsidic clinopyroxenes are not always associated with the most enstatitic orthopyroxene as would be expected from phase equilibria studies.

Chromite

The compositions of chromites (and chrome spinel) from the Oman harzburgite are plotted in projections of Stevens' (1944) spinel prism in fig.3.7. The projections clearly show that the main compositional variation in the chromite is in the Cr/Cr+Al ratio at low levels of Fe³⁺. There is a negative correlation between Cr/Cr+Al and Mg/Mg+Fe²⁺ of chromite with Cr-Al exchange exceeding the Mg-Fe²⁺ substitution by more than 2:1 on an atom for atom comparison. The Oman harzburgite chromite compositions fall within the compositional field for chromites from Alpine type peridotites (Irvine, 1965). Chromite, unlike the associated silicates, has a larger range of solid solution in alpine type peridotites than in any other terrestrial rock type. It must be noted that the Irvine Alpine type peridotite field contains chromite compositions from dunite and chromitite also but the compositions from the Oman harzburgite cover a large proportion of the compositional field. The field of composition for spinels from peridotite nodules (Irvine and Findlay, 1972) shows similar compositions at the Al rich end of the Alpine type field. The fields of composition for stratiform intrusions show a far more restricted range in Cr-Al substitution but a larger range in Fe contents. MnO and TiO₂ contents of accessory chromites from the Oman harzburgite are shown in figs.3.8 and 3.9, both occur at low levels. MnO shows a negative correlation with (Mg/Mg+Fe²⁺)_{sp} which may represent substitution of Mn²⁺ for Fe²⁺ in the spinel lattice (Dick, 1977). TiO₂ shows no correlation with (Cr/Cr+Al)_{sp} within this restricted range of TiO₂ contents.

3.5 Covariance of harzburgite mineral chemistry

The covariance of various compositional parameters in harzburgite olivine, orthopyroxene and spinel is shown in fig.3.10. The Mg/Mg+Fe

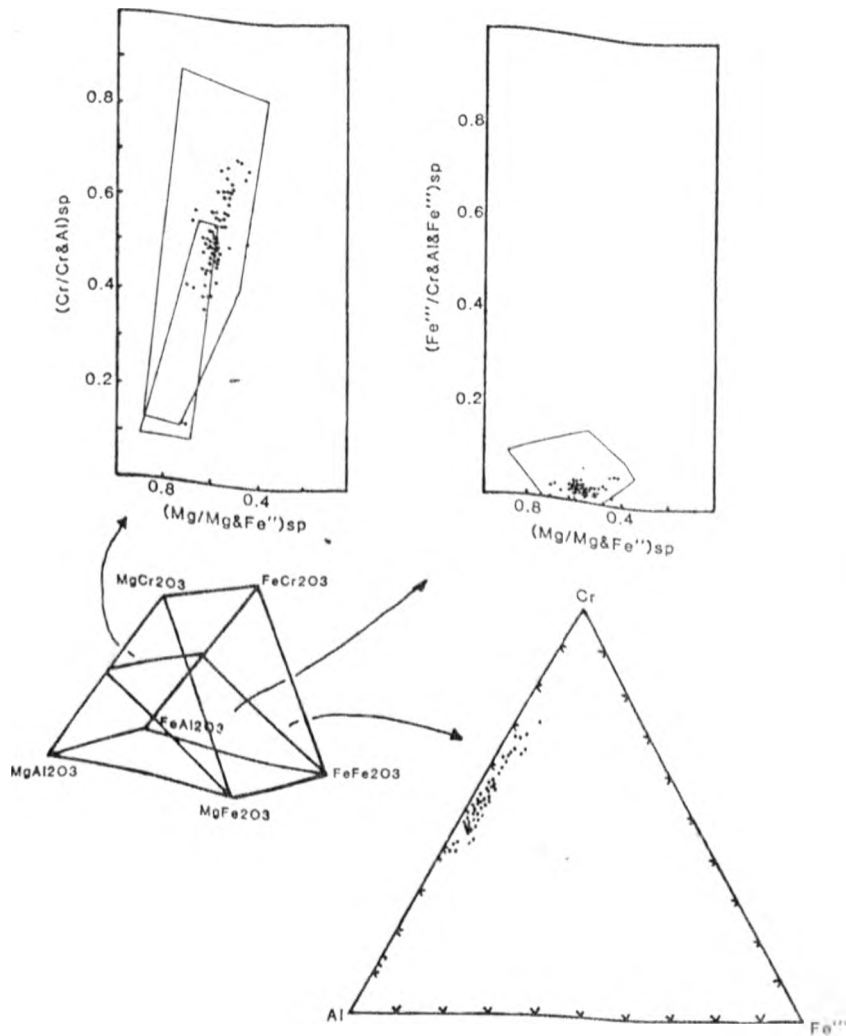


fig. 3.7 Compositions of accessory chromite from the Oman harzburgite plotted in Steven's (1944) spinel prism. The analyses fall within the alpine peridotite field (Irvine & Findlay, 1972). Chromites from mantle nodules have similar to more Al rich compositions. The main compositional variation is in the Cr/Cr and Al ratio with a concomitant slight increase in Mg/Mg+Fe'' ratio with decrease in Cr/Cr and Al ratio. All chromites from the Oman harzburgite have low Fe''' contents. Compositional fields shown are alpine type (larger) and mantle nodule chromite in upper left diagram and alpine type chromite in upper right diagram (from Irvine 1967 and Irvine & Findlay, 1972).

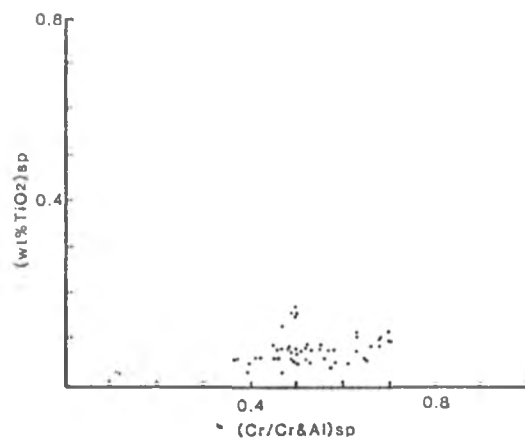


fig. 3.8 TiO₂ x Cr/Cr and Al ratios in Oman harzburgite accessory chromites.

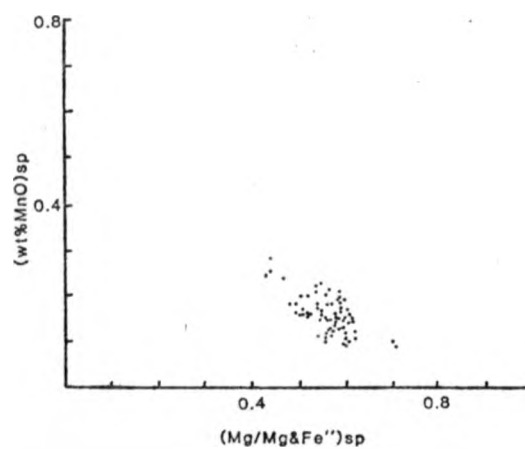


fig. 3.9 MnO Wt.% x Mg/Mg and Fe ratios in Oman harzburgite accessory chromites. There is an approximate negative correlation suggesting that Mn²⁺ follows Fe²⁺ in the spinel lattice.

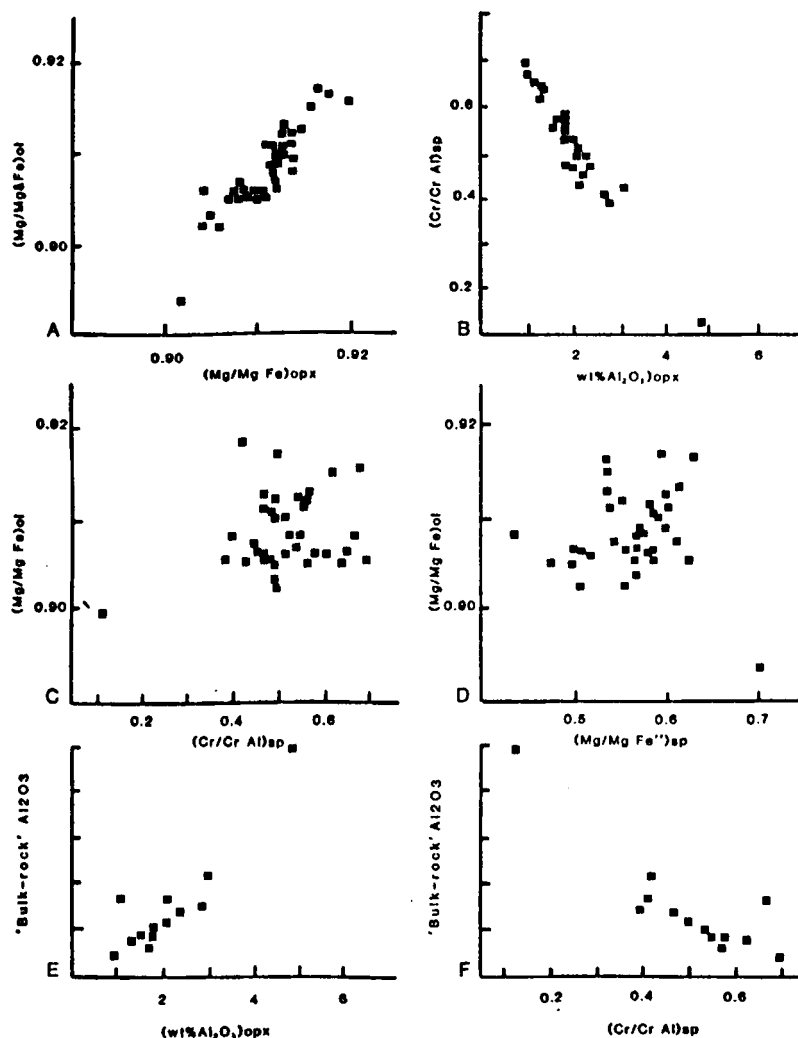


fig. 3.10 Covariance diagrams of olivine, orthopyroxene and chromite chemistry with modal orthopyroxene content of the Oman harzburgite.

- A $(\text{Mg}/\text{Mg}+\text{Fe})_{\text{ol}} \times (\text{Mg}/\text{Mg}+\text{Fe})_{\text{opx}}$. These ratios show a positive correlation and together approximate the $\text{Mg}/\text{Mg}+\text{Fe}$ variations of the whole rock.
- B $(\text{Cr}/\text{Cr}+\text{Al})_{\text{sp}} \times (\text{Wt}\% \text{Al}_2\text{O}_3)_{\text{opx}}$. These parameters show a negative correlation. Variation represents bulk rock Al_2O_3 variation as pyroxene and chromite bear all Al_2O_3 in harzburgite.
- C $(\text{Mg}/\text{Mg}+\text{Fe})_{\text{ol}} \times (\text{Cr}/\text{Cr}+\text{Al})_{\text{sp}}$. There is no correlation between these parameters within the limited compositional ranges encountered.
- D $(\text{Mg}/\text{Mg}+\text{Fe})_{\text{ol}} \times (\text{Mg}/\text{Mg}+\text{Fe})_{\text{sp}}$. As above there is no correlation between the compositions of olivine and chromite.
- E $^{*}\text{'Bulk rock' Al}_2\text{O}_3 \times (\text{Wt}\% \text{Al}_2\text{O}_3)_{\text{opx}}$. There is a positive correlation between these two compositional parameters.
- F $^{*}\text{'Bulk rock' Al}_2\text{O}_3 \times (\text{Cr}/\text{Cr}+\text{Al})_{\text{sp}}$. There is a negative correlation between these two compositional parameters.

(* 'Bulk rock' analyses are synthetic - calculated from mineral and modal analyses).

ratios of olivine and orthopyroxene have a positive correlation (fig. 3.10A) and the variation represents variation in bulk rock Mg/Mg+Fe ratio since the silicates make up >99% of the rock. The Cr/Cr+Al ratio of spinel has a positive correlation with Al₂O₃ Wt% in enstatite (fig. 3.10B) again representing bulk rock variations as spinel and pyroxene contain all the Al₂O₃ in harzburgite. The Mg/Mg+Fe and (Cr/Cr+Al) ratios in spinel are plotted against Mg/Mg+Fe ratio in olivine in fig. 3.10C and D and show no apparent correlation. Thus the Mg/Mg+Fe of spinel in the Oman harzburgite depends on the Cr/Cr+Al ratio of the spinel (fig. 3.7) rather than the Mg/Mg+Fe ratios of associated silicates.

The relations of aluminium contents of orthopyroxene and spinel to the bulk rock Al₂O₃ contents (calculated from modal and microprobe analyses of pyroxene and spinel) are shown in fig. 3.10E and F. Both orthopyroxene and spinel Al₂O₃ contents show a positive correlation with bulk rock Al₂O₃ contents, demonstrating that the primary influence on Al₂O₃ content of orthopyroxene is bulk-rock chemistry and not pressure (see Chapter 7.1).

3.6 Spatial variations in harzburgite mineral chemistry

Investigation of the spatial variation in the Oman harzburgite mineral chemistry has been by means of analysis of samples from two traverses from the top to the base of the mantle sequence. The relationship between chemical composition of the harzburgite minerals and relative horizons within the sequence was examined. Sample locations are shown in figs. 3.11 and 3.12. The limitation of this investigation of spatial variation are twofold:- 1) there is no lithological control on horizon as there is in cumulate sequences, and 2) there is no lateral control on the chemistry at each particular horizon due to sampling limited by accessibility.

The chemistry of harzburgite minerals from 27 samples across a harzburgite outcrop width of 19km, between W.Rajmi in the east and W.Rayy in the west, are plotted in fig.3.13 against distance across the outcrop. The diagram shows the correlations between mineral compositions seen in fig. 3.10. The (Cr/Cr+Al)_{sp} ratio varies most between samples and least within samples (Mg/Mg+Fe)_{sp} and (Al₂O₃ Wt%)_{opx} have

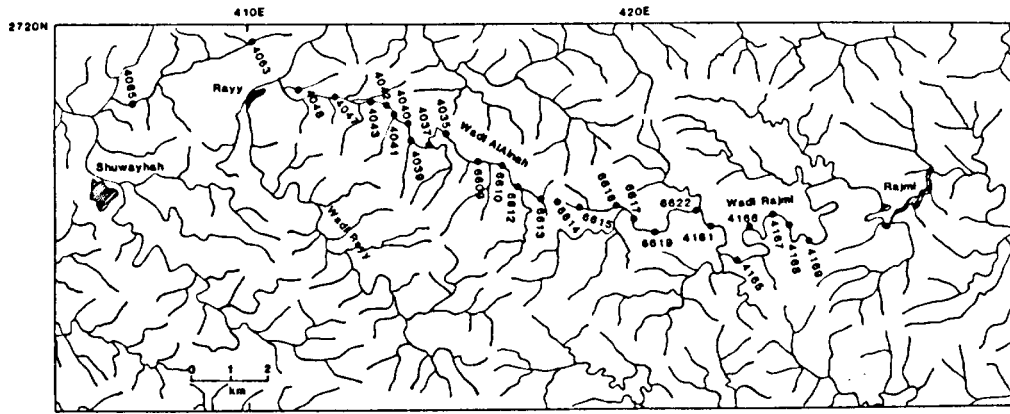


fig. 3.11 Sample locations on the Rayy-Rajmi harzburgite traverse.

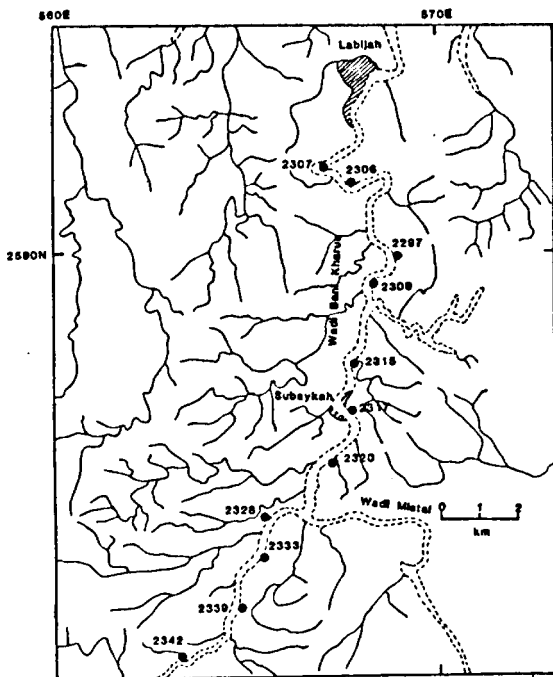
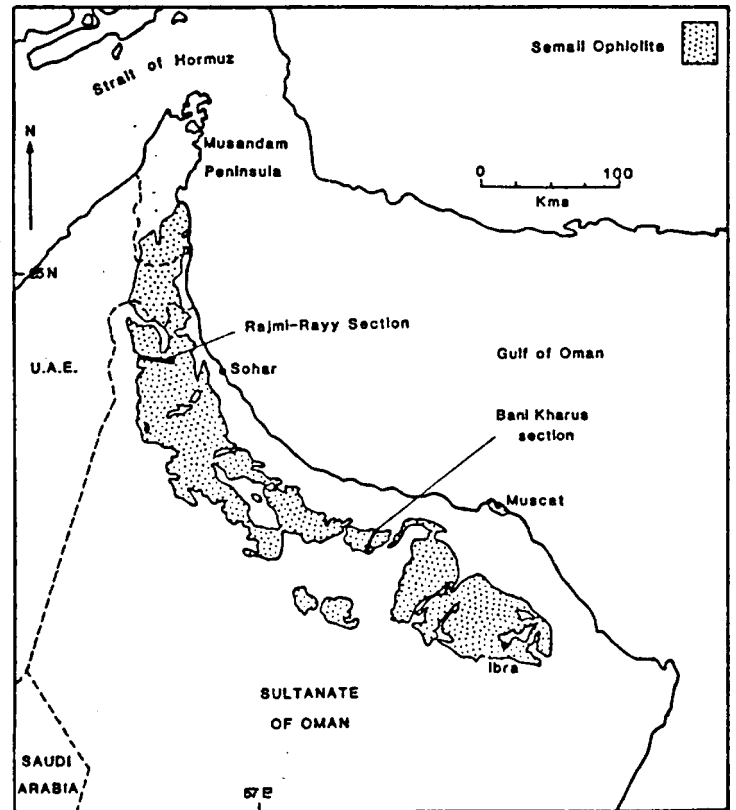
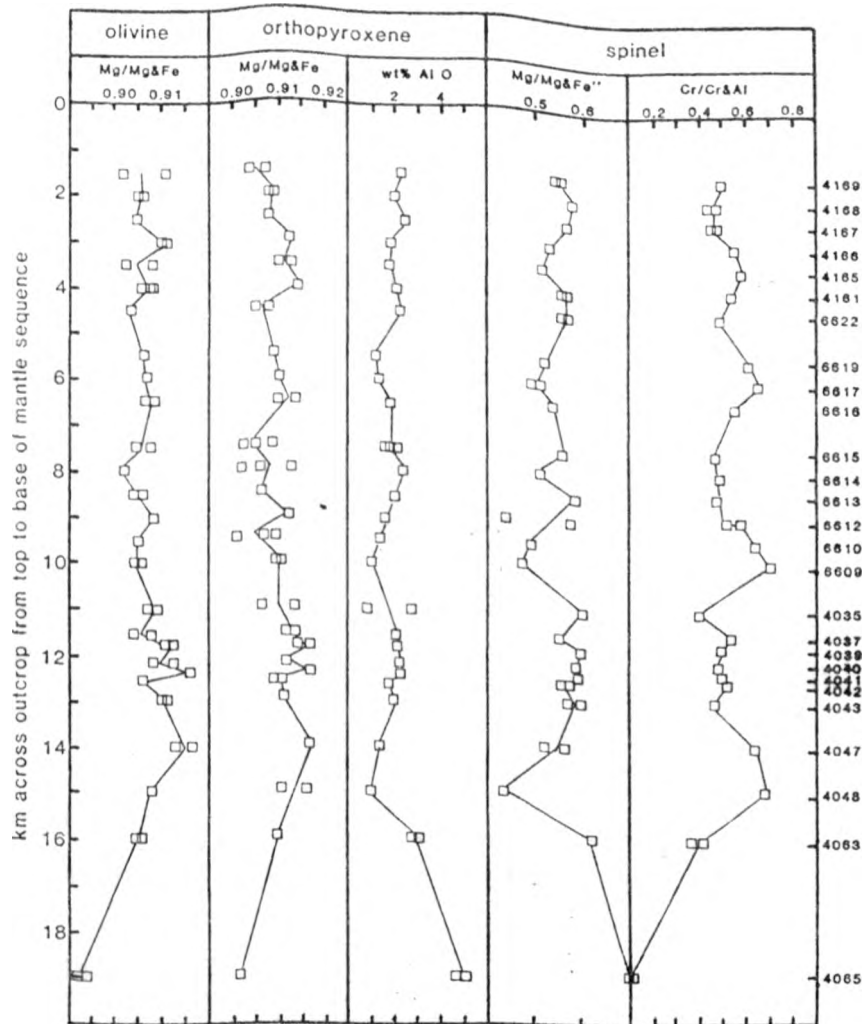


fig. 3.12 Sample locations on the Bani Kharus harzburgite traverse.





Spatial variation in harzburgite mineral chemistry :

Rayy-Rajmi Traverse

fig. 3.13 Chemical compositions of olivine, orthopyroxene and chromite plotted against distance from the upper boundary of the mantle sequence. Data is from 27 samples collected across a 19 km wide outcrop of the Oman harzburgite. There is no simple relationship between mineral chemistry and "depth" within the sequence.

good negative correlations with $(Cr/Cr+Al)_{ap}$. The $Mg/Mg+Fe$ ratios of orthopyroxene and olivine appear to have a positive correlation with $(Cr/Cr+Al)_{sp}$ on the extreme values in fig. 3.11 and the lack of correlation in fig. 3.10 between these parameters is due to the small ranges of variation of the silicate minerals and the occurrence of large percentages of these variations within single samples.

In the Rayy-Rajmi section (fig.3.13) there is a tendency for the $(Cr/Cr+Al)_{sp}$ ratio to increase with "depth" over intervals, i.e. 4169-4165, 6622-6617, 6615-6609 and 4035-4048. The two samples at the base of the sequence are comparatively alumina-rich. If the two limitations mentioned above did not apply and each trend was defined by more points then these patterns could be interpreted as cryptic chemical variation in the harzburgite. Due to the limitations, however, such an interpretation could not be statistically substantiated and the profile in fig.3.11 may represent the random distribution of harzburgites with varying bulk rock Al_2O_3 contents. Those rocks with higher Al_2O_3 also tend to be slightly enriched in FeO.

The Wadi Bani Kharus section (fig.3.14) shows the variation of harzburgite mineral chemistry in 11 samples from a mantle sequence outcrop width of 13km. The chemical parameters show the same covariance as in the Rayy-Rajmi section and similarly there is no simple correlation between mineral chemistry and depth. The chemical profiles on the composition x distance across outcrop plots bear no similarity between the two sections and although they are quite a distance apart (appendix 2) and there is a difference in thickness between them, this lends weight to the conclusion that the profiles represent random variations in bulk rock Al_2O_3 and FeO contents.

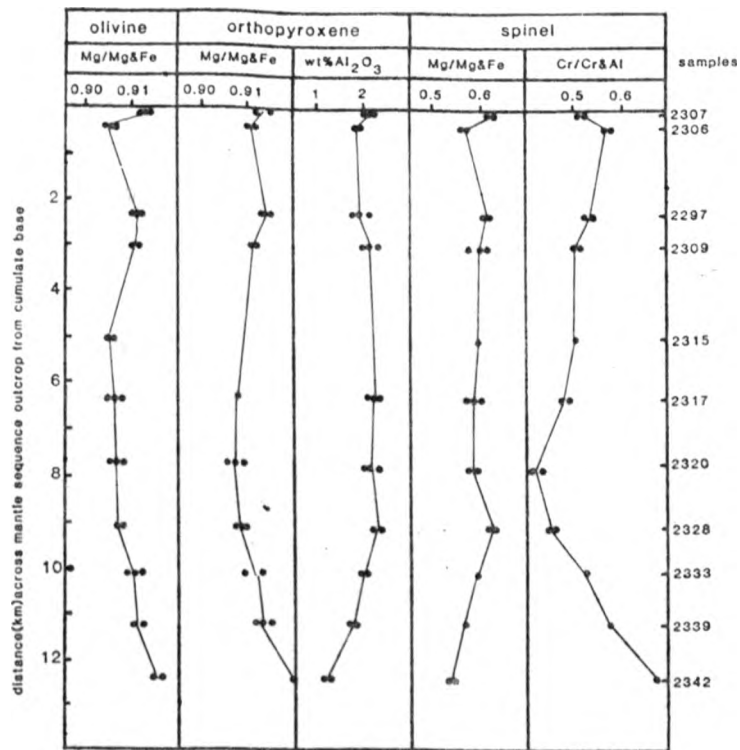


fig. 3.14 Wadi Bani Kharus harzburgite traverse. Chemical compositions of olivine, orthopyroxene and chromite plotted against distance from the upper boundary of the mantle sequence. Data is from 11 samples collected across a 13km wide outcrop of the Oman harzburgite. There is no simple relationship between mineral chemistry and "depth". Points represent 3 analyses for each mineral in each sample.

CHAPTER FOUR

Dunite and Chromitite

4.1 Introduction

Dunite is the most abundant rock type after harzburgite in the Oman mantle sequence and constitutes the remaining 5-15%. (These figures are visual estimates of relative abundances from various areas of the mantle sequence outcrop). Chromite is always present in dunite usually as an accessory forming some 2% of the mode but concentrations of chromite occur and all gradations between end members dunite and chromitite are observed (table 4.1). In the lower parts of the mantle sequence, chromitite contains only interstitial olivine and dunite is clinopyroxene free. Towards the top of the mantle sequence dunite is more frequently clinopyroxene bearing and chromitites frequently contain interstitial clinopyroxene or amphibole and, more rarely, orthopyroxene and plagioclase feldspar.

4.2 Rock textures

Primary Igneous Textures

Dunite and chromitite in the Oman mantle sequence bear primary igneous textures similar to those in the overlying 'cumulate sequence' (Smewing, 1979), other Alpine peridotites (c.f. Thayer, 1969) and stratiform intrusions (Jackson, 1961; Wager et al, 1960), which have been interpreted as being due to gravity settling of crystals in a fluid magma. The textures in the Oman dunite/chromitites are here described under a series of headings from the most olivine rich to the most chromite rich rock types. The classification of Wager et al (1960) is retained for descriptive purposes but no genetic process is inferred at this stage. The genesis of these dunite/chromitite textures is dealt with in Chapter 7.

Olivine adcumulates: Dunite bodies in the Oman mantle sequence are dominantly olivine adcumulates with mainly sub-hedral chromites forming 2% of the mode at intercumulus sites. Clinopyroxene may be present in small amounts (< 4%) as small irregular grains at intercumulus sites (plate 4.1) resembling textures in olivine adcumulates in the overlying cumulate sequence (plate 4.2) and more rarely as large oikocrysts poikilitically enclosing olivine grains (plate 2.5).

Sample No.	3715	3805	3962	3997	4023	4037B	4045B	4080B	4021	4135
Olivine	10.0	11.0	10.2	2.0	27.8	96.5	98.6	97.9	77.9	98.9
Chromite	79.1	88.5	83.5	77.5	62.2	2.3	1.4	1.7	22.1	1.1
Clinopyroxene	-	0.5	3.2	-	-	1.2	-	0.4	-	-
Orthopyroxene	-	-	1.2	-	-	-	-	-	-	-
Plagioclase feldspar	-	-	-	20.0	-	-	-	-	-	-
Amphibole	10.9	-	1.9	0.5	-	-	-	-	-	-

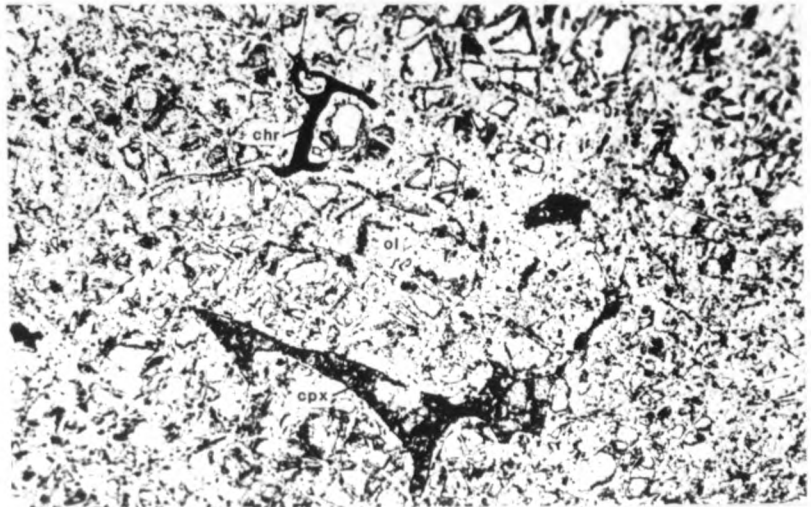
Table 4.1 Modal analyses of Oman mantle sequence dunite and chromite (1000 counts)

Plate 4.1 Mantle sequence dunite. Photomicrograph
Mag x 50 PPL
Cumulus olivine (lighter coloured, now serpentinised)
with irregular shaped intercumulus clinopyroxene
(darker coloured) and chromite (opaque).

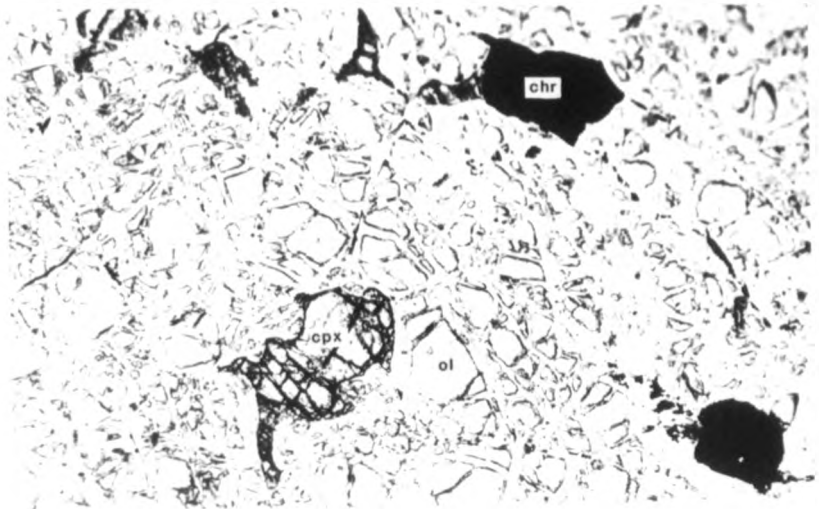
Plate 4.2 Cumulate sequence dunite. Photomicrograph
Mag x 50 PPL
This demonstrates the similarity between cumulate
sequence and mantle sequence (pl. 4.1) dunite.
Cumulus olivine is bordered by irregular shaped
intercumulus clinopyroxene and chromite.

Plate 4.3 Harrisitic olivine. Photo of large thin section.
Scale bar = 1cm
These large crystals of olivine (light colour) are
essentially one single grain although deformation
has induced the formation of sub-grains (seen in XPL).
The large olivine grains are surrounded by successive
zones of chromitite, olivine chromitite and
chromitiferous dunite and contain linear 'strings'
of included chromite parallel to their long axes.

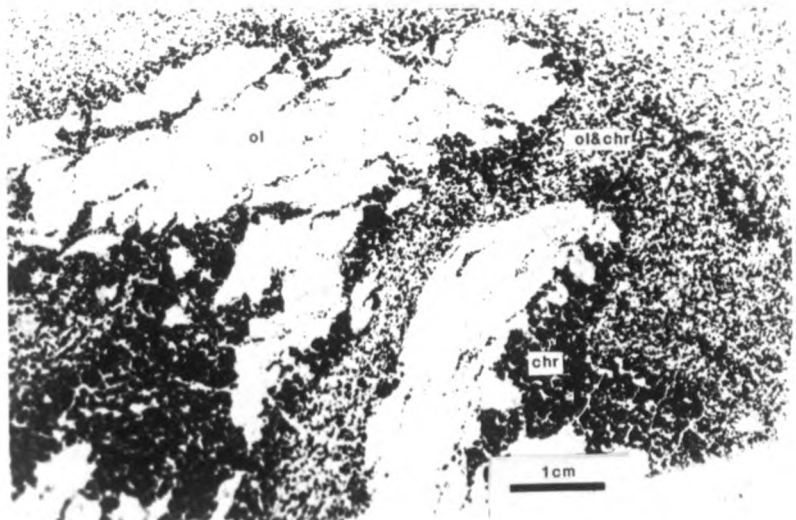
pl 4.1



pl 4.2



pl 4.3



Harrisitic cumulates: Large crystals of olivine up to 4-5cm long project up from near the base of a dunite body in Wadi Rajmi (plate 2.17, plate 4.3 and appendix 2). They resemble the 'type' harrisitic cumulates of the Rhum layered intrusion (Brown, 1956; Wadsworth, 1958; Wager et al, 1960) in their elongate parallel growth perpendicular to the cumulate layering. The Oman mantle sequence 'harrisitic' olivine crystals appear in the field to have successive phase and size graded layers of chromitite, olivine chromitite and chromitiferous dunite 'draped' over them (plate 2.17). Some sections show however that the phase variations are not in planar layers draped over an uneven surface but rather a zonation, around the 'harrisitic' olivine crystals of shells successively finer grained, poorer in chromite and richer in olivine (plate 4.4). The 'harrisitic' olivines appear to have been the loci for the successive crystallization of these chromite/olivine layers. One of the 'harrisitic' olivine crystals has a core of olivine chromitite and itself contains numerous isolated chromite grains (plate 4.5). These features suggest formation from a core or nucleus of zones of different chromite/olivine ratios. Differential outwards growth appears to have produced the large tooth-like 'harrisitic' olivine crystals which have in turn affected the morphology of ensuing concentric layers.

Chromite net texture: This texture, defined by Thayer, 1969 consists of large rounded to ovoid silicate grains or aggregates of grains, generally in contact with each other, surrounded by smaller sub-hedral chromites (plate 4.6). Chromite net texture is the most common textural variety in chromitiferous dunite in the Oman mantle sequence. This texture has been described from stratiform layered intrusions and Alpine type peridotites or ophiolite complexes (Jackson, 1961; Thayer, 1969; Mukherjee, 1969; Greenbaum, 1972) and has been interpreted as being due to the settling out from a magma of single large olivine grains or clusters of grains and the infilling of interstices by smaller chromite grains.

Occluded silicate texture: This texture, again defined by Thayer (1969) consists of isolated rounded to ovoid silicate grains or aggregates of grains in a matrix of chromitite (plate 4.7) and has also been described from stratiform and ophiolite complexes (see refs. above). It is the

Plate 4.4 Concentric chromite/olivine zones around large olivine crystals. Photo of polished slab.
Scale bar = 1cm.

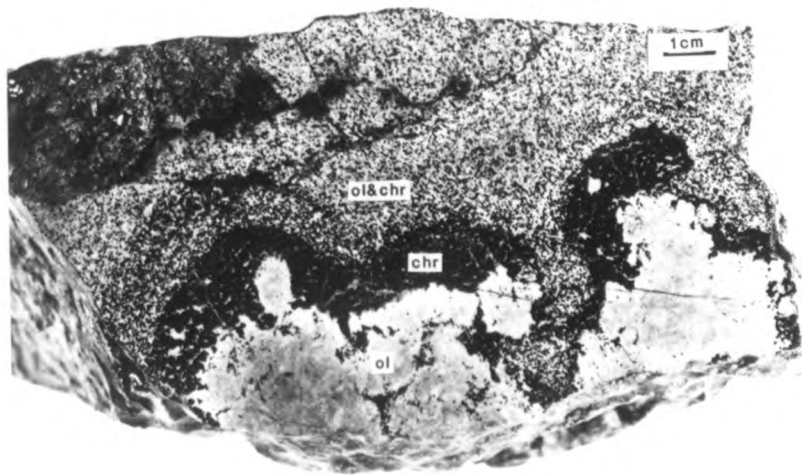
The large olivine crystals are more rounded and irregular in this specimen and less like harrisitic types. The concentric zonation around the large crystals of successive layers of chromitite, olivine chromitite and chromitiferous dunite and concomitant decrease in chromite grain size are clearly visible.

Plate 4.5 Harrisitic olivine crystal with core of olivine chromitite. Photo of polished slab.
Scale bar = 1cm.

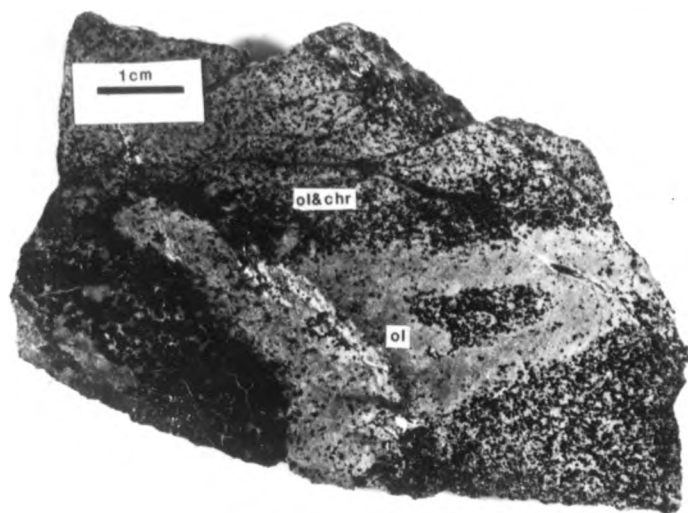
The large olivine crystal contains numerous included chromite grains, appears to be 'rooted' in olivine chromitite and contains a core zone of olivine chromitite. The margins of all mineralogical zones are slightly divided and then grade into each other.

Plate 4.6 Chromite net texture. Photo of polished slab.
Scale bar = 1cm.

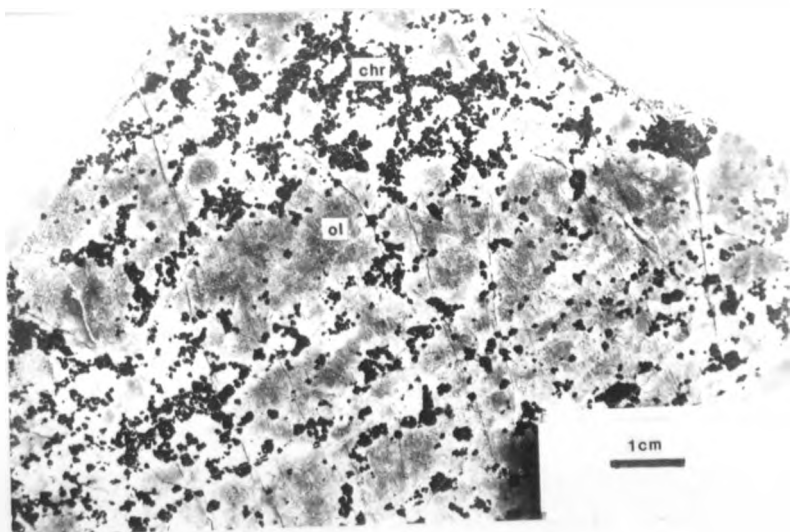
Larger rounded to ovoid olivine grains (now serpentinised, white-grey) generally in contact with each other are partially surrounded by smaller sub-hedral chromite grains (black).



pl 4.4



pl 4.5



pl 4.6

chromite-rich member of a continuous series with chromite net texture, the grain size of the chromite tending to increase with increasing chromite content. Occluded silicate volumes in Oman chromitites do not solely consist of olivine but also contain chromite grains (plate 4.8) that are invariably finer grained than those in the surrounding chromitite (plate 4.9).

Layered chromite: Phase and size graded chromitite/dunite layers occur in the Oman mantle sequence (plates 2.14, 2.16 and 4.10) with chromitite layers having a sharp basal margin with dunite and an upper gradational margin with dunite. Grain size of chromite tends to decrease upwards with increasing olivine content. Fine grained silicate-rich layers occur in chromitites in the Oman mantle sequence. These layers resemble the occluded silicate texture in the drastic reduction in grain size compared with the host chromitite and may be due to coalescence of occluded silicate volumes (plate 4.11). They may have a consistent grain size as in the last mentioned example or may be associated with larger olivine grains (plate 4.12).

Cluster texture: This term is suggested for agglomerations of chromite grains which may be irregular, rounded or ovoid, up to 1 cm or so in length, occurring in dunite bodies in the Oman mantle sequence. They coexist with chromitite layers with irregular margins up to a centimetre or so thick (plate 4.13).

Nodular texture: Nodular chromite has been described from many ophiolite complexes (e.g. Thayer, 1942; Flint et al, 1948; Bilgrami, 1963; Thayer, 1969 and Greenbaum, 1972) and has been variously known as leopard, grape, bean or shot ore. They are, according to Thayer (1969) a characteristic of podiform chromite deposits. Well developed nodular texture appears to be rare in Oman and has so far only been found as wadi cobbles and boulders near Rajmi (appendix 2.2). The nodular texture in Oman consists of ovoid nodules of chromite varying from 0.5-3cm long consisting of what appears to be a continuous rounded grain of chromite (plate 4.14). Most nodules have an ovoid silicate rich core consisting almost entirely of olivine (or its alteration products) varying between 0.3 and 0.7cm long. The matrix in between the nodules is almost exclusively olivine although small amounts of

Plate 4.7 Occluded silicate texture. Photo of polished slab.
Scale bar = 1cm.

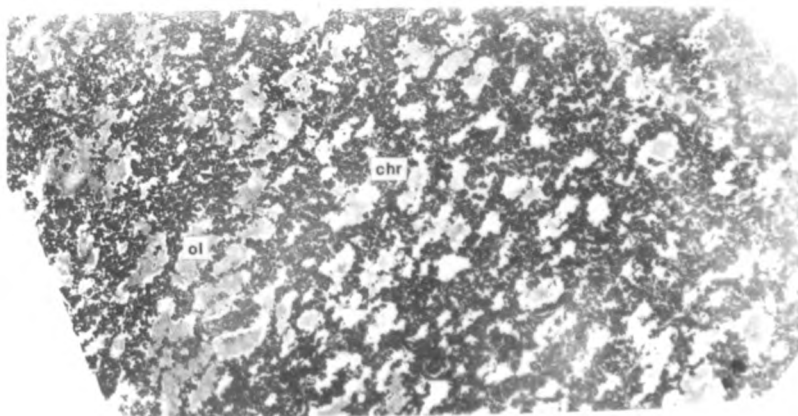
Larger rounded to ovoid olivine grains (now serpentinitised, white-grey) generally not in contact with each other are contained in a matrix of smaller sub-hedral black chromite grains.

Plate 4.8 Occluded silicate in chromitite. Photomicrograph.
Mag x 10

The occluded silicate volume consists of a tessellated array of straight to curvi-linear sided polygonal grains of olivine and chromite in an approximate 2:1 ratio. This ratio decreases outwards with increase in chromite grain size until olivine occurs only as occasional rounded or negative crystal inclusions in 'massive' chromitite.

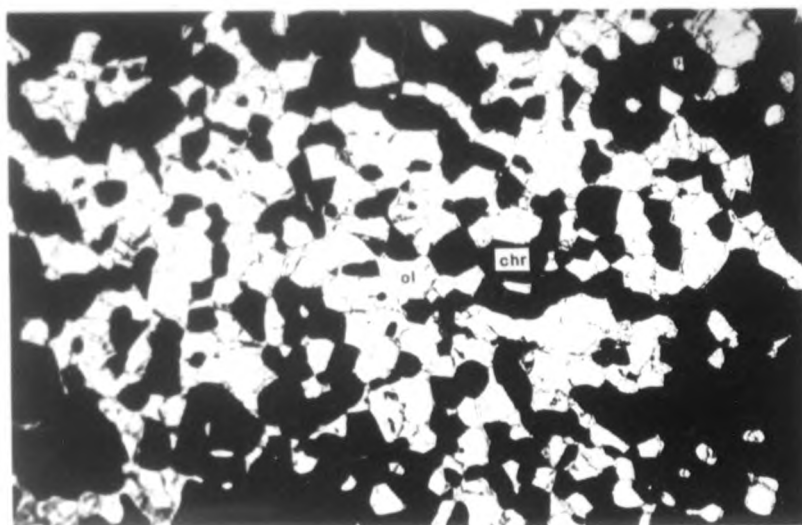
Plate 4.9 Occluded silicate in chromitite. Photo of polished slab.
Scale bar = 1cm.

The majority of the sample consists of coarsely granular 'massive' chromitite traversed by 'pull-apart' fractures, parallel to scale bar, filled with serpentine minerals, and containing rounded to irregular inclusions of olivine (now serpentinitised, white to grey). The occluded silicate in the top left of the sample is comprised of approximately 1:1 ratio of olivine and chromite. A clear reduction in grain size of the chromite can be seen between the host chromitite and the occluded silicate.

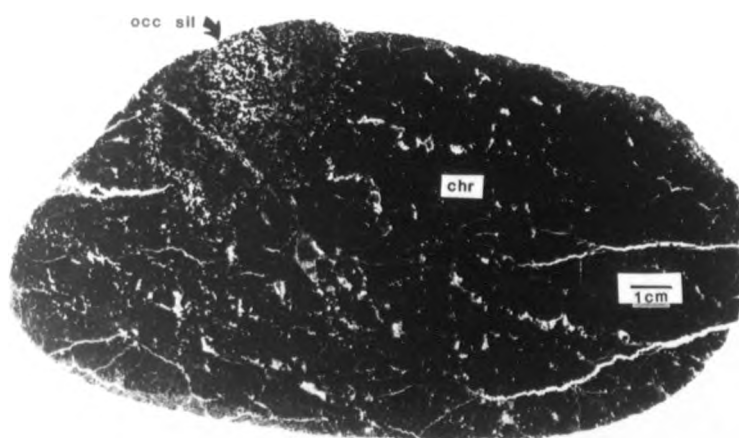


1cm

pl 4.7



pl 4.8



pl 4.9

Plate 4.10 Layered phase graded chromite. Photo of large thin section.
Scale bar = 1cm.

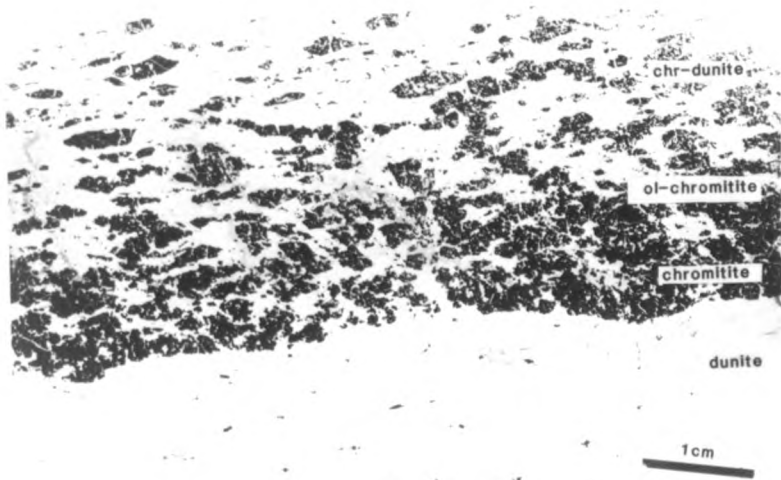
Olivine chromitite has a sharp, slightly undulating contact with underlying dunite. The olivine/chromite ratio increases upwards grading from coarsely granular olivine chromitite to dunite with small sub to anhedral chromite (the latter unit is not visible here but is similar to the unit below the basal layer). The chromite grains show evidence of stretching parallel to the layering in their elongate form and 'pull-apart' fractures roughly perpendicular to layering.

Plate 4.11 Fine grained silicate rich layer in chromitite. Photo of polished slab.
Scale bar = 1cm.

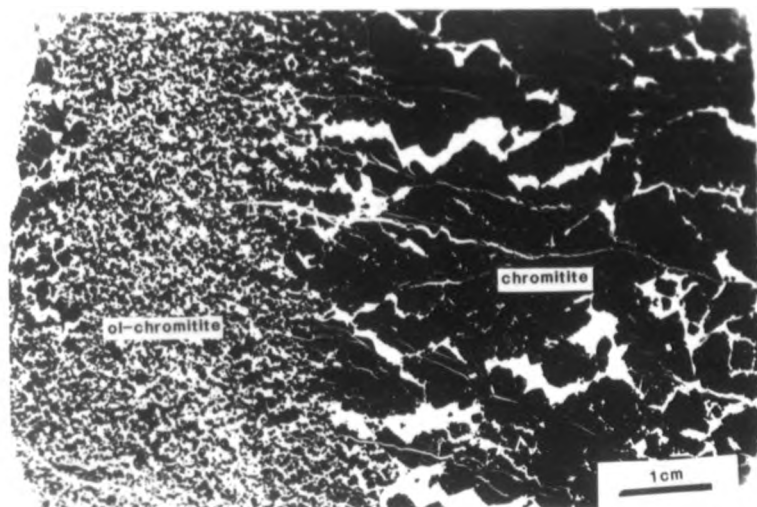
A continuous layer of olivine and chromite in approximate 1:1 ratio occurs in 'massive' chromitite. This layer resembles the occluded silicate (plate 4.9) in 'massive' chromitite with greatly reduced chromite grain size and a slight 'pinch and swell' in the layer margins suggests that layer formation might be due to the coalescing of two or more occluded silicate ovoid volumes. 'Pull-apart' cracks in the massive chromitite are perpendicular to the layering and filled mainly with serpentine minerals.

Plate 4.12 Fine grained olivine chromitite layer with large occluded olivine grains in massive chromitite. Photo of polished slab.
Scale bar = 1cm.

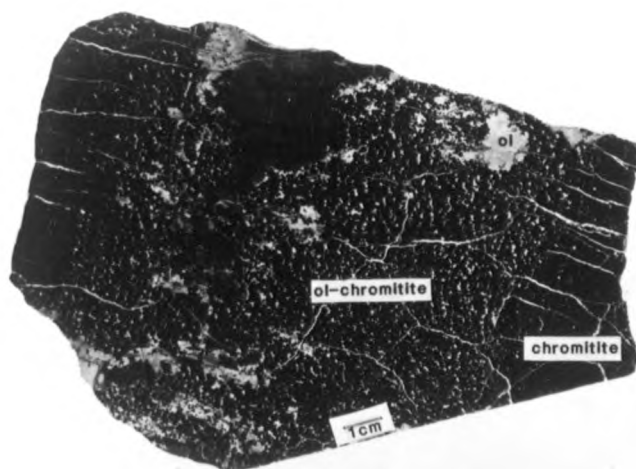
Massive chromitite (black) at the margins of the sample grade into a finer grained olivine (grey-dark grey) chromitite which contains large irregular grains, or aggregates of grains, of olivine. 'Pull-apart' cracks filled with serpentine (white) in the 'massive' chromitite are perpendicular to the layering but become less systematic in more olivine rich zones.



pl 4.10



pl 4.11



pl 4.12

Plate 4.13 Chromite 'cluster texture'. Photo of polished slab.
Scale bar = 1cm.

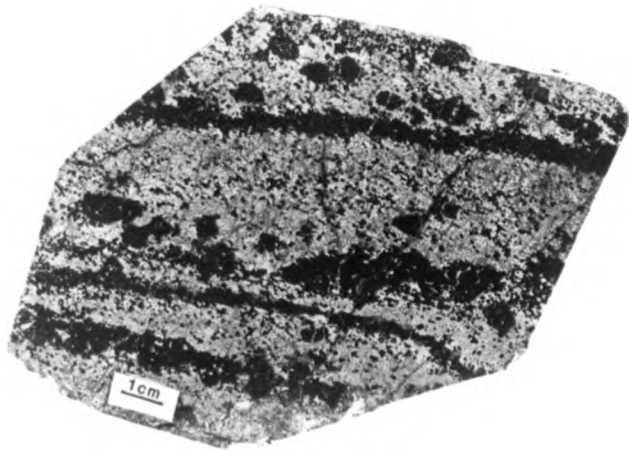
Irregular, rounded or ovoid clusters or agglomerations of chromite grains (< 1cm) coexist and are aligned parallel with chromitite layers in a matrix dominantly of chromitiferous dunite.

Plate 4.14 Nodular chromite. Photo of polished slab.

The chromite nodules (black) are round, ovoid or cigar-shaped and consist of a single chromite grain with smooth generally un-pitted margins. Nodules commonly have a core of silicate (grey) which is mainly olivine and its serpentine alteration products plus occasionally some clinopyroxene. The core material is indistinguishable both optically and chemically from the matrix between the nodules. The nodules appear to form a framework in the majority of specimens and contacts are common where nodules coalesce rather than become mutually flattened. Where coalescence is extensive, massive chromitite is formed.

Plate 4.15 Insipient nodular chromite. Photo of polished slab.
Scale bar = 1cm.

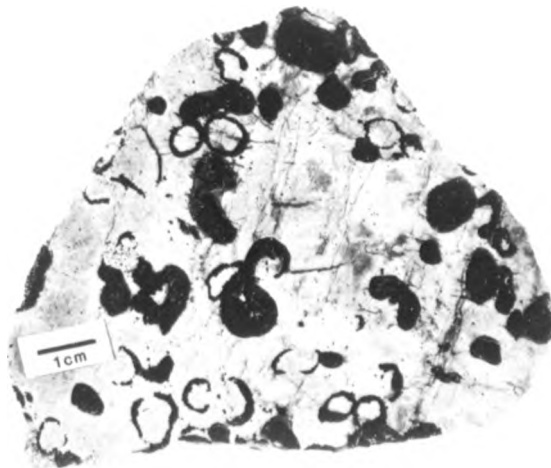
Thin 'shells' of chromite surround olivine cores and coexist with uncored nodules supported in a matrix of olivine. Most of the thin chromite 'shells' and nodules have smooth unpitted margins which suggest that this texture is due to insipient nodule formation rather than resorption of nodules. Some chromite 'shells' appear to have grown around the margins of rounded olivine grains and may not totally enclose them.



pl 4.13



pl 4.14



pl 4.15

clinopyroxene may occur. The nodules in most specimens appear to form a framework and contacts are common where coalescence rather than mutual flattening has taken place. This coalescence may be extensive where the nodules merge to form a solid mass of chromitite (plate 4.14) with very little interstitial silicate material. Some chromite nodules in the Oman mantle sequence appear ill-formed (plate 4.15). This is probably due to insipient formation of the nodules rather than resorption of the nodules by a host magma which would be expected to produce ragged nodules with pitted margins. The thin shells of these insipient nodules resemble the shells of the 'orbicular'* chromites described by Greenbaum (1972) from the Troodos ophiolite although no multiple shelled 'orbicules' have been found in Oman. Nodules and orbicules are found in intimate association with dendritic chromite growths in Troodos, this again has not been seen in the Oman.

Massive chromitite: This term is used here to describe chromitite consisting of large (< 5cm) irregular interlocking chromite grains with very little interstitial silicate material (plate 4.16). It is massive chromite which forms the bulk of the chromitite pods described in Chapter 2. As the constituent grains of massive chromitite are interlocking and irregular it appears that granulation took place by brittle fracture of larger masses of almost pure chromitite. Evidence of original smaller crystals is occasionally provided by euhedral crystal shapes projecting into interstitial silicates from massive chromitite and nodular shapes can be detected in massive chromite (plate 4.17). These features suggest that both crystal accumulation with subsequent postcumulus overgrowth (Jackson, 1961) and coalescence of nodules (seen in plate 4.13) may be contributory factors in the formation of massive chromitite.

Deformation textures

The primary igneous textures described above may bear evidence of modification by later deformation. Cigar shaped occluded silicates (plate 4.18) are probably due to stretching of ovoid or spheroidal occluded silicates. Pull-apart cracks (Thayer, 1964) are sub-parallel features produced by brittle fracture and extension of chromite, occur in the majority of chromite grains in the Oman mantle sequence, and are conspicuous in some massive chromitite samples (e.g. plate 4.10).

* 'Orbicular chromite' is used to describe quite different textures in Thayer (1969) and Greenbaum (1972).

Plate 4.16 Massive chromitite. Photo of polished slab.
Scale bar = 1cm.

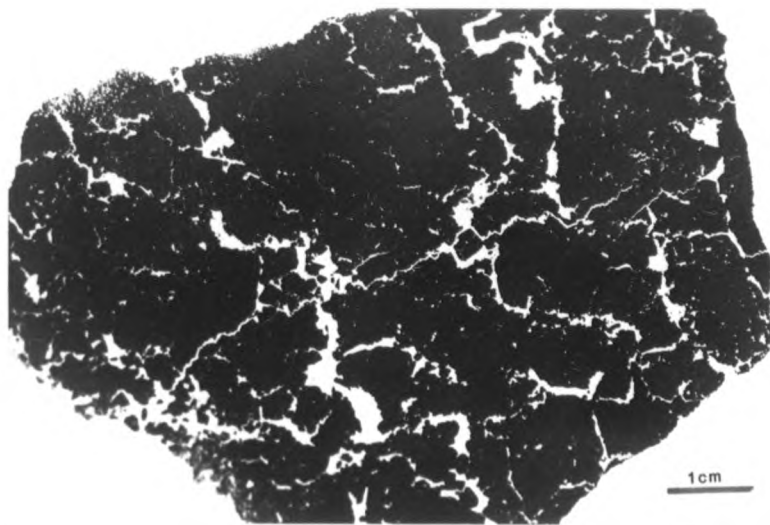
Large irregular interlocking grains of chromite (black) are bordered by thin irregular veins of silicate materials (white) much of which are secondary alteration minerals occupying veins and fractures produced by granulation of the chromitite. The large chromite grains are relatively featureless although some small rounded or negative crystal inclusions of olivine and sometimes diopside occur. The inclusions are often aligned and may represent an original, smaller, constituent grain boundary. The margins of the large chromite grains are jagged, suggestive of granulation although part-euhedral chromite crystal shapes may be present extending into the interstitial silicate.

Plate 4.17 Nodular chromite in massive chromitite.
Reflected light photomicrograph.
Mag x 50.

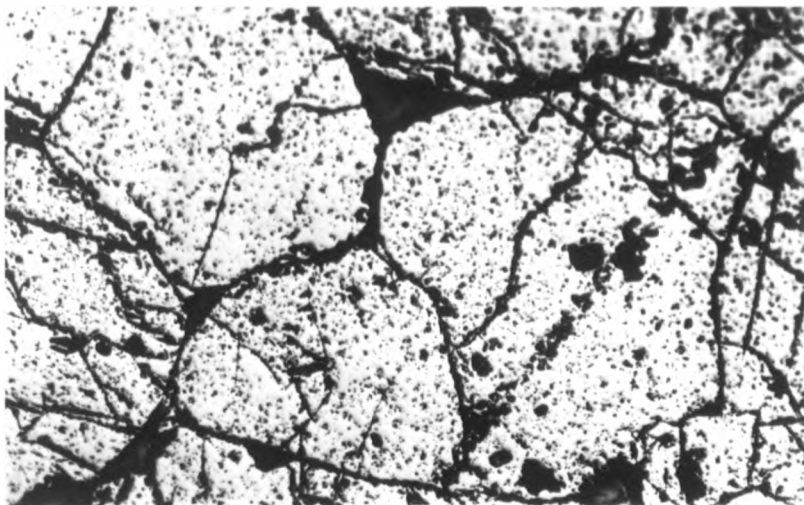
Nodules of chromite (grey) are mutually flattened at their margins and form massive chromitite with very little silicate interstitial material (dark grey to black). The grain margins seen clearly in reflected light are not easily distinguished in transmitted light and the chromite appears as 'massive' and featureless. At the centre of each nodule there is a small grain of silicate (black). Inclusions of silicate may also occur nearer the margins of the nodules.

Plate 4.18 Cigar-shaped occluded silicate. Photo of polished slab.
Scale bar = 1cm.

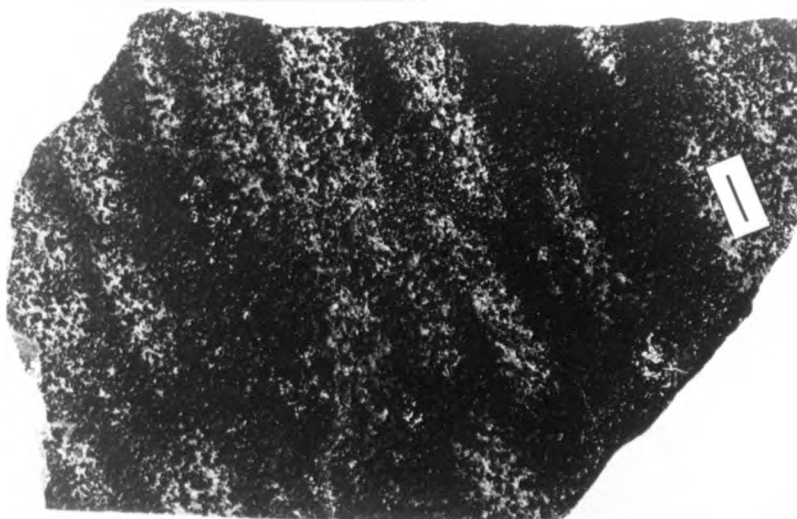
Occluded silicate texture originally comprised of spherical or ovoid silicate rich volumes in a chromitite matrix have been stretched to produce cigar-shapes. The matrix surrounding the occluded silicates is olivine chromitite rather than massive chromitite which has suppressed the formation of 'pull-apart' fractures.



pl 4.16



pl 4.17



pl 4.18

Where chromite grain boundaries are roughly parallel with pull-apart features the intergranular space may be widened and subsequently filled with secondary mineral assemblages (e.g. plate 4.9). Significantly the dominant set of pull-apart cracks in the Oman chromitite samples are consistently perpendicular to layering (e.g. plates 4.9 and 4.10). The lineation defined by the long axes of the nodules in plate 4.18, however, are not perpendicular to the pull-apart cracks in the lineation, and therefore may be a primary magmatic feature due to settling of nodules in a fluid magma or due to a high temperature plastic deformation prior to the brittle deformation which produced the pull-apart cracks.

Where dunite/chromitite bodies are cut by hydrothermal veins the silicate minerals are altered to hydrous secondary mineral assemblages mainly involving serpentine, chlorite, brucite and talc. Chromite reacts mainly by mechanical break-down on grains although a change in colour in thin section from deep red to opaque indicates an enrichment in Fe^{3+} due to oxidation.

4.3 Mineralogy and chemistry

Introduction

The variations in composition of mineral grains from 299 samples of mantle sequence dunite and chromitite are presented in table 4.2, (details of the sample preparation and analytical procedure are contained in appendix 3.1). Olivine in dunite/chromitite is generally more highly magnesian than olivine in harzburgites in the Oman mantle sequence and has greater ranges in both $\text{Mg}/\text{Mg}+\text{Fe}$ and $\text{NiO}\%$ values. Chromite in mantle sequence dunite/chromitites has a similarly large range of $\text{Cr}/\text{Cr}+\text{Al}$ values as the chromite in the harzburgite but at generally higher levels of $\text{Cr}/\text{Cr}+\text{Al}$ and $\text{Mg}/\text{Mg}+\text{Fe}$.

Olivine

Olivine in Oman mantle sequence dunite and chromitite has an optically positive interference figure (i.e. $> \text{Fo}_{87}$) like harzburgite olivine but has a greater variation in composition from $\text{Fo}_{91.5}$ to $\text{Fo}_{96.3}$ (table 4.2). This range extends to higher $\text{Mg}/\text{Mg}+\text{Fe}$ values in olivine than have been previously reported in ophiolite tectonites but is still limited compared with the compositional range of olivine in some layered intrusions (table 3.4). Olivine compositions in the Oman sequence dunite/chromitite suite are related to their mode of occurrence

Number of samples analysed = 240					
Mineral	Number of analyses	Zoning	Total compositional range	Max.compn.range in thin section or handsp.	
					% of total range
Olivine	23	None detected	(Mg/Mg + Fe)OL or FO 0.915 -0.963 NiO ₂ Wt% 0.35 -0.84	0.008 0.20	16% 41%
Clinopyroxene	2	None detected	(Mg/Mg + Fe + Ca)CPX or En 0.496 -0.702 (Fe/Mg + Fe + Ca)CPX or Fs 0.021 (Ca/Mg + Fe + Ca)CPX or Wo 0.277 -0.483	Insufficient data available	
Chromite	305	Post-cumulus overgrowth - slightly lower Cr Fe rich rims - secondary alteration	(Mg/Mg + Fe ²⁺)SP 0.380 -0.861 (Cr/Cr + Al)SP 0.440 -0.827 (Fe ³⁺ /Cr + Al + Fe ²⁺)SP 0 -0.119 TiO ₂ Wt% 0 - 1.06 MnO Wt%	0.066 0.064 0.016 0.30	14% 17% 13% 28%
Plagioclase Feldspar	2	None detected by optical methods	(Ca/Ca + Na)FSP or An 0.786 -0.789	Insufficient data available	
Amphibole	7	None detected	Mg/Mg + Fe* 0.892 - 0.937 TiO ₂ Wt% 0.67 - 1.23 Al ₂ O ₃ Wt% 9.18 - 12.67 Na ₂ O Wt% 1.84 - 2.75 Cr ₂ O ₃ Wt% 0.96 - 2.21	0.011 0.24 1.34 0.25 0.41	24.4% 42.9% 38.4% 27.5% 32.8%

Table 4.2 Dunite + chromitite mineral chemistry

(fig. 4.1A). Occluded olivine and olivine in primary inclusions in chromitite are richest in MgO and NiO. Interstitial olivine in chromitite and olivine chromitite and then olivine in chromitiferous dunite and dunite are successively poorer in MgO and NiO. With the greater variation in olivine $\text{Mg}/\text{Mg}+\text{Fe}$ values encountered within this suite a trend of decreasing NiO with decreasing $\text{Mg}/\text{Mg}+\text{Fe}$ can be seen. Olivine compositions in cumulate dunite from the base of the cumulate sequence lie at the end of this trend, (fig. 4.1A). Analysis of olivine from paired samples of dunite and harzburgite are shown in fig. 4.1B. Samples were collected close together each side of the contact between dunite and harzburgite. The paired samples clearly show that olivine in dunite has higher $\text{Mg}/\text{Mg}+\text{Fe}$ ratios but lower NiO values than the olivine in the adjacent sample of harzburgite. When dunite olivine and harzburgite olivine compositions are plotted as two groups however they show considerable overlap.

Pyroxene

Despite association with harzburgite that contains 20% orthopyroxene, dunite in the Oman mantle sequence contains no orthopyroxene, and chromitites contain only small amounts as isolated interstitial grains. The clinopyroxene present is of diopsidic composition (En_{70} , Fs_2 , Wo_{28}) (table 4.2). As the diopside is highly magnesian and thus very low in iron it is colourless and consequently non-pleochroic in plain polarised light. The interstitial clinopyroxene in chromitite lies at the Mg-rich end of an Fe enrichment/Mg depletion trend involving clinopyroxene compositions from the Oman mantle sequence and cumulate sequence (fig. 4.2) and is of similar composition to clinopyroxene in the harzburgite/Lherzolite samples.

Orthopyroxene in chromitite is colourless, non pleochroic and probably of similar composition to the enstatite in the surrounding harzburgite but differs in being unstrained and lacking exsolution lamellae of clinopyroxene. No analyses have been made of orthopyroxene in chromitite.

Chromite

Chromite in Oman mantle sequence dunite and chromitites varies in composition from $\text{Cr}/\text{Cr}+\text{Al}$ 0.44 to 0.70, $\text{Mg}/\text{Mg}+\text{Fe}^{\text{II}}$ 0.38 to 0.86, and

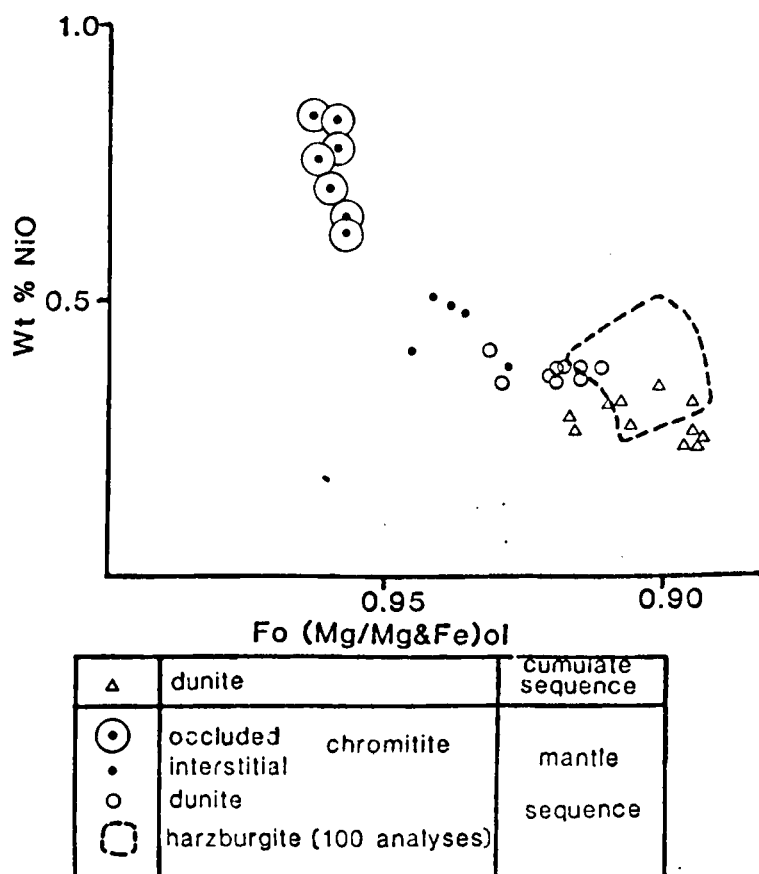


fig. 4.1A Olivine compositions Mg/Mg+Fe x NiO₂ Wt%

Olivine compositions in Oman mantle sequence chromites and dunites show a simple positive correlation between Mg/Mg+Fe and NiO₂ Wt%. There are two factors affecting the compositions: 1) The plots of olivine from cumulate dunite lie at the low Mg/Mg+Fe and NiO₂ end of the compositional trend suggesting that there is an original magmatic fractionation sequence represented by decreasing Mg/Mg+Fe and NiO₂, and 2) rocks with higher modal amounts of chromite tend to contain olivine with higher Mg/Mg+Fe ratios and NiO₂ Wt% values.

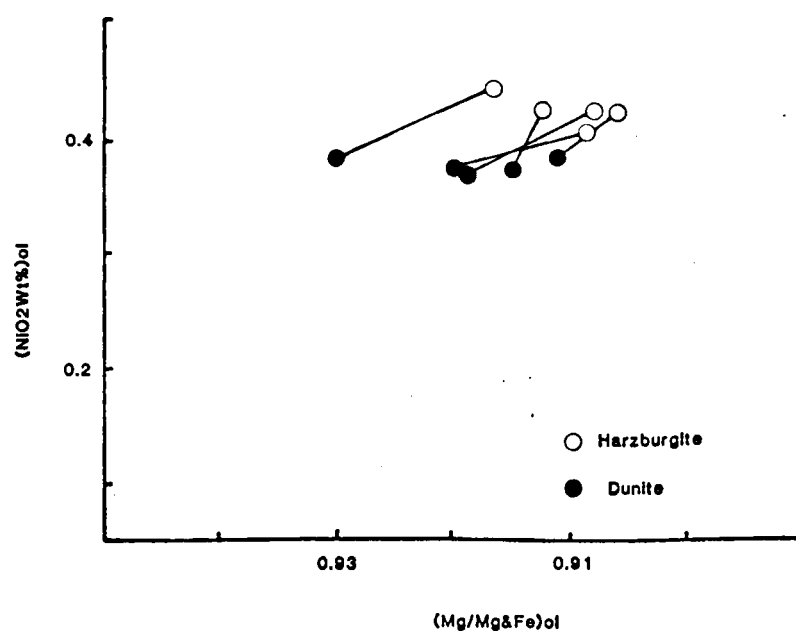


fig. 4.1b Olivine compositions from paired harzburgite and dunite samples.

This plot demonstrates that olivine in mantle sequence dunite has consistently higher Mg/Mg+Fe ratios but lower NiO₂ contents than olivine from the host harzburgite (in the immediate vicinity of the dunite body) but overlap does occur between olivine compositions from dunite and harzburgite when all localities are considered.

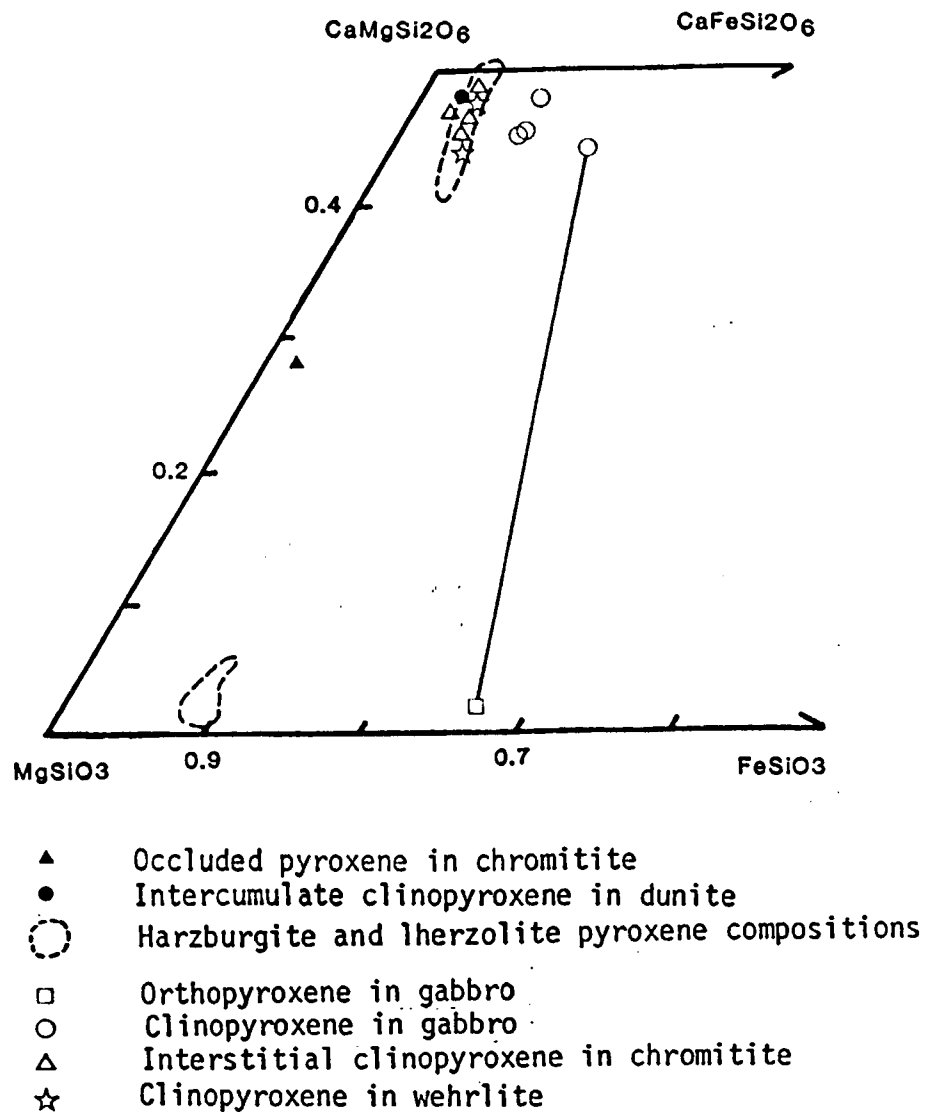


fig. 4.2

Pyroxene plots.

Clinopyroxene compositions from mantle sequence chromitite and cumulate sequence ultramafic rocks have similar compositions to those from mantle sequence cpx-harzburgite and lherzolite. Cumulate sequence gabbro contains clino and orthopyroxenes that are relatively Fe enriched. A clinopyroxene from a primary inclusion in chromitite plots in the two-pyroxene field of Boyd and Schairer (1964) (see fig. 3.2).

$\text{Fe}^{3+}/\text{Cr}+\text{Al}+\text{Fe}^{2+}$ 0-0.12 (table 4.2). The main chemical trend shown by chromite from chromitites and olivine chromitites is that of variation in Cr/Cr+Al ratio at fairly constant levels of Mg/Mg+Fe²⁺ (fig. 4.3). Chromite from mantle sequence chromitiferous dunite and dunite show a similar trend at lower levels of Mg/Mg+Fe²⁺. Chromite compositions from cumulate sequence chromitite, dunite and gabbro are also plotted in figs. 4.3 and 4.4 showing a markedly different trend. The cumulate sequence chromitite and dunite chromites plot at the Al and Fe³⁺ rich end of the mantle sequence compositional trends and the gabbro chromites define a trend of increasing Cr, Fe²⁺ and Fe³⁺ originating from cumulate chromitite and dunite compositions (fig. 4.3 and 4.4). Chromite analyses from paired samples of harzburgite and dunite are plotted in fig. 4.3B and show that dunite chromite consistently has higher Cr/Cr+Al and lower Mg/Mg+Fe²⁺ ratios.

The titanium content of chromite in mantle sequence chromitites and dunites is generally low (< 0.4%, see table 4.2 and fig. 4.5) but is markedly higher in some chromitites where the Cr/Cr+Al ratio falls in the range 0.5 to 0.6. Most chromite compositions from cumulate chromitite and dunite also plot in this lower Cr/Cr+Al, higher (< 1% TiO₂) zone. Chromite in cumulate gabbro contains rather more titanium (< 4.3% TiO₂) and increase in TiO₂ content may be accompanied by a slight increase in Cr/Cr+Al ratio (fig. 4.5).

Manganese contents of chromites from mantle sequence chromitites and dunites vary between 0 and 0.3% MnO (table 4.2, fig. 4.6) and show a simple trend of increasing Mn with decreasing Mg/Mg+Fe²⁺, suggesting that Mn may substitute for Fe²⁺ in the chromite lattice as in the harzburgite chromite (Chapter 3.3). Chromite from cumulate chromitite, dunite and gabbro generally has lower Mg/Mg+Fe²⁺ ratios and contains correspondingly more Mn²⁺ (up to about 0.7% MnO, fig. 4.6).

Feldspar

So far feldspar has been identified in the mantle sequence dunite/chromitite suite in only one chromitite body (Farfar 6 - see appendix 2.2). Optical determination of the plagioclase feldspar in this

fig. 4.3A Chromite compositions
Cr/Cr+Al x Mg/Mg+Fe"

Mantle sequence chromitite chromite compositions vary in their Cr/Cr+Al ratios at constant levels of Mg/Mg+Fe". Mantle sequence dunite chromites show similar variation at lower Mg/Mg+Fe" levels. Cumulate sequence chromitite and dunite chromites plot at the Al rich end of the chromitite and dunite trends respectively. Chromite from cumulate sequence wehrlite and gabbro show a different compositional trend of decreasing Mg/Mg+Fe" with a concomitant increase in Cr/Cr+Al. Chromites from both chromitite and dunite from the mantle sequence have generally higher Cr/Cr+Al ratios than chromite from mantle sequence harzburgite.

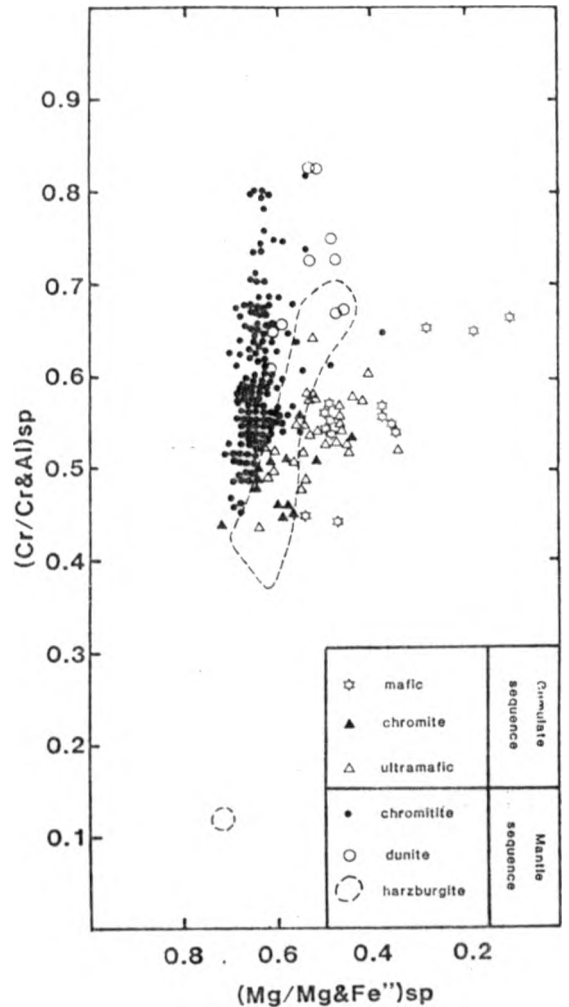
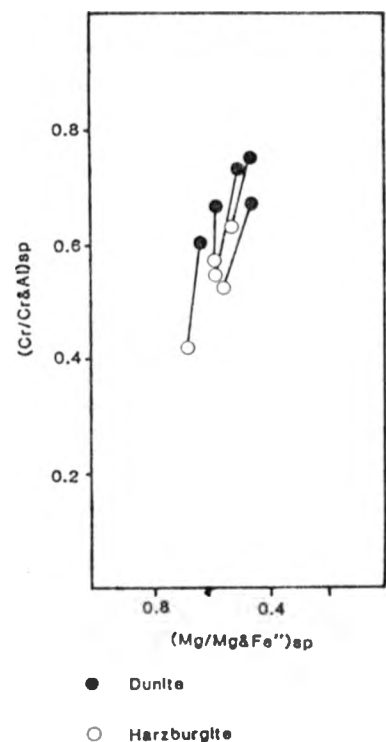


fig. 4.3B Chromite compositions from paired harzburgite and dunite samples

The chromite from mantle sequence dunite has consistently higher Cr/Cr+Al ratios but lower Mg/Mg+Fe" ratios than chromite from the host harzburgite but when considered together there is overlap in composition between the groups (compare with olivine analyses fig. 4.1B).



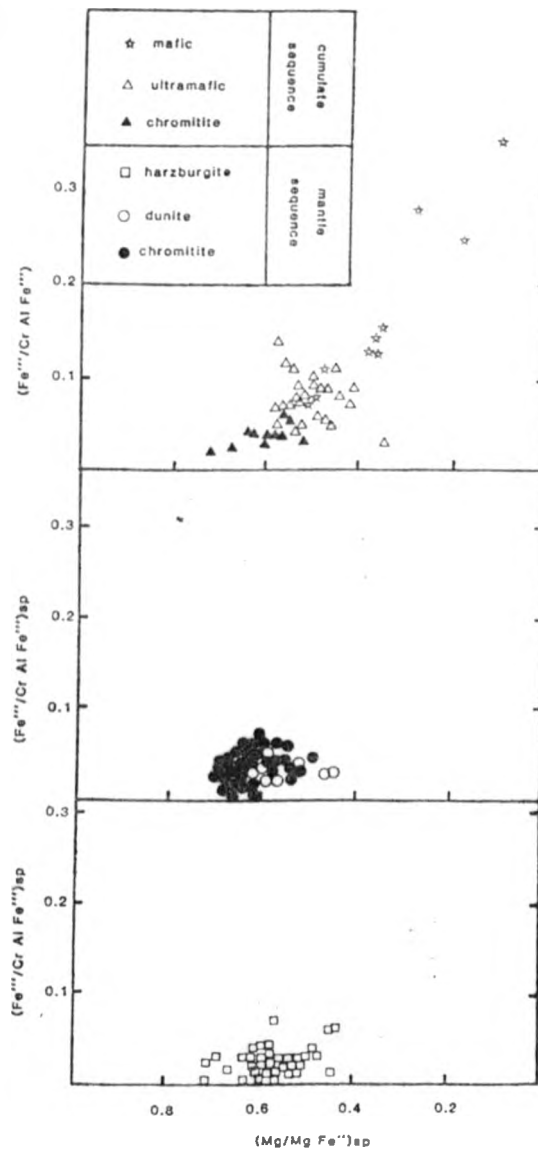


fig. 4.4 Chromite compositions $\text{Mg}/\text{Mg}+\text{Fe}'' \times \text{Fe}''' / \text{Cr}+\text{Al}+\text{Fe}'''$

Mantle sequence chromitite and dunite chromite compositions are lowest in Fe''' , the dunite chromite also has lower $\text{Mg}/\text{Mg}+\text{Fe}''$ ratios. Chromite from cumulate sequence chromitite has similar $\text{Mg}/\text{Mg}+\text{Fe}''$ and $\text{Fe}''' / \text{Cr}+\text{Al}+\text{Fe}'''$ ratios to those from mantle sequence chromitite. Cumulate sequence dunite, wehrlite and particularly gabbro are relatively enriched in Fe'' and Fe''' producing the overall trend running from the Mg/Fe'' to the Fe''/Fe''' join.

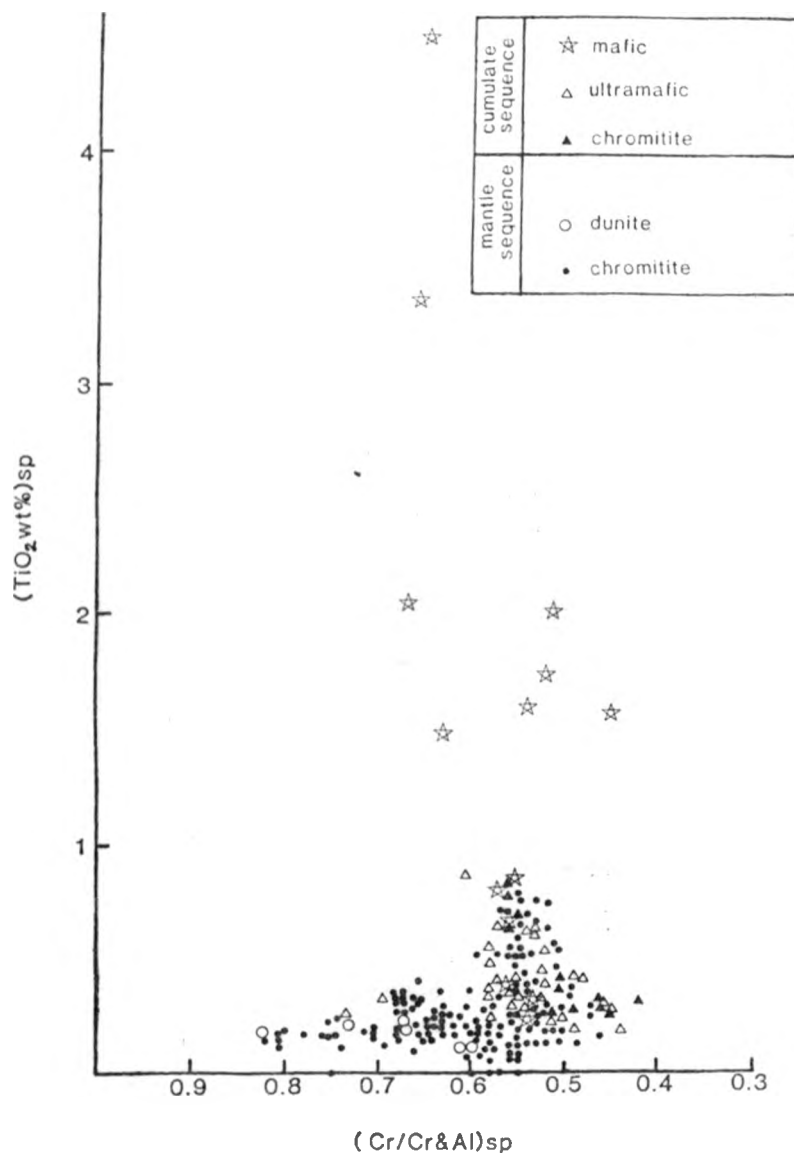


fig. 4.5 Chromite compositions $\text{Cr/Cr+Al} \times \text{TiO}_2 \text{ Wt\%}$

Most mantle sequence chromite from dunite and chromitite has low ($< 0.4\%$) TiO_2 content. Chromite with Cr/Cr+Al ratios between 0.4 and 0.6 (most cumulate sequence chromite) have higher TiO_2 contents ($< 1.0\%$). Chromite from gabbro cumulates may have much higher TiO_2 contents ($< 4.3\%$).

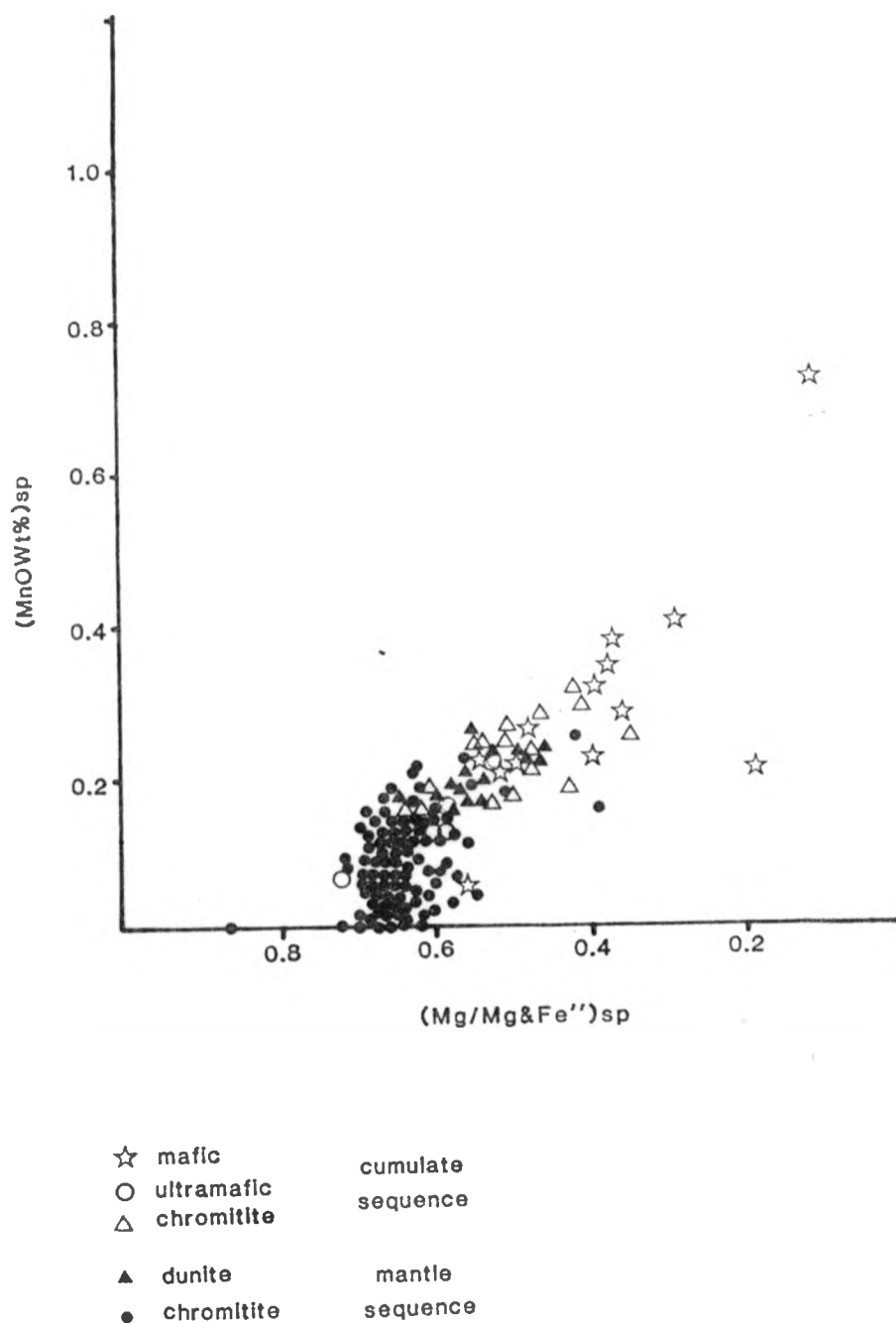


fig. 4.6 Chromite compositions $\text{Mg/Mg+Fe}'' \times \text{MnO Wt}\%$

The MnO content of chromite from mantle sequence dunite and chromitite shows a simple negative correlation with the $\text{Mg/Mg+Fe}''$ ratio as did the chromite in harzburgite (fig.3.9). This shows a strong preference by Mn^{2+} for the Fe^{2+} site in the chromite lattice.

chromitite using the Michel Lévy method on sections normal to {010} revealed that the feldspar is bytownite and microprobe analyses confirmed this with compositions of An_{76-79} . No zoning of the feldspar could be determined optically and not enough microprobe analyses are presently available to investigate the possibility of zoned grains.

Amphibole

Primary magmatic amphibole in Oman mantle sequence chromitites occurs as an interstitial mineral, often poikilitically enclosing chromite grains, and as primary inclusions within chromite grains. The amphibole is a highly magnesian, chrome rich pargasitic hornblende (table 4.2, fig. 4.7), colourless and non-pleochroic, due to its low iron content, with a prismatic habit. Secondary tremolite after clinopyroxene is distinguished from primary amphibole in having a distinct fibrous habit (Chapter 6).

Sulphides

Small grains ($< .01\text{mm}$) of Ni-Fe sulphide (pentlandite) occur in Oman mantle sequence chromitites, interstitial to the chromite grains. They are only distinguishable in reflected light on polished specimens where the creamy-white pentlandite contrasts with grey-white chromite. When polished specimens have a carbon coating the pentlandite appears pale red whilst the chromite colour does not appear to be affected. Qualitative X-ray scans have been made on these grains and confirm the conclusion from optical data that they are Ni-Fe sulphide (appendix 3.2).

Platinum group elements (PGE)

Determinations of Pd, Pt, Rh, Ir and Ru concentrations by spectrographic analysis have been made on 18 whole rock samples of Oman mantle sequence chromitites by J.Haffty and A.Haubert at the U.S.G.S., Menlo Park, California, (appendix 3.3). Platinum group elements in Oman chromitite samples occur in the overall ratio of $Ru_{20} : Ir_8 : Pt_2 : Pd_1$ with extremely low values of Rh and overall PGE abundances of 0.03 to 0.60 ppm. The order of abundance of the PGE is similar to that reported for Cyprus chromitites by Constantinides et al (1980) but Oman mantle sequence chromitite PGE concentrations are smaller by a factor of ten. The PGE concentrations in the Oman chromitite bear no relation

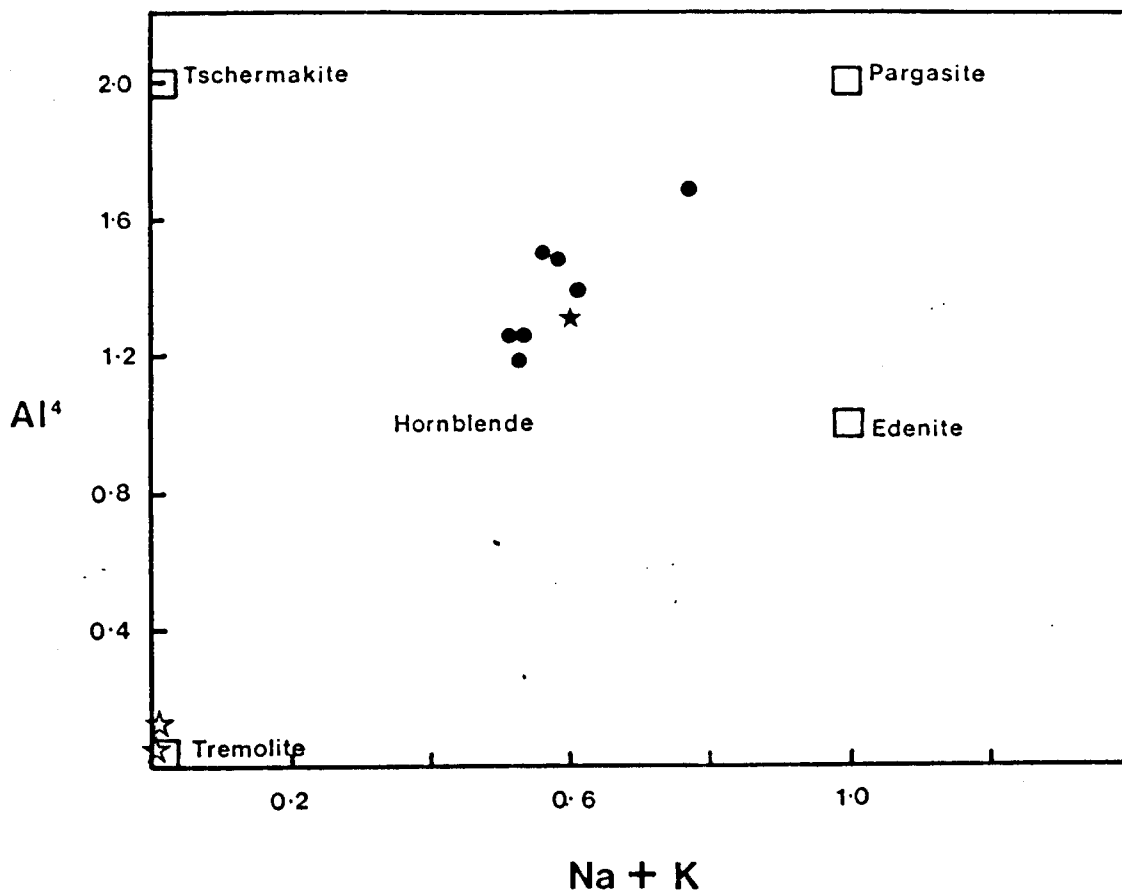


fig. 4.7 Amphibole compositions in Oman mantle sequence chromitites. Filled circles are primary pargasitic hornblende, open stars are secondary tremolite and the filled star is amphibole from a cumulate sequence hornblende gabbro.

to chromite chemistry of stratigraphic position within the mantle sequence and no discrete PGE bearing mineral phases have been identified although that is not surprising considering the low PGE abundances.

The PGE may be present in platinum group minerals (PGM) and/or in the chromite lattice and evidence for both modes of occurrence has been put forward (Razin and Khomenko, 1969; Hagen, 1954; Gijbels et al, 1974; and Constantinides et al, 1980), but there is little evidence available from Oman chromitites to support either mode of occurrence. It is clear, however, that either 1) the source magma for Oman chromitites was depleted in PGE with respect to source magma for Cyprus chromitites and especially chromitites in stratiform intrusions, or 2) the concentration mechanism for PGE in chromitites active particularly within the Bushveld (of Cousins, 1969) and Stillwater (Page and Jackson, 1967) complexes and perhaps partially in the Cyprus chromitite (Constantinides et al, 1980) was very limited or absent during the formation of Oman mantle sequence chromite.

4.4 Covariance of dunite and chromitite mineral chemistry

The covariances of the main compositional parameters in pairs of adjacent olivine and chromite grains from Oman mantle sequence dunite and chromitite are shown in fig. 4.8. The $Mg/(Mg+Fe)$ ratios of olivine and chromite show a positive correlation (fig. 4.8A) representing bulk rock $Mg/(Mg+Fe)$ variation but the $Cr/(Cr+Al)$ ratio of the chromite bears no relation to the olivine composition (fig. 4.8B). The $Mg/(Mg+Fe)$ ratios of olivine are also related to the modal percentage of chromite in the rock (figs. 4.8C and D), the higher $Mg/(Mg+Fe)$ ratios occurring in chromitites and the lower ratios in dunites. This could also be observed in the spinel prism plots (figs. 4.3 and 4.4). The $Cr/(Cr+Al)$ ratio is independent of the modal composition of the rock (fig. 4.7E).

4.5 Spatial variation in mantle sequence dunite and chromitite mineral chemistry

Single grains: No systematic zoning has been identified in olivine grains from mantle sequence dunite and chromitite although detailed investigation is hampered by alteration of olivine grains to serpentine minerals (see Chapter 6). Serpentinisation involves criss-crossing of

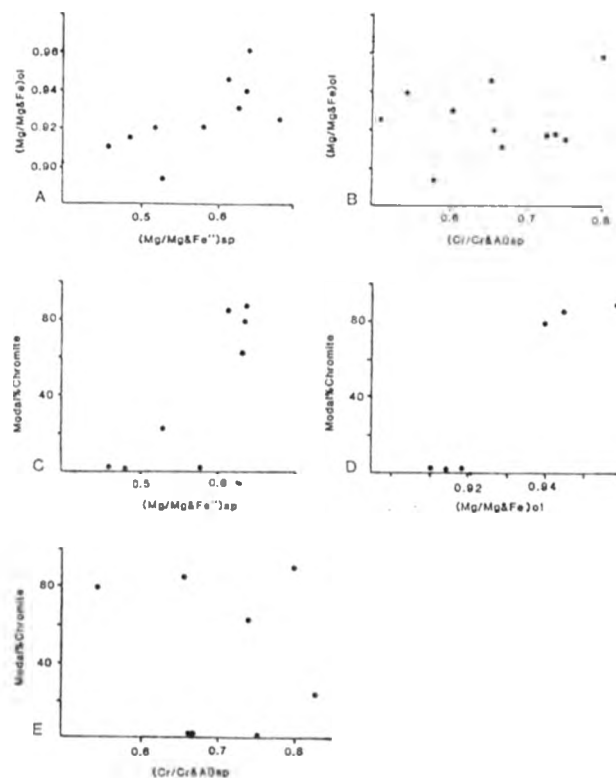
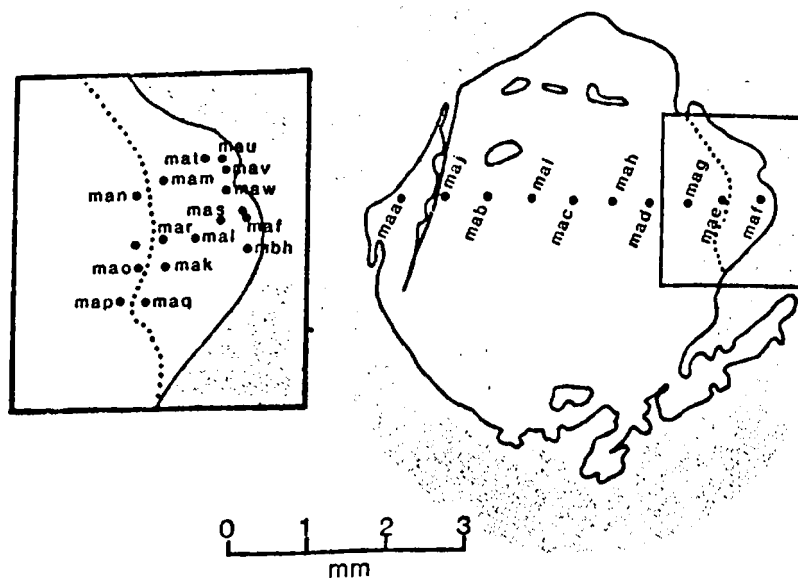


fig. 4.8 Covariance of mantle sequence dunite and chromitite mineral chemistry

- A The $Mg/Mg+Fe$ ratios of olivine and chromite show a positive correlation.
- B There is no correlation between $Mg/Mg+Fe$ ratio of olivine and the $Cr/Cr+Al$ ratio of chromite.
- C&D The $Mg/Mg+Fe$ ratios of chromite and olivine depend on the modal content of chromite, both ratios increasing with increasing chromite content.
- E The $Cr/Cr+Al$ ratio of chromite has no relation to the modal content of chromite.



Variation of chromite chemistry: single grain

fig. 4.9 Analysis points in single chromite grain (OM 3962)

The diagram shows the individual microprobe analysis points on a single chromite grain from a mantle sequence chromite (OM 3962). The analyses are listed in appendix 3.3 and presented with statistical treatment in table 4.3. The analysis groups show differences in composition between the main body of the grain and the marginal area delineated by the broken line.

Table 4.3 Microprobe traverse across a single chromite grain (OM 3962)

- 1) Main area of grain, 12 points: MAA, MAB, MAC, MAD, MAE, MAG, MAH, MAI, MAJ, MAN, MAO, MAP

	Mean \bar{x}	Standard deviation σ_{n-1}
MgO	14.45	0.10
Al ₂ O ₃	23.51	0.10
TiO ₂	0.57	0.02
Cr ₂ O ₃	43.39	0.16
MnO	0.14	0.01
FeO (tot)	17.99	0.07
TOTAL	100.05	

- 2) Lobate marginal area of grain, 13 points: MAF₁, MAF₂, MAK, MAL, MAM, MAP, MAR, MAS, MAT, MAU, MAV, MAQ, MAW

	Mean \bar{x}	Standard deviation σ_{n-1}
MgO	14.70	0.34
Al ₂ O ₃	24.50	0.70
TiO ₂	0.45	0.07
Cr ₂ O ₃	42.34	0.81
MnO	0.13	0.02
FeO (tot)	17.72	0.41
TOTAL	99.84	

olivine grains by a meshwork of serpentine which obscures original olivine grain boundaries and reduces the surface area of olivine grain available for analysis by microprobe. Chromite grains, on the other hand, are practically unaltered and more detailed investigation of composition is possible. A chromite grain with a marginal lobate overgrowth is shown in fig. 4.9 with analysis points marked. Table 4.3 contains the means and standard deviations of two sets of data points, one from the main body of the grain and the other from the marginal lobate area. The analyses from the main body of the grain are characterised by small values for the standard deviations, i.e. the grain is fairly homogeneous. The second set of analyses from the smaller marginal area of the grain have higher Al_2O_3 , lower Cr_2O_3 and lower TiO_2 mean values and much larger standard deviations on all compositional parameters, i.e. the marginal area is significantly different in composition from the main body of the grain and shows greater, albeit still very limited, compositional variations. The compositional change from the main body of the grain to the margin area is sharp, across the arbitrary boundary marked on fig. 4.9 and is not the type produced by alteration of chromite (see Chapter 6). The lower Cr_2O_3 , higher Al_2O_3 and greater range in composition are consistent with post-cumulus overgrowths from a progressively evolving inter-cumulus liquid but the lower TiO_2 values are not, (table 4.3).

Variation within chromitite bodies

It has been demonstrated that single chromite grains may have compositional zonation produced by successive crystallization/precipitation from an evolving magma and that textural evidence suggests that either of these processes or both are instrumental in producing concentrations of chromite to produce chromitite layers, lenses and pods. These bodies of chromitite, therefore, may contain compositional layering produced by successive crystallization/precipitation from a progressively evolving magma. The variation in composition of chromite grains from varying horizons within some chromitite bodies is shown in fig. 4.10. There is no simple pattern of compositional variation within the investigated chromitite bodies. The pattern expected would be one of decreasing Cr/Al with possibly slightly decreasing Mg/Fe and

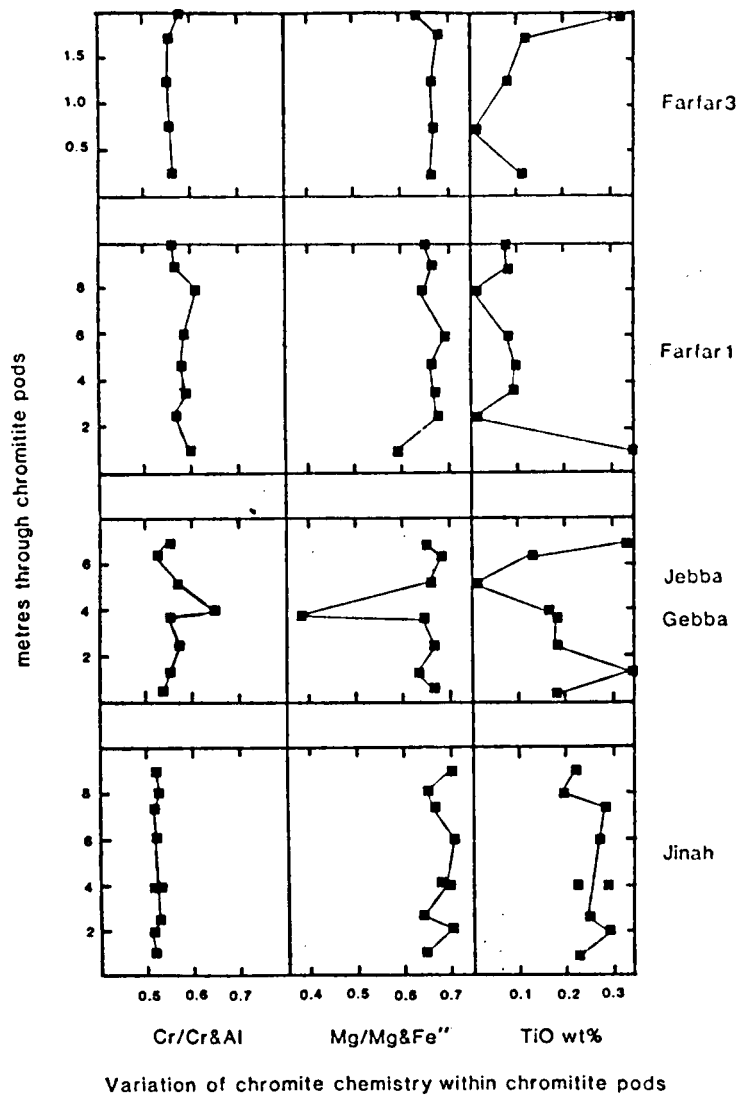


fig. 4.10 Chromite compositions plotted against horizon within chromite deposits

Variation in chromite composition through 4 separate chromite deposits is shown. There is no simple or common relation between composition and horizon within the deposits.

increasing TiO_2 from base to top of the chromitite body if it was formed by successive cumulate layers from a single evolving magma pulse, or if several magma pulses were involved then a repetition of these trends might be expected. Problems with the method of investigation are that: 1) identification of horizon within a single deposit is difficult as much of it appears homogeneous and structureless as 'massive' chromitite and 2) the analyses points may be primary grains or possibly the marginal overgrowths identified earlier in this section. Another possibility is that the massive chromitite bodies were formed from immiscible chromite liquids in a silicate melt and thus chemical trends up through layers as soon as chromite cumulates in stratiform intrusions may not be present at all.

Spatial variations in chromite chemistry throughout the Oman mantle sequence

The relative positions of eighteen chromitite bodies in the mantle sequence of the Fizh block (appendix 2) of the Oman ophiolite are plotted in fig. 4.11. The datum for their position within the mantle sequence is taken as the position of the upper boundary of the mantle sequence with the cumulate sequence due east of the deposit, the exception being the Aleya deposit, which occurs in the basal dunite of the cumulate sequence and is thus assigned a value of 0km. Locations of the deposits are shown in appendix 2.2. The $\text{Mg}/(\text{Mg}+\text{Fe})$ ratios of the chromite grains do not show any pattern of difference between the deposits related to their positions within the mantle sequence. The overall variation (0.75 - 0.46) is encountered within one single deposit (Rajmi 1, see appendix 2.2). The $\text{Cr}/(\text{Cr}+\text{Al})$ ratios of the chromites, on the other hand, do show variations between deposits related to their position in the mantle sequence. The chromite deposits can be conveniently divided into 3 groups: 1) the upper group (0-1km), 2) the middle group (1-8km) and 3) the lower group (8-12km). The upper group $\text{Cr}/(\text{Cr}+\text{Al})$ ratios vary from 0.619 to 0.414, the middle group from 0.764 to 0.512 and the lower group from 0.831 to 0.579. There is some overlap between these ranges and one deposit (Heylah 2) contains a

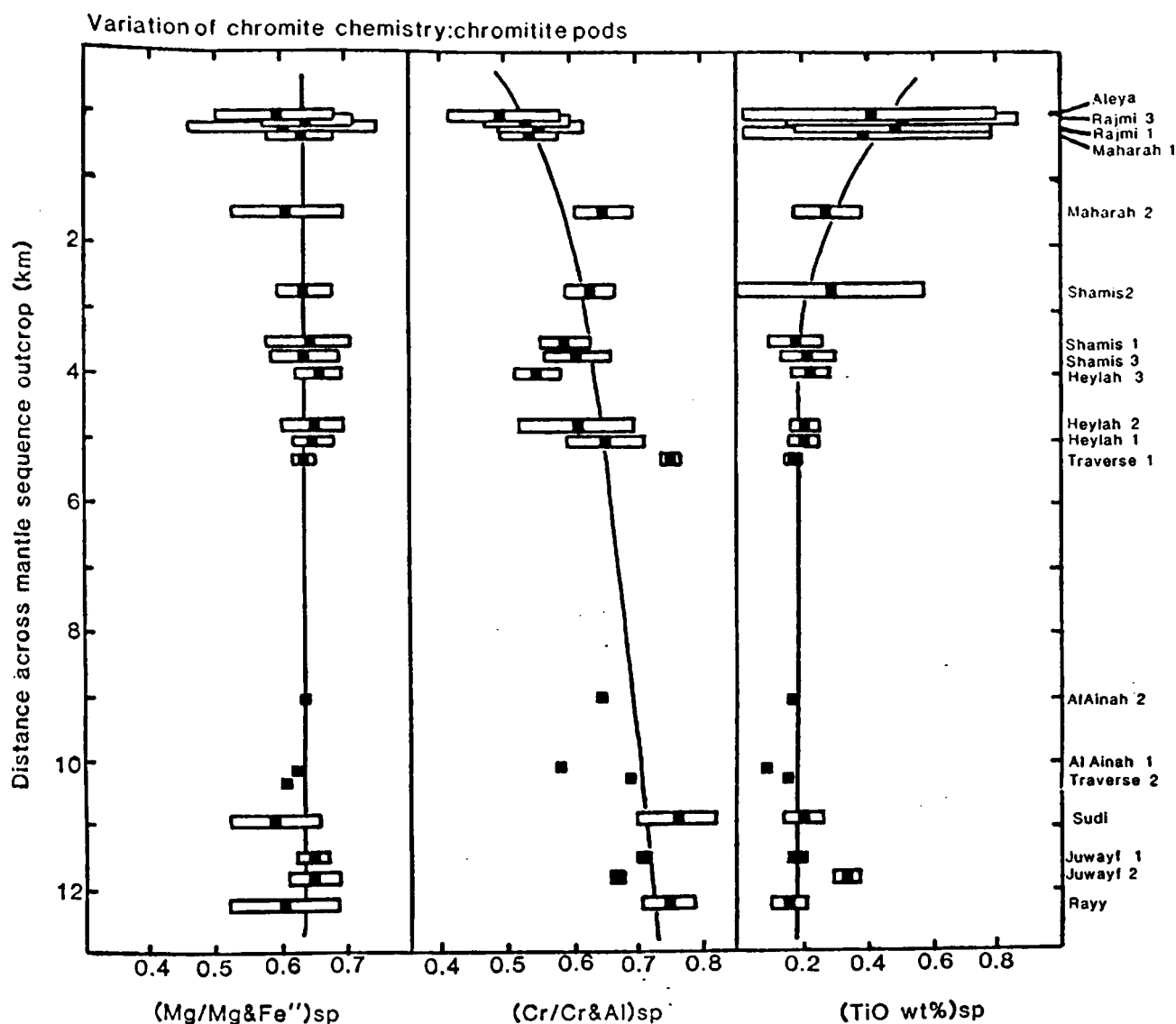


fig. 4.11 Chromite compositions plotted against horizon within mantle sequence

Plot shows mean and 2σ limits of group of analyses for each deposit.

The criterion for estimation of relative depths within the sequence is taken as the distance across outcrop from the mantle sequence upper boundary. The $Mg/Mg+Fe^{''}$ ratio of chromite shows no correlation with 'depth' and the overall total range in composition is encountered in one deposit. The $Cr/Cr+Al$ ratios group into low, medium and high values corresponding the upper, middle and lower parts of the mantle sequence. There is overlap in composition between the groups but the collective distinction is clear. The lower and middle groups contain mostly low TiO_2 chromite whilst the upper group contains higher TiO_2 averages with larger variations. All chromite deposit locations are shown in appendix 2.

range of Cr/Cr+Al ratios of 41% of the total range but a general progressive increase of Cr/Cr+Al ratio in chromite from chromitite bodies with depth within the mantle sequence is clear from fig. 4.10. TiO_2 values are generally low with small variations in the lower and middle groups whilst higher mean TiO_2 contents with greater variations characterise the upper chromitite group.

ETHOS SCANNING JOB SHEET

EPID: 348844

IMAGE OUTPUT

Admin Copy

Date received from 13/03/2020

University:

Author (s): Brown , M. A

University: Open University



Admin Team Comments

2 VOLS. DO NOT SCAN ITEMS IN ENVELOPE AT BACK OF VOL 2. PLS ADD TARGET

Scan Process Details

Hrs Mins

Date Scanned

Time Taken

Scanner No

Total Pages

Scanned by

Comments

Post Process Details

Hrs Mins

Date Processed

Time Taken

Processed by

Date Returned to Admin

ETHOS SCANNING JOB SHEET

EPID: 348844

IMAGE

OUTPUT

Scanning Copy

Date received from 13/03/2020

University:

Author (s): Brown , M. A

University: Open University



Admin Team Comments

2 VOLS. DO NOT SCAN ITEMS IN ENVELOPE AT BACK OF VOL 2. PLS ADD TARGET

KIRTAS download

Date

Downloaded by

Finalise

Finalise 1

Finalise 2

Scan Process Details

Hrs Mins

Date Scanned

Time Taken

Scanner No

Total Pages

Scanned by

Comments

Post Process Details

Hrs Mins

Date Processed

Time Taken

Processed by

Total pages Post